https://ntrs.nasa.gov/search.jsp?R=19760016328 2020-03-22T15:39:50+00:00Z

NASA CR-135022

FINAL REPORT
on

LOW-CYCLE FATIGUE OF TYPE 347 STAINLESS STEEL AND HASTELLOY ALLOY X IN HYDROGEN GAS AND IN AIR AT ELEVATED TEMPERATURES

by

Carl E. Jaske, Richard C. Rice, Richard D. Buchheit,
Donald B. Roach, and Theodore L. Porfilio

May 1976

(NASA-CR-135022) LOW-CYCLE FATIGUE OF TYPE 347 STAINLESS STEEL AND HASTELLOY X ALLOY X IN HYDROGEN GAS AND IN AIR AT ELEVATED TEMPERATURES Final Report (Battelle Columbus Labs., Ohio.) 111 p HC $5.50 CSCL 11F G3/26 Unclas 23227

Prepared under Contract No. NAS3-20078

for

NATIONAL AERONAUTICS AND SPACE ADMINISTRATION
LEWIS RESEARCH CENTER

BATTELLE
Columbus Laboratories
505 King Avenue
Columbus, Ohio 43201

JUN 1976
RECEIVED
NASA STI FACILITY
INPUT BRANCH

NASA-CR-135022

LOW-CYCLE FATIGUE OF TYPE 347 STAINLESS STEEL AND HASTELLOY ALLOY X IN HYDROGEN GAS AND IN AIR AT ELEVATED TEMPERATURES

By Carl E. Jaske, Richard C. Rice, Richard D. Buchheit,
Donald B. Roach, and Theodore L. Porfilio

Prepared under Contract No. NAS3-20078
BATTELLE
Columbus Laboratories
Columbus, Ohio

for

NATIONAL AERONAUTICS AND SPACE ADMINISTRATION

EXPLANATORY NOTE

Between July, 1970, and April, 1972, an extensive low-cycle fatigue investigation of Type 347 stainless steel and Hastelloy Alloy X was performed at Battelle-Columbus under the sponsorship of Aerojet Nuclear Systems Company. The program was under the auspices of the NASA-Space Nuclear Systems Office, Cleveland Extension, Contract SNP-1, Project 187, Purchase Order 900105. Messrs. W. Emmons, H. Spaletta, L. Pickering, and P. Dessau of Aerojet provided technical direction and monitoring of the program. In addition, Aerojet documented the chemistry and fabrication history of the materials used, and the supplementary experiments in air at 538 and 871°C (1000 and 1600°F) were supported through a Battelle-Columbus in-house project.

In order to ensure that the above information would not be lost to the general technical community and to provide it to the public in a single, complete document, a program was initiated at Battelle-Columbus in January, 1976, under the sponsorship of NASA-Lewis Research Center through Contract No. NAS3-20078. Dr. Gary R. Halford of NASA-Lewis served as the technical monitor for the program. The purpose of this program was to prepare the following report, documenting the research performed previously, and distribute the report to appropriate members of the technical community.

CONTENTS

	Page
SUMMARY	1
INTRODUCTION	2
SYMBOLS	4
MATERIALS	5
Heat Treatment	7
Chemistry	7
Microstructure	10
Hardness	10
EXPERIMENTAL PROCEDURES	17
Specimen Preparation	17
Tensile Testing Apparatus	20
Fatigue Testing Apparatus	20
Fatigue Data Acquisition	25
EXPERIMENTAL RESULTS AND DISCUSSION	34
Tensile Properties	35
Cyclic Stress-Strain Response	39
Fatigue Resistance	54
Fractographic and metallographic studies of failed Type 347 stainless steel specimens	74
CONCLUSIONS	80
RECOMMENDATIONS	82
APPENDIX A	83
APPENDIX B	89
REFERENCES	101

PRECEDING PAGE BLANK NOT FILMED

ILLUSTRATIONS

Figure		Page
1	Comparison of chemical compositions	9
2	Microstructure of heat A (X-11585) of Type 347 stainless steel after simulated brazing (samples etched with 30HCl, 10HNO_3 solution).	11
3	Microstructure of heat B (G-5617) of Type 347 stainless steel after simulated brazing (samples etched with 30HCl, 10HNO_3 solution).	12
4	Microstructure of heat C (G-4943) of Type 347 stainless steel after simulated brazing (samples etched with 30HCl, 10HNO_3 solution).	13
5	Microstructure of heat D (2610-0-4007) of Hastelloy Alloy X after simulated brazing (samples etched with aquaregia solution)	14
6	Microstructure of heat E (2610-0-4008) of Hastelloy Alloy X after simulated brazing (samples etched with aquaregia solution)	15
7	Specimen configurations	18
8	Closed-loop electrohydraulic fatigue system	19
9	Waveforms of axial strain and stress for continuous cycling	22
10	Illustration of hysteresis loop for strain cycle with hold time at peak compressive strain	23
11	Cyclic waveforms of axial strain and stress for compression strain hold-time tests	24
12	Hydrogen test chamber with specimen installed	26
13	Load-axial displacement hysteresis loops for Type 347 stainless steel and Hastelloy Alloy X at 538°C (1000°F). . . .	28
14	Load-axial displacement hysteresis loops for Type 347 stainless steel and Hastelloy Alloy X at 760°C (1400°F). . . .	29
15	Load-axial displacement hysteresis loops for Type 347 stainless steel and Hastelloy Alloy X at 871°C (1600°F). . . .	30

Figure		Page
16	Load-Time histories of Type 347 stainless steel and Hastelloy Alloy X at 538°C (1000°F)	31
17	Load-time histories of Type 347 stainless steel and Hastelloy Alloy X at 760°C (1400°F)	32
18	Load-time histories of Type 347 stainless steel and Hastelloy Alloy X at 871°C (1600°F)	33
19	Effect of temperatures on average material properties of Type 347 stainless steel and Hastelloy X	38
20	Monotonic stress-strain curves for Type 347 stainless steel	40
21	Monotonic stress-strain curves for Hastelloy Alloy X	41
22	Stress amplitude versus fatigue cycles for Type 347 stainless steel and Hastelloy Alloy X in hydrogen gas at 538°C (1000°F)	42
23	Stress amplitude versus fatigue cycles for Type 347 stainless steel and Hastelloy Alloy X in hydrogen gas at 760°C (1400°F)	43
24	Stress amplitude versus fatigue cycles for Type 347 stainless steel and Hastelloy Alloy X in hydrogen gas at 871°C (1600°F)	44
25	Effect of temperature on stress response in hydrogen gas and at a total axial strain range of 3 percent	46
26	Monotonic and stabilized cyclic (at $N_f/2$) stress response of Type 347 stainless steel and Hastelloy Alloy X in hydrogen gas	47
27	Stress amplitude versus fatigue cycles for Type 347 stainless steel and Hastelloy Alloy X in air	48
28	Monotonic and stabilized cyclic (at $N_f/2$) stress response of Type 347 stainless steel and Hastelloy Alloy X in air	49
29	Relaxation stress response for Type 347 stainless steel in hydrogen gas at 760°C (1400°F)	51
30	Relaxation stress response for Type 347 stainless steel in hydrogen gas at 871°C (1600°F) and at a total axial strain range of 3 percent	52

Figure		Page
31	Relaxation stress response for Hastelloy Alloy X in hydrogen gas and at a total axial strain range of 3 percent	53
32	Fatigue life as a function of strain range for Type 347 stainless steel and Hastelloy Alloy X in air and at an axial strain rate of 10^{-3} sec^{-1}	57
33	Fatigue life as a function of temperature and total axial strain range for Type 347 stainless steel and Hastelloy Alloy X in air	59
34	Fatigue life as a function of strain range for Type 347 stainless steel and Hastelloy Alloy X in hydrogen gas at 538°C (1000°F) and at a strain rate of 10^{-3} sec^{-1} . . .	61
35	Fatigue life as a function of strain range for Type 347 stainless steel and Hastelloy Alloy X in hydrogen gas at 760°C (1400°F) and at a strain rate of 10^{-3} sec^{-1}	62
36	Fatigue life as a function of strain range for Type 347 stainless steel and Hastelloy Alloy X in hydrogen gas at 871°C (1600°F) and at a strain rate of 10^{-3} sec^{-1}	63
37	Fatigue life versus total strain range for Type 347 stainless steel and Hastelloy Alloy X in hydrogen gas at elevated temperature and at strain rate of 10^{-3} sec^{-1} . . .	64
38	Comparison of fatigue life in air with that in hydrogen gas at 538, 760, and 871°C (1000, 1400, and 1600°F) and at a strain rate of 10^{-3} sec^{-1}	66
39	Fatigue life as a function of temperature for Type 347 stainless steel at 3 percent total axial strain range	68
40	Comparison of continuous cycling and 10-minute compressive hold time fatigue data for heat A of Type 347 stainless steel in hydrogen gas at 760°C (1400°F) and at an axial strain rate of 10^{-3} sec^{-1}	71
41	Comparison of continuous cycling and 10-minute compressive hold time fatigue data for heat A of Type 347 stainless steel in hydrogen gas at 871°C (1600°F) and at an axial strain rate of 10^{-3} sec^{-1}	72
42	Photomicrographs of specimen A18 tested under continuous strain cycling at 1.5 percent total axial strain range and in hydrogen gas at 760°C (1400°F)	77
43	Photomicrographs of specimen A49 tested at 1.5 percent total axial strain range with a 10-minute compressive hold time and in hydrogen gas at 760°C (1400°F)	79

TABLES

Table		Page
I	IDENTIFICATION OF MATERIALS	6
II	CHEMICAL COMPOSITION	8
III	ESTIMATED GRAIN SIZES AFTER HEAT TREATMENT	16
IV	HARDNESS VALUES	16
V	TENSILE PROPERTIES OF TYPE 347 STAINLESS STEEL AT A STRAIN RATE OF 0.005 MIN^{-1}	36
VI	TENSILE PROPERTIES OF HASTELLOY ALLOY X AT A STRAIN RATE OF 0.005 MIN^{-1}	37
VII	SUMMARY OF STRESS RELAXATION DATA FOR COMPRESSIVE-STRAIN HOLD-TIME EXPERIMENTS ON TYPE 347 STAINLESS STEEL AND HASTELLOY ALLOY X	55
VIII	SUMMARY OF ELASTIC AND INELASTIC SLOPE AND INTERCEPT VALUES FOR CONTINUOUS CYCLING FATIGUE TESTS ON TYPE 347 STAINLESS STEEL AND HASTELLOY ALLOY X IN AIR AND HYDROGEN GAS	58
IX	COMPARISON OF AVERAGE FATIGUE LIFE AND STRESS RANGE VALUES FROM COMPRESSIVE HOLD-TIME TESTS WITH THOSE FROM CONTINUOUS CYCLING TESTS OF TYPE 347 STAINLESS STEEL AND HASTELLOY ALLOY X IN HYDROGEN GAS	70
B1	SUMMARY OF CONTINUOUS CYCLING FATIGUE DATA FOR TYPE 347 STAINLESS STEEL IN AIR AND AT AN AXIAL STRAIN RATE OF 10^{-3} SEC^{-1}	91
B2	SUMMARY OF CONTINUOUS CYCLING FATIGUE DATA FOR HASTELLOY ALLOY X IN AIR AND AT AN AXIAL STRAIN RATE OF 10^{-3} SEC^{-1}	92
B3	SUMMARY OF CONTINUOUS CYCLING FATIGUE DATA FOR TYPE 347 STAINLESS STEEL IN HYDROGEN GAS AT 538°C (1000°F) AND AT AN AXIAL STRAIN RATE OF 10^{-3} SEC^{-1}	93
B4	SUMMARY OF CONTINUOUS CYCLING FATIGUE DATA FOR HASTELLOY ALLOY X IN HYDROGEN GAS AT 538°C (1000°F) AND AN AXIAL STRAIN RATE OF 10^{-3} SEC^{-1}	94
B5	SUMMARY OF CONTINUOUS CYCLING FATIGUE DATA FOR TYPE 347 STAINLESS STEEL IN HYDROGEN GAS AT 760°C (1400°F) AND AT AXIAL STRAIN RATE OF 10^{-3} SEC^{-1}	95
B6	SUMMARY OF CONTINUOUS CYCLING FATIGUE DATA FOR HASTELLOY ALLOY X IN HYDROGEN GAS AT 760°C (1400°F) AND AN AXIAL STRAIN RATE OF 10^{-3} SEC^{-1}	96

TABLES

Table		Page
B7	SUMMARY OF CONTINUOUS CYCLING FATIGUE DATA FOR TYPE 347 STAINLESS STEEL IN HYDROGEN GAS AT 871°C (1600°F) AND AT AN AXIAL STRAIN RATE OF 10^{-3} SEC^{-1}	97
B8	SUMMARY OF CONTINUOUS CYCLING DATA FOR HASTELLOY ALLOY X IN HYDROGEN GAS AT 871°C (1600°F) AND AN AXIAL STRAIN RATE OF 10^{-3} SEC^{-1}	98
B9	SUMMARY OF CONTINUOUS CYCLING FATIGUE DATA FOR TYPE 347 STAINLESS STEEL IN HYDROGEN GAS AT 593, 649, AND 704°C (1100, 1200, AND 1300°F) AND AT AXIAL STRAIN RATE OF 10^{-3} SEC^{-1}	99
B10	SUMMARY OF FATIGUE DATA FOR TYPE 347 STAINLESS STEEL AND HASTELLOY ALLOY X IN HYDROGEN GAS AT 760 AND 871°C (1400 AND 1600°F) WITH A 10-MINUTE COMPRESSIVE-STRAIN HOLD TIME AND AT AN AXIAL STRAIN RATE OF 10^{-3} SEC^{-1}	100

LOW-CYCLE FATIGUE OF TYPE 347 STAINLESS STEEL AND HASTELLOY ALLOY X IN HYDROGEN GAS AND IN AIR AT ELEVATED TEMPERATURES

Carl E. Jaske, Richard C. Rice, Richard D. Buchheit, Donald B. Roach, and Theodore L. Porfilio*

Battelle's Columbus Laboratories

SUMMARY

An experimental investigation was conducted to assess the low-cycle fatigue resistance of two alloys, Type 347 stainless steel and Hastelloy Alloy X, that were under consideration for use in nuclear-powered rocket vehicles. Constant-amplitude, strain-controlled fatigue tests were conducted under compressive strain cycling at a constant strain rate of 10^{-3} sec^{-1} and at total axial strain ranges of 1.5, 3.0, and 5.0 percent. Work was carried out in both laboratory-air and low-pressure [108 kN/m^2 (15.7 psi)], hydrogen-gas environments at temperatures from 538 to 871°C (1000 to 1600°F).

Specimens were obtained from three heats of Type 347 stainless steel bar and two heats of Hastelloy Alloy X bar that had been subjected to a simulated brazing heat-treatment cycle. After characterization of chemistry, microstructure, and hardness, the tensile properties of each heat were determined at 21, 538, 649, and 760°C (70, 1000, 1200, and 1400°F).

Using three replicates of each test condition for Type 347 stainless steel and four replicates for Hastelloy Alloy X, the continuous cycling fatigue resistance in hydrogen gas was determined for each heat at each of the three strain ranges of interest and at temperatures of 538, 760, and 871°C (1000, 1400, and 1600°F). Similar fatigue experiments (except with no or only limited replication) were conducted on specimens from all five heats of material in air at 760°C (1400°F) and on specimens from one heat of each alloy at 538 and 871°C (1000 and 1600°F). Also, continuous cycling fatigue experiments were conducted on specimens from one heat of Type 347 stainless steel in hydrogen gas at 3.0 percent strain range at 593, 649, and 704°C (1100, 1200, and 1300°F) and at 1.5 percent strain range at 649°C (1200°F).

---

* Formerly at Battelle-Columbus, but presently at Dialight, Brooklyn, New York.

Information on both cyclic stress-strain response and fatigue life was developed for all of the above conditions. In hydrogen gas, the fatigue resistance of both alloys was lowest at 760°C (1400°F) and highest at 871°C (1600°F), with results at 538°C (1000°F) falling intermediate to those at the other two temperatures. The supplementary experiments in hydrogen gas showed that the Type 347 stainless steel had a minimum fatigue resistance at 704°C (1300°F) that was slightly lower (about 10 percent) than that at 760°C (1400°F).

The Type 347 stainless steel exhibited equal or superior fatigue resistance to the Hastelloy Alloy X in hydrogen gas at all conditions of this study. The fatigue resistance of both materials in air was close to or slightly below that in hydrogen gas for temperatures up to 760°C (1400°F), but the fatigue resistance was significantly degraded in air at 871°C (1600°F) where oxidation became more severe than at lower temperatures. In air, the Type 347 stainless steel had slightly superior fatigue resistance to the Hastelloy Alloy X at 538 and 760°C (1000 and 1400°F), but it had inferior fatigue resistance at 871°C (1600°F).

Exploratory, 10-minute, compressive hold-time experiments were conducted on specimens from one heat of each alloy in hydrogen gas at 760 and 871°C (1400 and 1600°F). Compared with continuous cycling at comparable total axial strain ranges, the compressive hold times caused a small improvement in the fatigue resistance of the Type 347 stainless steel and a small degradation in the fatigue resistance of the Hastelloy Alloy X. The improvement of Type 347 stainless steel was qualitatively explained by the method of strain range partitioning. Also, cyclically stable (at $N_f/2$) stress relaxation behavior was quantitatively characterized.

A limited fractographic and metallographic examination was conducted on specimens from one heat of Type 347 stainless steel tested in hydrogen gas at 760°C (1400°F). Both hold-time and continuous-cycling specimens had some grain boundary voids near the fracture. However, the size of these voids indicated that compressive hold time tended to either inhibit or close voids.

INTRODUCTION

During operation of a nuclear-powered rocket engine, some areas of the rocket nozzle are exposed to hydrogen gas and subjected to temperature

fluctuations that are of sufficient magnitude to produce large cyclic compressive strains. Since it was determined that these cyclic strains could produce fatigue cracks or failures in less than 1,000 cycles, it was important to know the low-cycle fatigue resistance of the two materials, Type 347 stainless steel and Hastelloy Alloy X, that were being considered for use in this application. This program was conceived to experimentally evaluate the low-cycle fatigue behavior of these two alloys in both hydrogen-gas and laboratory-air environments at temperatures from 538 to 871°C (1000 to 1600°F). A strain rate of 10^{-3} sec^{-1} was selected for these studies because this was the approximate rate of straining anticipated in service.

Although sheet material would be used in fabrication of nozzles, bar stock was selected to avoid difficulties in experimentation. Uniaxially loaded cylindrical specimens are normally used for low-cycle-fatigue evaluation of metallic materials (for example, see ref. 1) because both strain and stress can be easily determined. Potential buckling under compressive straining made uniaxial loading of sheet material impractical for the temperature range of this study. Since it was not considered feasible to take cylindrical specimens from sheet stock and since it was expected that bar stock would have approximately the same low-cycle-fatigue behavior as sheet stock, 19 mm (0.75 in.) diameter bar stock was selected for use in this program. Materials were obtained in the solution-treated condition and then subjected to a simulated brazing heat treatment before experimental work was performed on them. This brazing process was completed because it was anticipated that fatigue-critical areas in the nozzle would be joined by brazing.

Type 347 stainless steel is one of the 300 series of chromium-nickel austenitic stainless steels. It is columbium/tantalum stabilized to provide resistance to intergranular environmental attack and is normally used in applications where oxidation, corrosion, and heat resistance are required at temperatures up to 816°C (1500°F). Its use at this high temperature is limited to cases where low strength is acceptable, as in the present case of thermally induced cyclic straining. Hastelloy Alloy X is an austenitic nickel-base superalloy used in components that require oxidation resistance up to 1204°C (2200°F). In contrast to the Type 347 stainless steel, it has relatively high strength above 816°C (1500°F). However, such strength is usually more important for creep/rupture and for long-life fatigue resistance than for low-cycle (high-strain) fatigue resistance.

No relevant data were available on the fatigue behavior of these alloys in hydrogen gas. Baldwin, et al (ref. 2), conducted an extensive low-cycle fatigue study of Type 347 stainless steel in air at temperatures up to 600°C (1112°F) and at total axial strain ranges of less than 2 percent. An extensive review of available low-cycle fatigue data on three comparable austenitic alloys (Types 304 and 316 stainless steel and Alloy 800) in air at temperatures up to 816°C (1500°F) was conducted by Jaske, et al (ref. 3). The review included an extensive collection of low-cycle fatigue information on Types 304, 316, and 348 stainless steels in air at 427, 649, and 816°C (800, 1200, and 1500°F) from the work of Berling and Slot (ref. 4). A limited low-cycle fatigue study of Hastelloy Alloy X in argon gas at 427, 704, 816, and 982°C (800, 1300, 1500, and 1800°F) was performed by Carden and Slade (ref. 5). Low-cycle fatigue data on Hastelloy Alloy X in air at 21 and 649°C (70 and 1200°F) were also recently reported (ref. 6).

This work was conducted using the U. S. customary system of units. Conversion to the International System of Units (SI) was made for reporting purposes only.

SYMBOLS

A	optimized constant in stress relaxation equation
A_T	area of specimen at temperature, mm^2 ($in.^2$)
D_T	minimum specimen diameter at temperature, mm (in.)
E	modulus of elasticity, GN/m^2 (ksi)
K	compliance constant, N^{-1} (lb^{-1})
M	optimized constant in stress relaxation equation
N_o	number of cycles to detectable cracking
N_s	number of cycles to significant cracking
N_f	number of cycles to total fracture
P	load on specimen, N (lb)
ΔP	load range, N (lb)

t	instantaneous time, min
$t_{\epsilon-}$	compression strain hold time, min
ϵ_d	diametral strain
ϵ_{de}	elastic component of diametral strain
$\dot{\epsilon}_t$	total axial strain rate, sec^{-1}
$\Delta\epsilon_{cc}$	reversed creep strain range
$\Delta\epsilon_{de}$	change in elastic component of diametral strain
$\Delta\epsilon_e$	elastic strain range
$\Delta\epsilon_{ed}$	elastic strain range under decreasing load
$\Delta\epsilon_{ei}$	elastic strain range under increasing load
$\Delta\epsilon_{in}$	inelastic strain range
$\Delta\epsilon_{pc}$	plastic strain range reversed by creep strain
$\Delta\epsilon_{pp}$	reversed plastic strain range
$\Delta\epsilon_t$	total axial strain range
ν_e	Poisson's ratio, elastic
ν_{in}	Poisson's ratio, inelastic
σ	stress, MN/m^2 (ksi)
σ_o	initial stress value
$\Delta\sigma$	stress range, MN/m^2 (ksi)
$\Delta\sigma_{r-}$	stress relaxation during hold, MN/m^2 (ksi)
$\Delta\sigma/2$	stress amplitude, MN/m^2 (ksi)

MATERIALS

Three heats of Type 347 stainless steel and two heats of Hastelloy Alloy X were evaluated in this study. Both alloys were supplied by the Aerojet Nuclear Systems Company (ANSC) in the form of 19 mm (0.75 in.) diameter bar stock in the amounts listed in table I. As indicated, all bar stock was originally obtained

REPRODUCIBILITY OF THE
IS POOR

TABLE I. — IDENTIFICATION OF MATERIALS

Alloy	Specimen letter prefix	Vendor	Vendor heat number	Number of 19 mm (0.75 in.) diameter by 1.22 m (4 ft) long bars	
				Originally supplied	Remaining unused
Type 347 Stainless Steel, AMS 5654A	A	Crucible Speciality Metals Division, Colt Industries, Inc.	X-11585	24	14
	B	Universal-Cyclops Speciality Steel Division, Cyclops Corporation	G5617	24	14
	C	Universal-Cyclops Speciality Steel Division, Cyclops Corporation	G4943	24	14½
Hastelloy Alloy X, AMS 5754F	D	Stellite Division, Cabot Corporation	2610-0-4007	26½	17½
	E	Stellite Division, Cabot Corporation	2610-0-4008	26½	20

by ANSC from three different suppliers. The specimen letter prefix which was assigned to each heat and the applicable Aerospace Material Specification (AMS) number are also listed.

Heat Treatment

All 5 heats of material were originally obtained in the annealed condition. However, examination of the hardness and tensile properties of the Type 347 stainless steel indicated that it had undergone about 5 to 10 percent of cold working.

Since these alloys were being evaluated for possible use in nozzles of nuclear-powered rocket vehicles, they were subjected to a heat treatment that simulated the brazing operations to be used in fabrication of such nozzles. Before shipment of the bar stock to Battelle-Columbus, it was given the following simulated brazing heat treatment by Pyromet Industries:

(1) Heat to 1010°C (1850°F) at a rate of 83 to 111°C (150 to 200°F) per hour. Furnace cool to 538°C (1000°F); then air cool to room temperature.

(2) Reheat to 982°C (1800°F) at a rate of 83 to 111°C (150 to 200°F) per hour. Furnace cool to 538°C (1000°F); then air cool to room temperature.

(3) Reheat to 968°C (1775°F) at a rate of 83 to 111°C (150 to 200°F) per hour. Furnace cool to 538°C (1000°F), and finally air cool to room temperature.

None of the heats of material were soaked while at the peak heat treatment temperatures. Elapsed time for the three-step brazing cycle was approximately 30 hours.

Chemistry

The chemical compositions of the 5 heats of material were reported by ANSC as listed in table II and comparatively illustrated in figure 1. Values from the appropriate AMS specifications are also listed and shown. Compositions of heats B, C, D, and E fell within the specified values. The phosphorous and sulfur contents of heat A were slightly above the specified maximum levels, even though all other elements were within the specified levels. However, the

TABLE II. – CHEMICAL COMPOSITION[a]

Alloy	Specimen letter prefix	Composition, wt. %														
		C	Mn	P	S	Si	Cr	Ni	Mo	Cu	Cb + Ta	Fe	W	Co	B	Others
Type 347 Stainless Steel	A	0.050	1.64	0.026	0.028	0.72	17.70	10.20	0.34	0.37	0.81	Remainder	--	--	--	--
	B	0.053	1.62	0.016	0.008	0.76	17.03	10.06	0.28	0.23	0.76	Remainder	--	--	--	--
	C	0.056	1.47	0.015	0.006	0.87	17.18	9.98	0.26	0.16	0.72	Remainder	--	--	--	--
AMS 5654A		≤0.08	≤2.00	≤0.020	≤0.020	≤1.00	17.00-19.00	9.00-13.00	≤0.75	≤0.50	10 x C - 1.10	Remainder	--	--	--	--
Hastelloy Alloy X	D	0.09	0.74	0.003	0.006	0.40	22.10	Remainder	9.10	0.01	--	17.40	0.47	2.03	<.001	0.01 Al, 0.01 Ti, 0.01 Zr and 0.01 V
	E	0.08	0.76	0.001	0.006	0.38	22.00	Remainder	9.05	0.01	--	18.65	0.43	1.97	0.001	0.01 Al, 0.01 Ti, 0.01 Zr and 0.01 V
AMS 5754F		0.05-0.15	≤1.00	≤0.040	≤0.030	≤1.00	20.50-23.00	Remainder	8.00-10.00	--	--	17.00-20.00	0.20-1.00	0.50-2.50	≤.010	--

[a]Values reported by Aerojet Nuclear Systems Company.

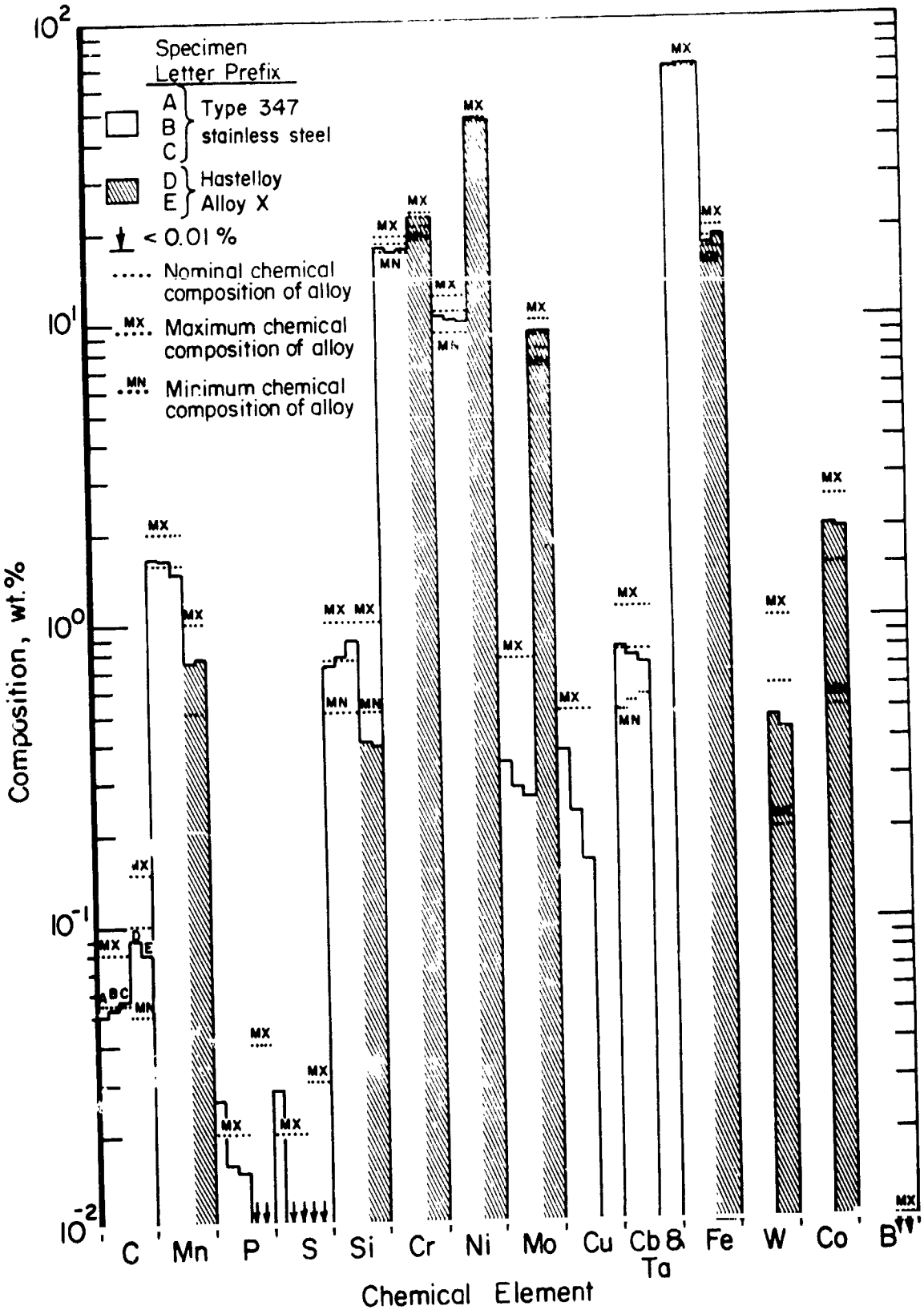

Figure 1.– Comparison of chemical compositions.

phosphorous and sulfur levels of heat A were within AMS 5512D specifications (P ≤ 0.040 wt % and S ≤ 0.030 wt %) covering sheet material. Since nozzles would be fabricated from sheet material and bar stock was evaluated to avoid experimental difficulties as discussed earlier, these levels were considered acceptable. Also, the nickel contents of heats A, B, and C were below the maximum level of 12.00 wt % specified for sheet in AMS 5512D (in contrast to the maximum levels of 13.00 wt % specified for bar in AMS 5654A). The specified chemical composition of Hastelloy Alloy X sheet in AMS 5536G is the same as that for bar in AMS 5754F.

Microstructure

Photomicrographs of typical microstructures (after heat treatment) for all 5 heats of material are presented in figures 2 through 6. These were obtained from both longitudinal and transverse samples of each heat. The Type 347 stainless steel was etched with 30HCl, 10HNO_3 solution, and the Hastelloy Alloy X was etched with aquaregia solution. Both alloys had a relatively fine grain size for bar stock to simulate that usually found in sheet material.

Grain sizes of the Type 347 stainless steel samples were estimated using a comparison procedure in accordance with ASTM Designation E-112 (see table III). For all three heats, the longitudinal grain size was slightly smaller than the transverse. Heats B and C had the same grain size, and heat A had a slightly smaller grain size.

Grain sizes of the Hastelloy Alloy X samples were estimated using both a comparison procedure (as was the Type 347 stainless steel) and an intercept procedure in accordance with the previously mentioned standard (see table III). Because of the presence of some rather small grains, the estimates made by the comparison procedure tended to overestimate the grain size. Thus, the estimates determined by the intercept method were probably more indicative of the actual average grain size. For the Hastelloy Alloy X, there was no significant variation in grain size as either a function of heat or orientation.

Hardness

Hardness measurements were made by ANSC before heat treatment and by Battelle-Columbus after heat treatment as summarized in table IV. The heat treatment caused a reduction in hardness of the Type 347 stainless steel and

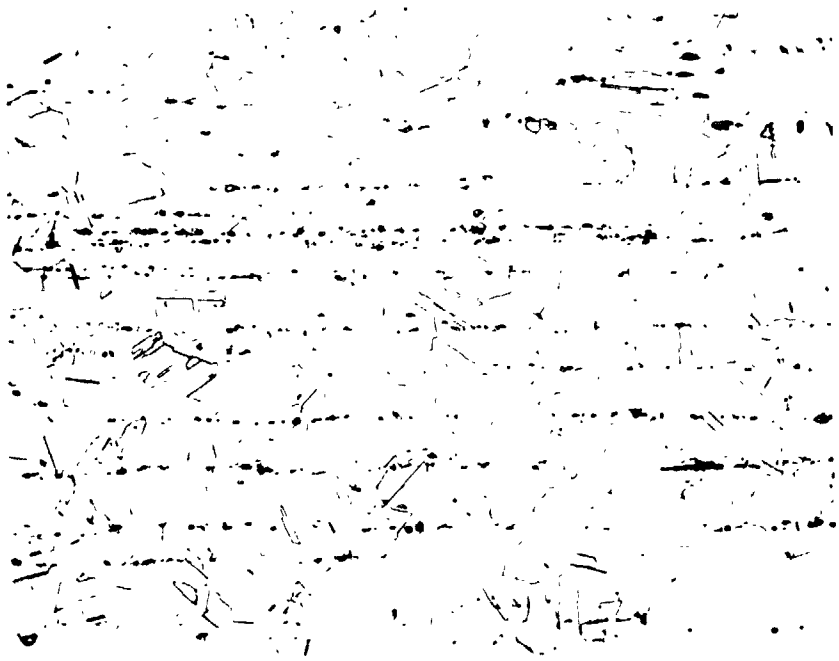

250X 1F051

(a) Longitudinal

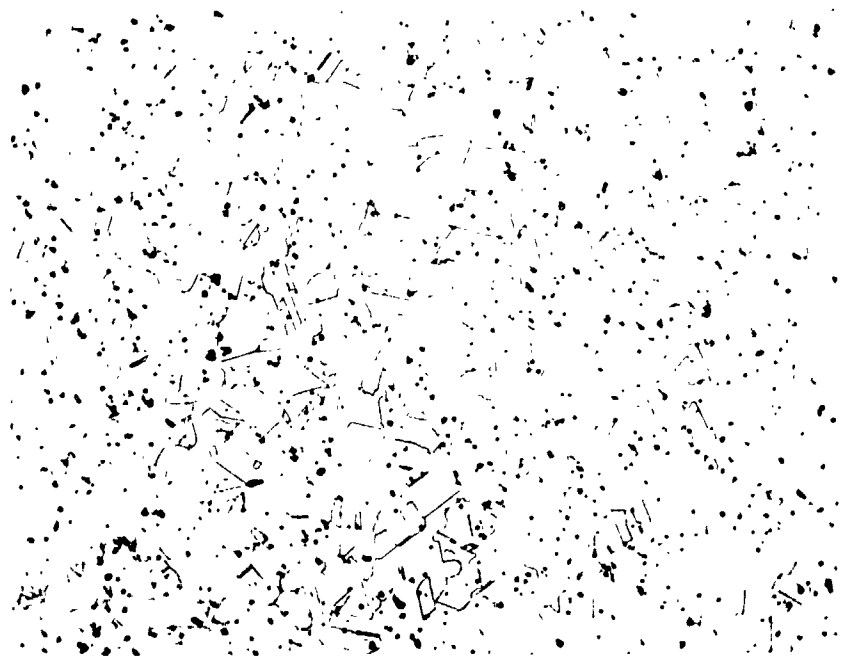

250X 1F050

(b) Transverse

Figure 2.—Microstructure of heat A (X-11585) of Type 347 stainless steel after simulated brazing (samples etched with 30HCl, 10HNO_3 solution).

REPRODUCIBILITY OF THE
ORIGINAL PAGE IS POOR

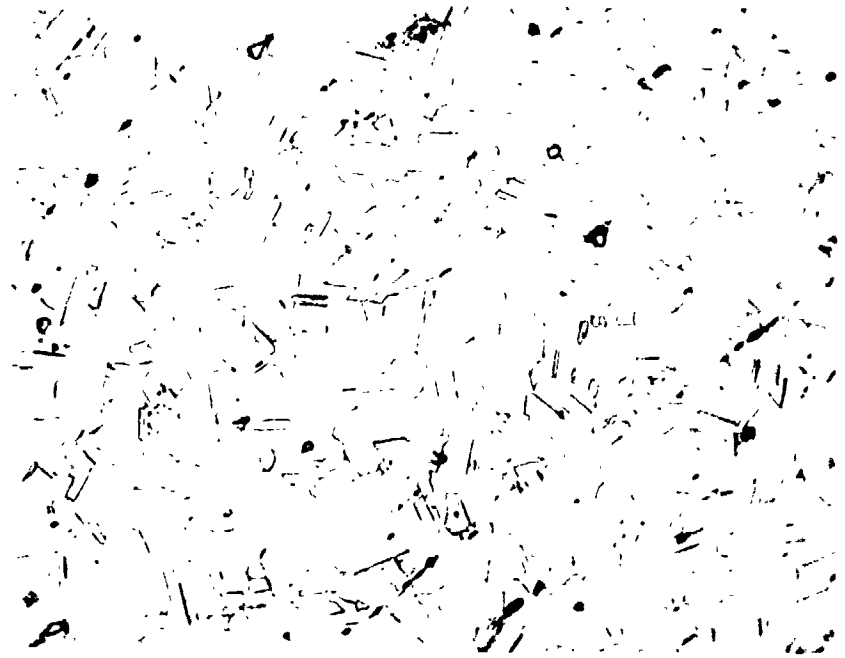

250X 1F053

(a) Longitudinal

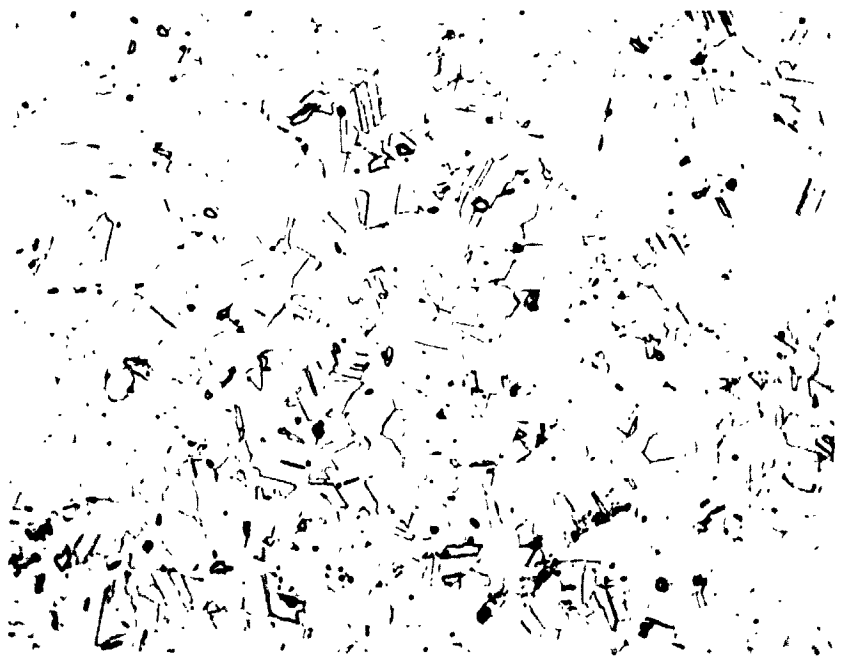

250X 1F052

(b) Transverse

Figure 3. – Microstructure of heat B (G-5617) of Type 347 stainless steel after simulated brazing (samples etched with 30HCl, 10HNO_3 solution).

REPRODUCIBILITY OF THE ORIGINAL PAGE IS POOR

250X 1F055

(a) Longitudinal

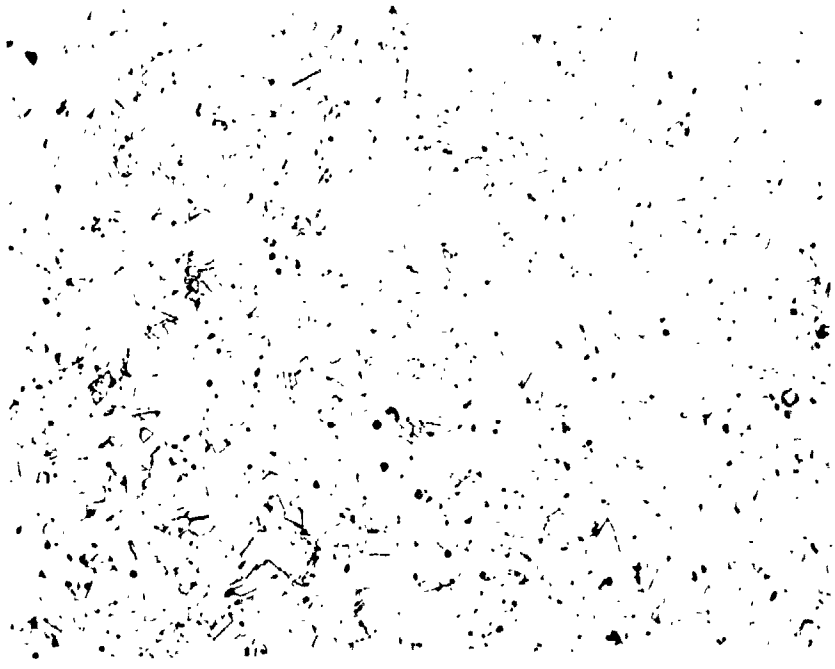

250X 1F054

(b) Transverse

Figure 4. – Microstructure of heat C (G-4943) of Type 347 stainless steel after simulated brazing (samples etched with 30HCl, 10HNO_3 solution).

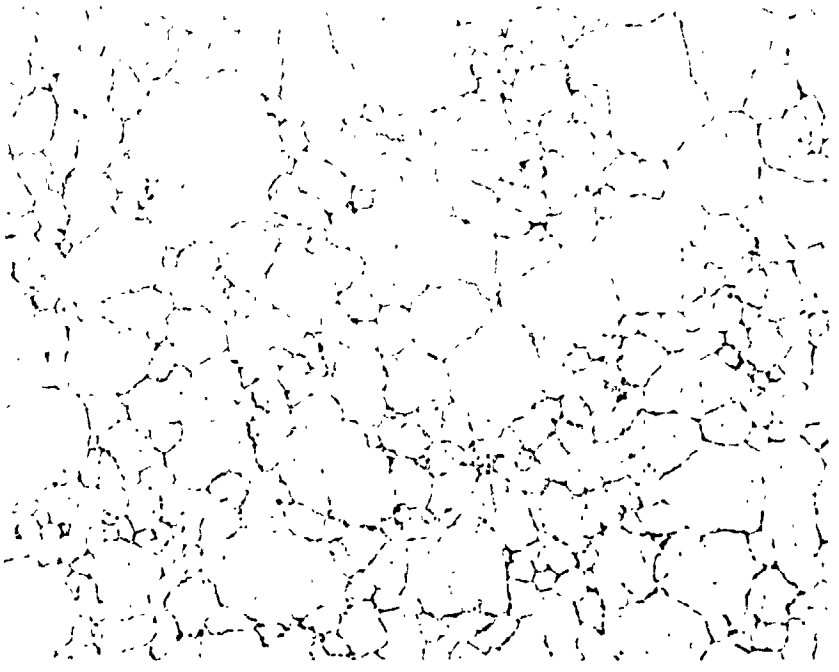

250X 3F281

(a) Longitudinal

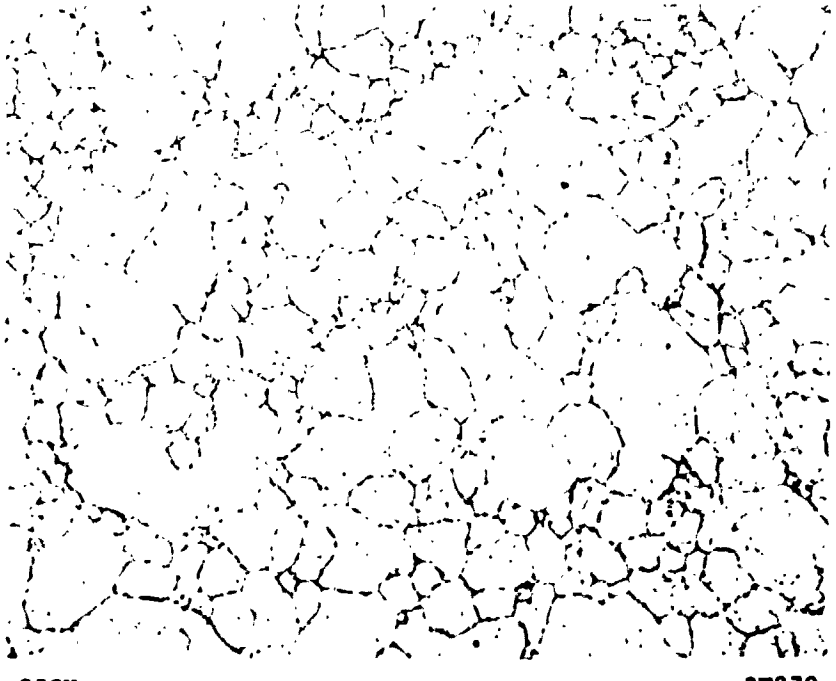

250X 3F279

(b) Transverse

Figure 5. — Microstructure of heat D (2610-0-4007) of Hastelloy Alloy X after simulated brazing (samples etched with aquaregia solution).

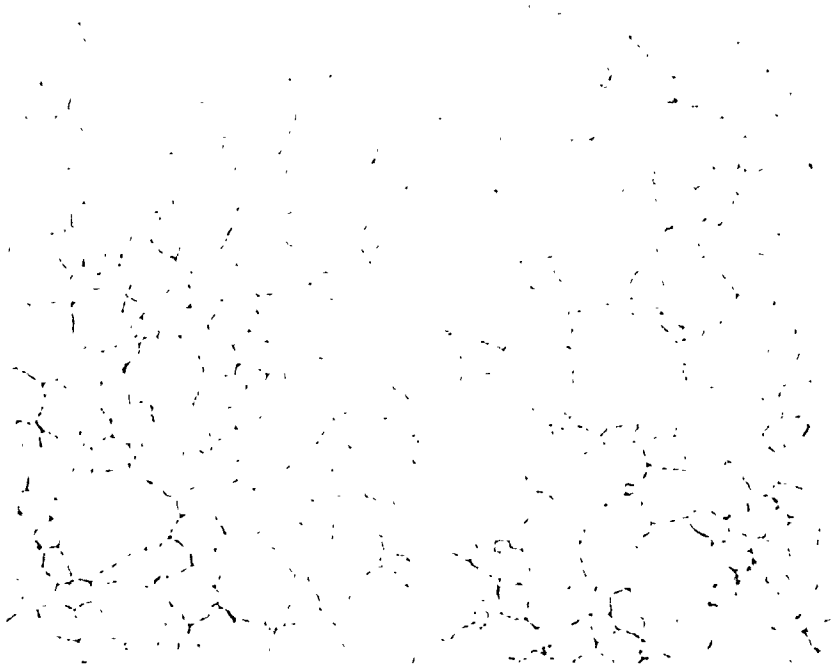

250X 3F282

(a) Longitudinal

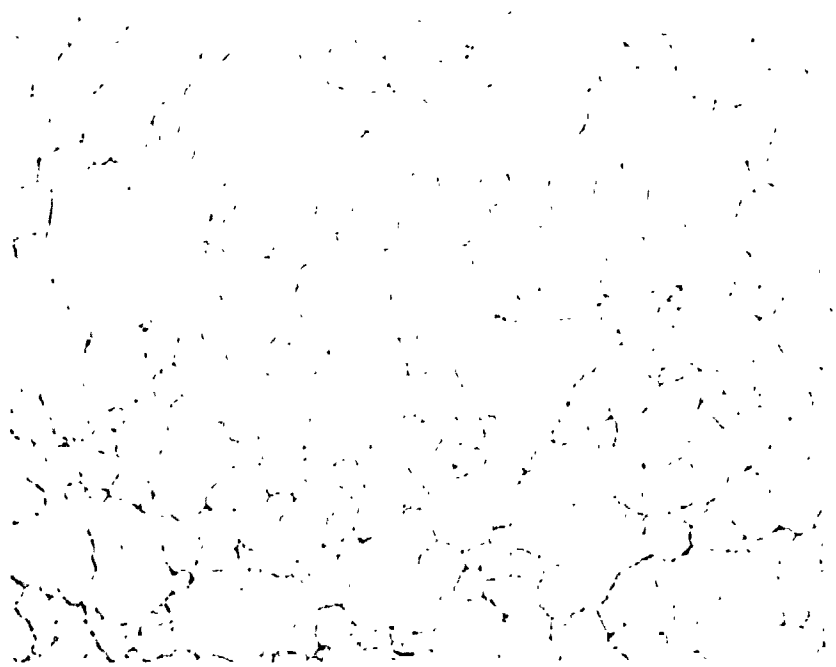

250X 3F280

(b) Transverse

Figure 6. – Microstructure of heat E (2610-0-4008) of Hastelloy Alloy X after simulated brazing (samples etched with aquaregia solution).

TABLE III. – ESTIMATED GRAIN SIZES AFTER HEAT TREATMENT[a]

Specimen letter prefix	ASTM grain size number			
	By comparison procedure		By intercept procedure	
	Longitudinal	Transverse	Longitudinal	Transverse
Type 347 stainless steel				
A	7.5	7	--	--
B	8.5	8	--	--
C	8.5	8	--	--
Hastelloy alloy X				
D	6 to 6.5	6 to 6.5	7.3	7.6
E	6 to 6.5	6 to 6.5	7.9	7.1

[a] In accordance with ASTM Designation: E-112.

TABLE IV. – HARDNESS VALUES

Specimen letter prefix	Hardness numbers[a]	
	Before heat treatment[b]	After heat treatment
Type 347 stainless steel		
A	187 BHN	143 BHN
B	222 BHN	188 BHN
C	231 BHN	149 BHN
Hastelloy alloy X		
D	87 R_B	93 R_B
E	85 R_B	94 R_B

[a] BHN indicates standard Brinell hardness number and R_B indicates Rockwell B hardness number.

[b] Measured by ANSC.

REPRODUCIBILITY OF THE
is Poor

an increase in hardness of the Hastelloy Alloy X. The values for Type 347 stainless steel before heat treatment fell within the range of 170 to 255 Brinell hardness specified for bar stock up to 19.05 mm (0.75 in.) diameter in AMS 5654A, but they were below this range for heats A and C after heat treatment. However, they were still above the minimum Brinell hardness of 140 specified for bar greater than 19.05 mm (0.75 in.) diameter. The values of hardness for Hastelloy Alloy X, both before and after heat treatment, are below the maximum value of 100 Rockwell B (241 Brinell) specified in AMS 5754F. The observed order of magnitude increase in hardness is expected when this alloy is aged at elevated temperatures.

EXPERIMENTAL PROCEDURES

Experimental tasks included specimen preparation, tensile testing in an air environment, and fatigue testing in both hydrogen-gas and air environments. Most fatigue experiments were under continuous cycling conditions; however, a few were performed with compressive strain hold times. Details regarding each of these three areas are described in the following subsections.

Specimen Preparation

Tensile specimens were machined to the configuration shown in figure 7(a) and fatigue specimens were machined to the configuration shown in figure 7(b). The test section of each fatigue specimen was polished with successively finer grades of silicon carbide paper to produce a surface finish of 0.41 μm (16 μin.) rms or better, with finishing marks parallel to the longitudinal axis of the specimen. All specimens were penetrant inspected in accordance with MIL-I-6866, Type I, Method B.

After completing all machining operations, the specimens were degreased with trichlorethylene, followed by reagent acetone. Immediately prior to installation in the test system, the specimens were recleaned with a reagent grade acetone.

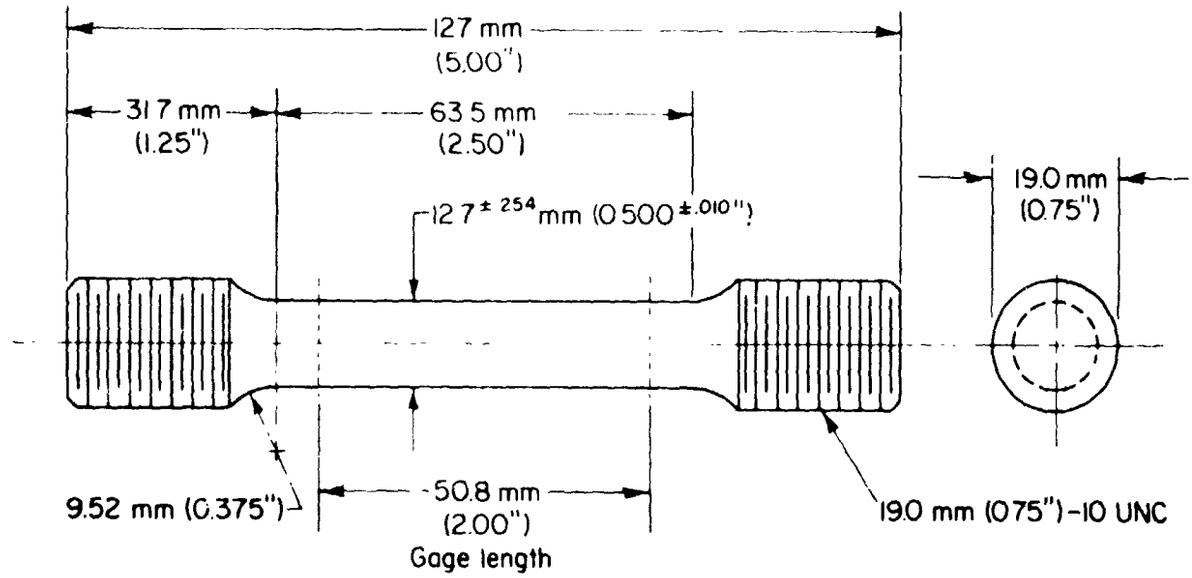

(a) Tensile specimen

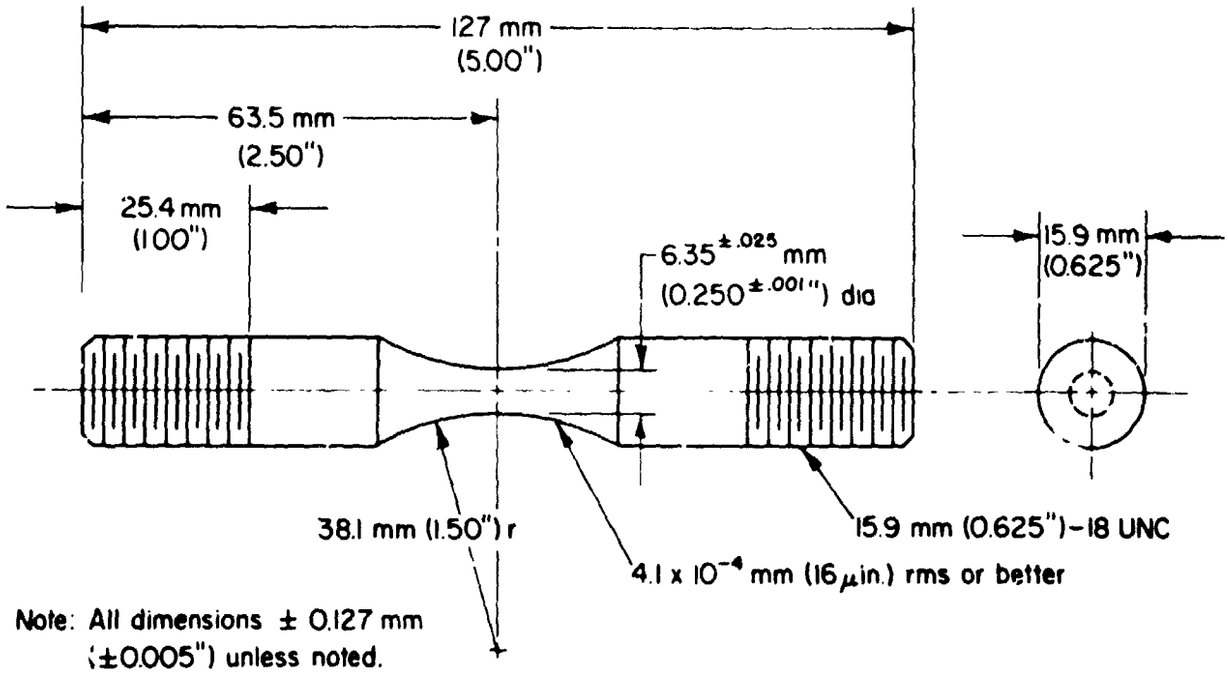

(b) Fatigue specimen

Figure 7. – Specimen configurations.

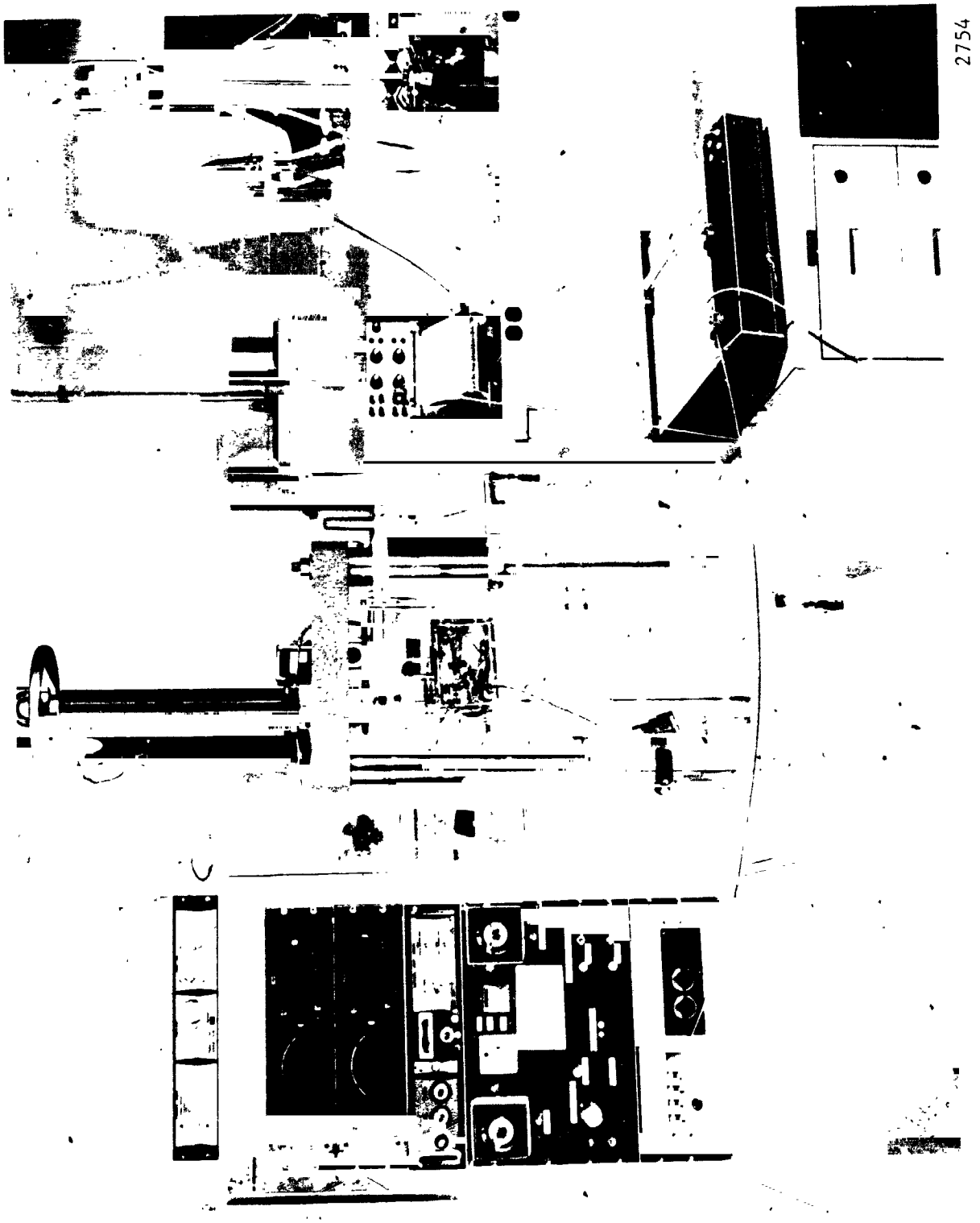

Figure 8. – Closed-loop electrohydraulic fatigue system.

REPRODUCIBILITY OF THE
ORIGINAL PAGE IS POOR

Tensile Testing Apparatus

All of the tensile tests were conducted at a constant strain rate of 0.005 min^{-1} using a standard hydraulic universal testing machine. Specimens were brought up to and held at temperature by an electrical-resistance heating furnace. Room-temperature tests were conducted in accordance with the methods described in ASTM Designation: E8, and elevated-temperature tests were performed in accordance with the procedures of ASTM Designation: E21.

Fatigue Testing Apparatus

For the fatigue experiments, axial load was applied to the specimen using a servocontrolled, electrohydraulic system operated in closed-loop axial strain control (see fig. 8). Diametral changes in the specimen were measured with a special extensometer and load was measured with a strain-gaged load cell in series with the specimens. Diametral strain and load signals were combined and converted to an equivalent axial strain signal using an analog computer (ref. 7).

The extensometer consisted of adjustable sensing arms of high-purity alumina connected to a bracket made with two parallel beams joined by a flexible ligament that acted as an elastic hinge. Diameter changes were mechanically multiplied by a factor of three before they were measured at the other end of the extensometer by a sensitive and magnetically shielded linear variable differential transformer (LVDT). The transformer and armature of the LVDT were mounted on opposite beams and the position of the armature relative to the transformer was adjusted after each test specimen was brought to the desired temperature. The output signal obtained from the LVDT was proportional to the diameter change in the specimen.

Specimens were heated by high-frequency induction, and temperature was controlled with a standard proportional-type power controller. The geometry of the heating coil was designed to minimize temperature gradients in the test section. A specimen instrumented with several thermocouples along the central 12.7 mm (0.50 in.) portion was used to verify this design. Three Chromel-Alumel thermocouples were spot-welded to the surface in the gage section of each specimen. Two of the thermocouples were 4.76 mm (0.188 in.) on one side of the minimum diameter. One of the first two thermocouples provided the feedback signal to the controller. The other two were used to make minor adjustments in the coil position and obtain a uniform temperature profile along the specimen.

Specimens were gripped using a fixture arrangement similar to that described by Feltner and Mitchell (ref. 8). The lower end of the specimen was threaded into an adapter attached to the load cell which was, in turn, attached to the hydraulic actuator. The upper end of the specimen was attached to the loadframe crosshead through a Wood's metal type liquid-solid grip (ref. 9). Both the upper and lower adapters were continuously water cooled to avoid overheating of the fixtures.

Continuous Strain-Controlled Cycling.—For the continuous cycling experiments, the computed axial strains (from the analog computer) were programmed to follow a fully compressive triangular waveform [see fig. 9(a)] with a constant axial strain rate of 10^{-3} sec^{-1}. Because of large inelastic deformation in the two alloys at the total strain ranges and temperatures used in this study, the corresponding stress cycles were essentially fully reversed as illustrated in figure 9(b). Calibration of the equipment was in accordance with MIL-C-45662.

During each fatigue test, load was continuously recorded using a time-base strip chart recorder. These records were used to obtain hardening behavior and information on when cracking occurred just prior to specimen failure. Load-axial strain hysteresis loops (e.g., see fig. 10) were periodically recorded during each test using an X-Y recorder. These loops were used to obtain values of total, inelastic, and elastic strain range. For a symmetrical continuous cycle, the value of $\Delta\sigma_{r-} = 0$ and $\Delta\epsilon_{ei} = \Delta\epsilon_{ed}$.

Compressive Hold-Time Strain Cycling.—The same equipment was used for the compressive hold-time experiments as was used for the continuous cycling ones, except for the addition of timers which were used to closely control the time intervals during which the desired strain levels were maintained. The timers were calibrated with a stop watch and had a repeat accuracy of 0.2 percent or ± 7.2 seconds.

The cyclic compressive axial strain waveform with compressive hold times is illustrated in figure 11(a), and the corresponding stress response for the alloy-temperature-strain range conditions of this study is shown in figure 11(b). As also indicated in figure 11(b), such a hold time at elevated temperature will result in appreciable compressive stress relaxation as a direct result of inelastic flow. The effect of this inelastic flow on stress-strain response is i lustrated in figure 10.

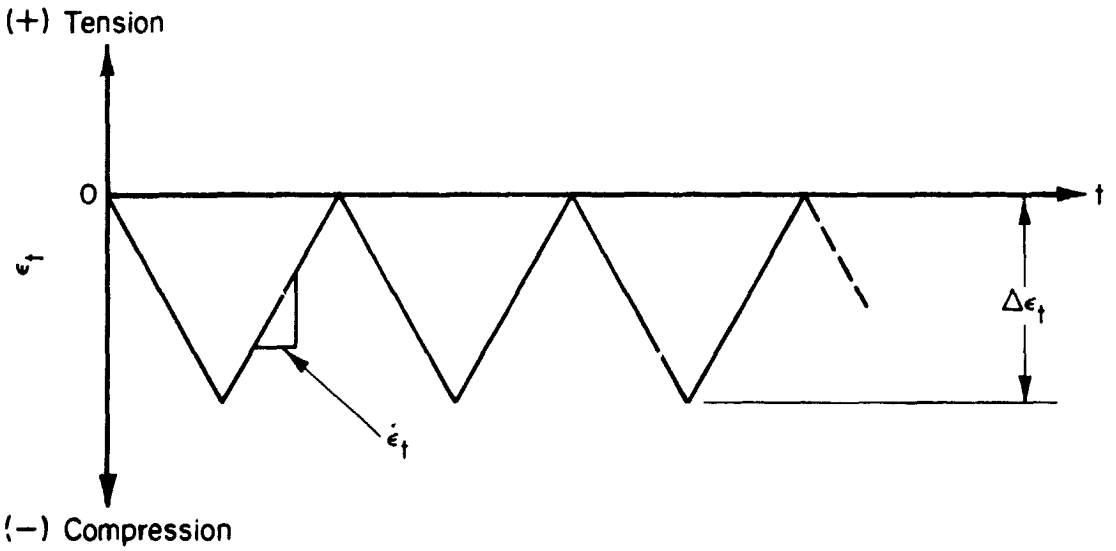

(a) Compression strain-cycling waveform

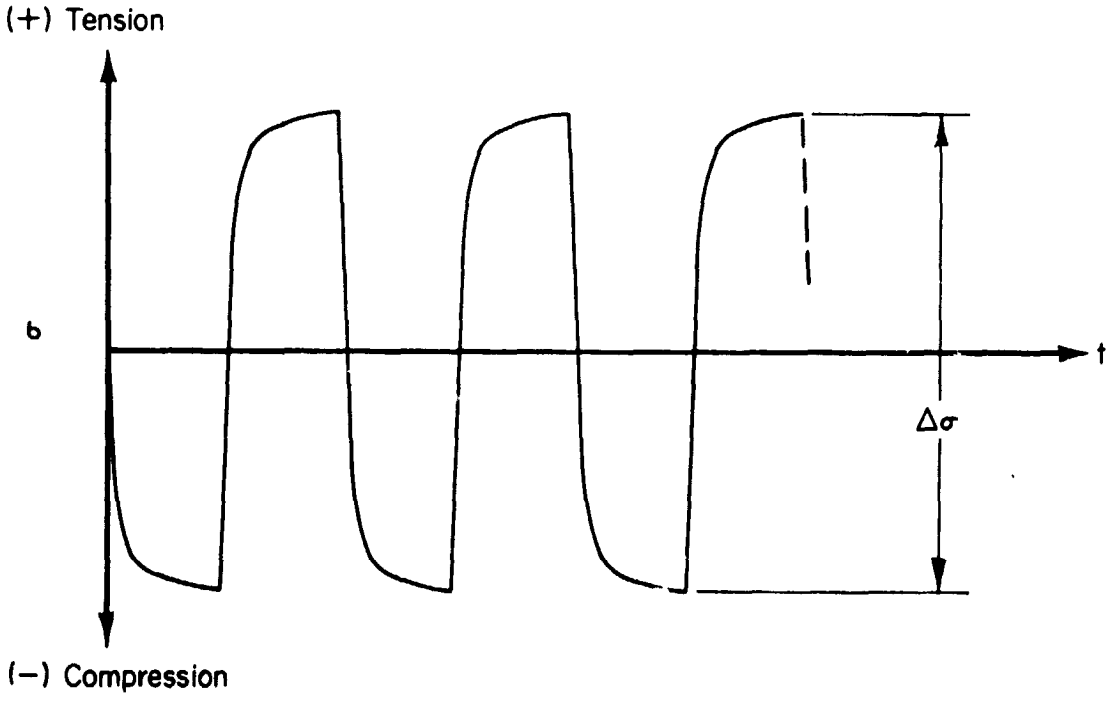

(b) Cyclic stress waveform

Figure 9. – Waveforms of axial strain and stress for continuous cycling.

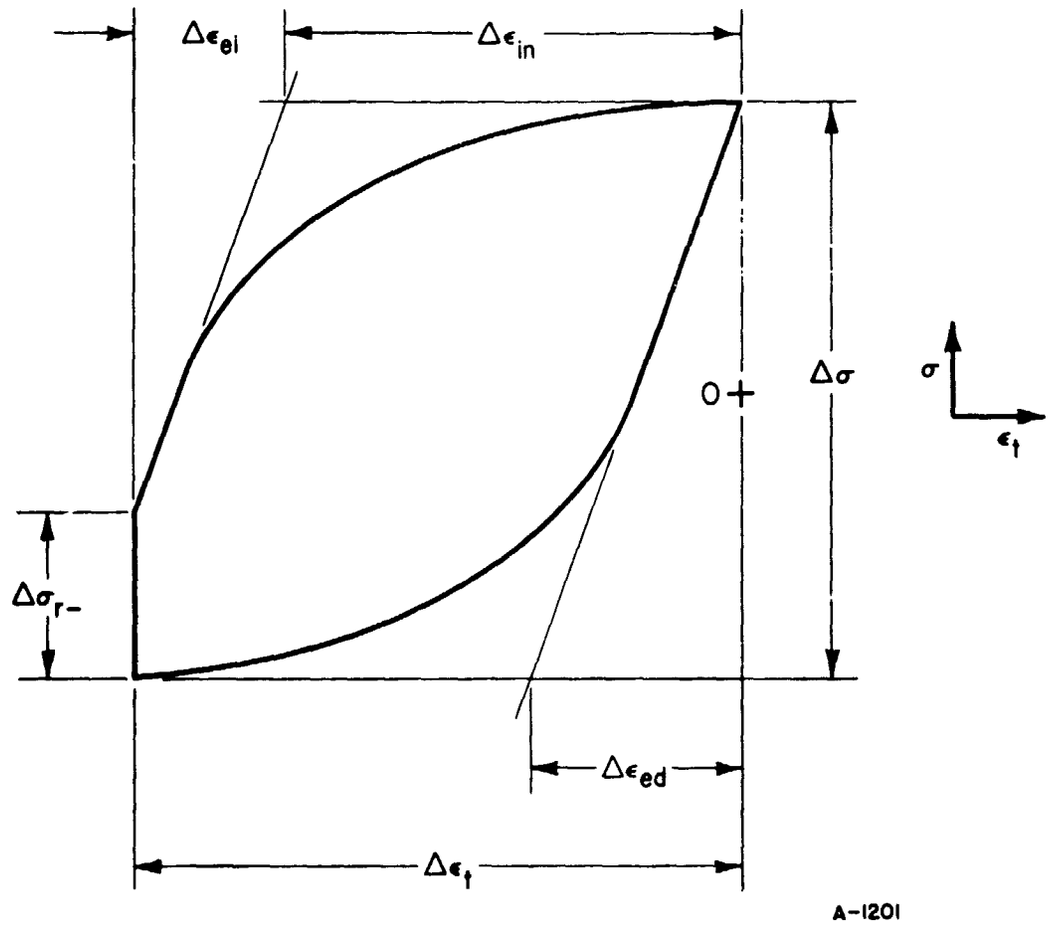

Figure 10. – Illustration of hysteresis loop for strain cycle with hold time at peak compressive strain.

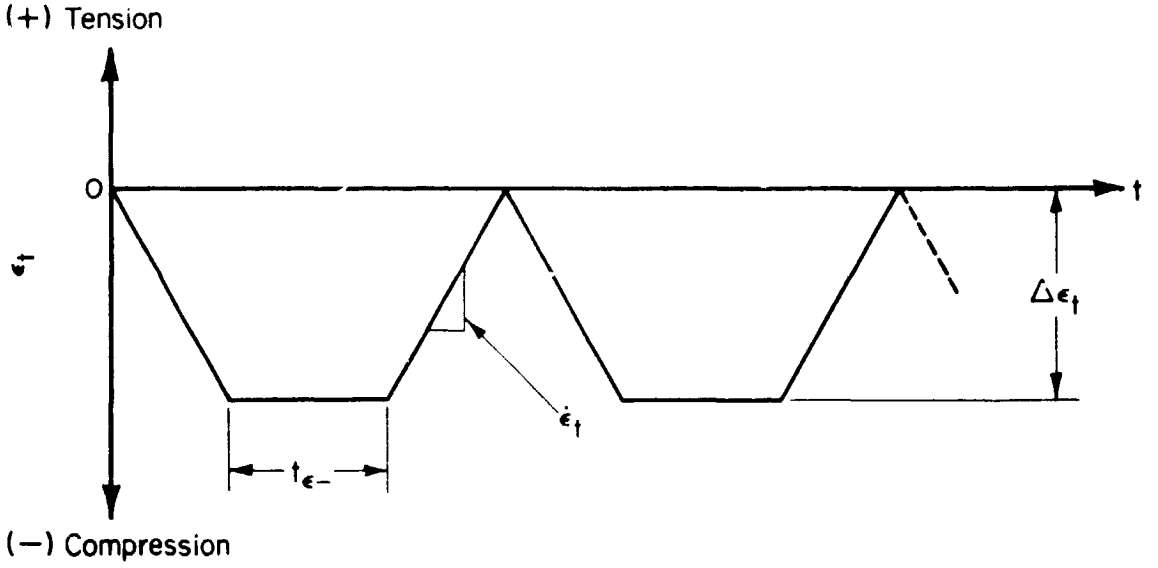

(a) Compression strain-cycling waveform with maximum strain hold time

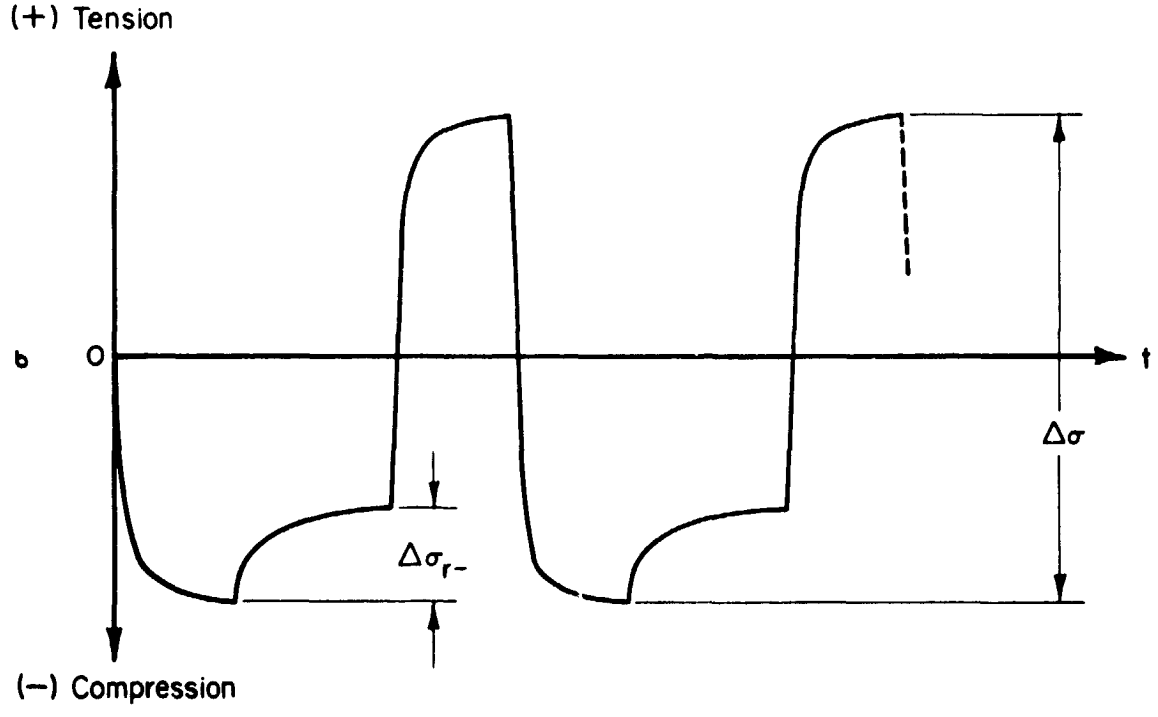

(b) Cyclic stress waveform

Figure 11. – Cyclic waveforms of axial strain and stress for compression strain hold-time tests

Hydrogen Gas Environment.—The high-purity hydrogen gas environment was obtained by use of a palladium alloy diffusion process. Commercial high-purity hydrogen (better than 99.95 percent) was supplied to a palladium catalyst purifier (Englehard Industries, Model HPD 20-150) which was capable of delivering 0.56 cubic meters (20 cubic feet) per hour of ultrapure hydrogen (i.e., the extent to which contaminants are present in the gas is not measurable by any known means of detection). The test chamber, as shown in figure 12, was constructed of acrylic plastic sheet. It was sealed at the lower specimen grip by an "O" ring arrangement and sealed at the upper grip by a bellows. The chamber was first purged for 20 to 30 minutes with nitrogen. The high-purity hydrogen was then permitted to flow into the purged environment for approximately the same period of time before the induction heating of the specimen began. A flow of between 0.14 and 0.28 cubic meters (5 and 10 cubic feet) per hour was maintained throughout the experiment, which amounted to roughly 8 to 16 volume changes of the hydrogen environment per hour. A gage pressure of at least 6.9 kN/m^2 (1 psi) was maintained inside the chamber, and the gas which egressed from the chamber was burnt at a remote point.

Laboratory Air Environment.—The air within the laboratory was maintained at $20 \pm 1^{\circ}C$ ($70 \pm 2^{\circ}F$) and at 50 ± 5 percent relative humidity. When tests were conducted in air, the chamber described above was not used and the specimens were heated by the same induction heating method.

Fatigue Data Acquisition

Since an hourglass-type specimen [previously shown in fig. 7(b)] was used for the fatigue experiments, it was necessary to measure diametral rather than axial strain. Because axial strain was the desired control variable, the diametral strain was converted to axial strain; this was done by determining the elastic and plastic components of diametral strain and relating them to the same components of axial strain, which could then be summed to give total axial strain. The equations necessary for computations of axial strain and the analog circuits required for such computations have been described in detail by Slot, et al (ref. 7).

Figure 12. – Hydrogen test chamber with specimen installed.

REPRODUCED
ORIGINAL

To complete the computations, electric analogs of diametral strain and applied load were supplied as inputs, and the values of elastic Poisson's ratio and the specimen compliance constant were programmed in the computer. The inelastic Poisson's ratio was assumed to be constant at a value of 0.5 (assuming constant-volume, inelastic deformation of an isotropic material).

The value of elastic Poisson's ratio was determined in the laboratory for each specimen. This was done by placing the specimen in the test fixture, applying the desired temperature and environment, and then cycling the specimen briefly in load control under low loads within the range of elastic material response. While the specimen was being cycled in this manner, the analog specimen compliance was adjusted to reduce the apparent plastic strain to zero. The elastic Poisson's ratio was then determined from the equation

$$\nu_e = - \frac{\Delta\varepsilon_{de} A_T E}{\Delta P} \quad , \tag{1}$$

where the values of $\Delta\varepsilon_{de}$ and ΔP were determined from the slope of the load versus diametral extension X-Y plot recorded during load cycling. The modulus of elasticity values at temperatures up to 760°C (1400°F) were taken from data tabulated later in this report. Values of E used for the tests at 871°C (1600°F) were 134 GN/m^2 (19.5 x 10^3 ksi) for Hastelloy Alloy X and 128 GN/m^2 (18.6 x 10^3 ksi) for Type 347 stainless steel. These values were taken from reference 10.

Values of the cyclically stable elastic and inelastic strain range were obtained from the stable load versus axial extension hysteresis loops (see figs. 13 through 15) near half the fatigue life ($N_f/2$). Strain values were calculated by dividing the appropriate value of the extension by the gage length (minimum specimen diameter at the test temperature). Figures 13 through 15 show representative hysteresis loops for the materials used in the program. The hysteresis loops shown for the beginning of the test illustrate the tendency of the material to harden due to cyclic straining. The other loops shown are typical of a stable hysteresis loop (or as near to stability as possible) for the corresponding conditions and material.

In addition to the recording of the load versus axial extension behavior, continuous cyclic load-time histories were recorded for every test. Representative samples of the load histories during the early cycles are presented in figures 16 through 18. These strip charts correspond to the displayed hysteresis loops described above. Examination of these charts reveals the materials'

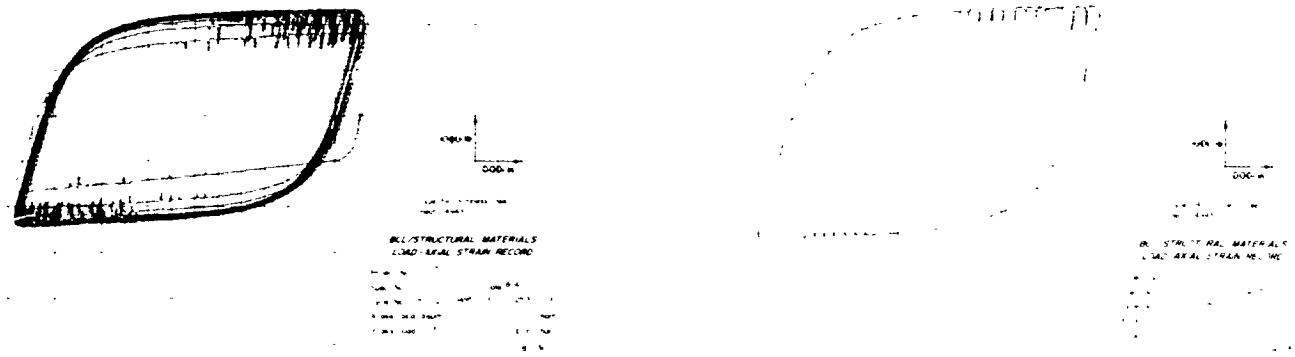

(a) Type 347 stainless steel, $\Delta\epsilon_t$ = 2.95 percent

(b) Hastelloy X, $\Delta\epsilon_t$ = 2.95 percent

Figure 13. – Load-axial displacement hysteresis loops for Type 347 stainless steel and Hastelloy Alloy X at 538° C (1000° F).

REPRODUCTIBILITY OF THE ORIGINAL PAGE IS POOR

(a) Type 347 stainless steel, $\Delta\varepsilon_t$ = 2.96 percent

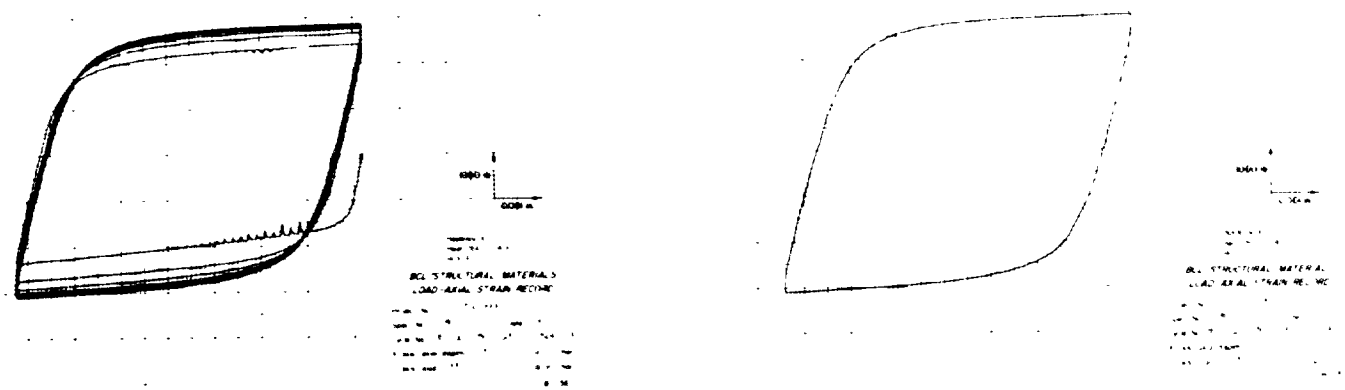

(b) Hastelloy X, $\Delta\varepsilon_t$ = 2.96 percent

Figure 14. – Load-axial displacement hysteresis loops for Type 347 stainless steel and Hastelloy Alloy X at 760°C (1400°F).

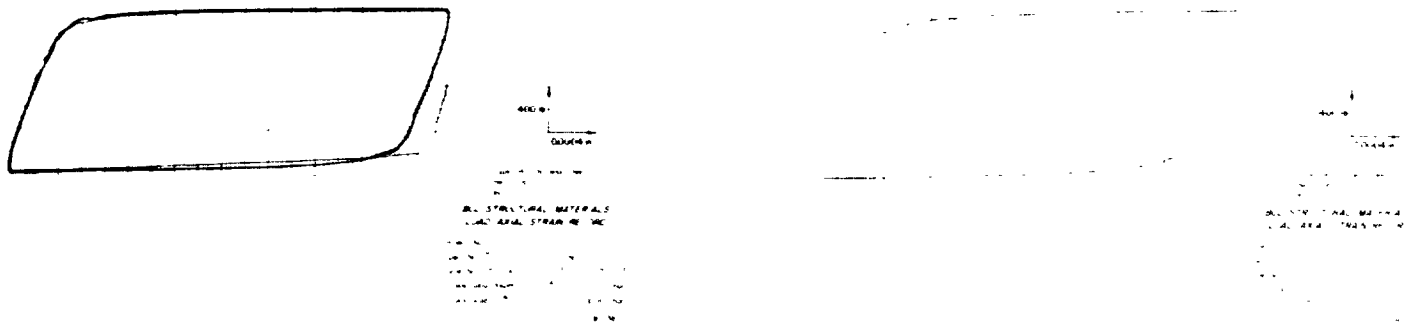

(a) Type 347 stainless steel, $\Delta\varepsilon_t$ = 1.51 percent

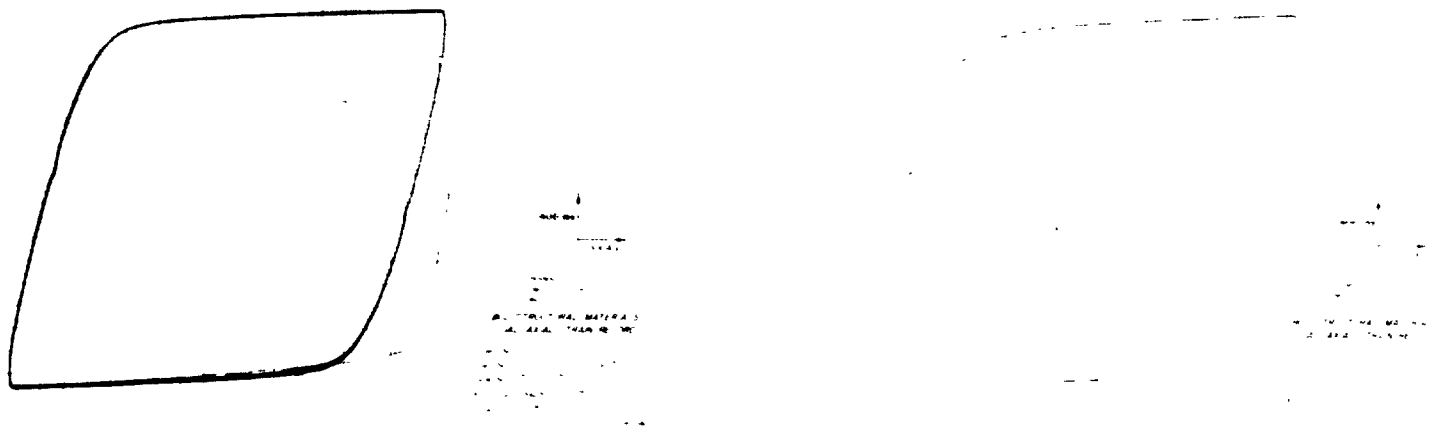

(b) Hastelloy Alloy X, $\Delta\varepsilon_t$ = 1.91 percent

Figure 15. – Load-axial displacement hysteresis loops for Type 347 stainless steel and Hastelloy Alloy X at 871° C (1600° F).

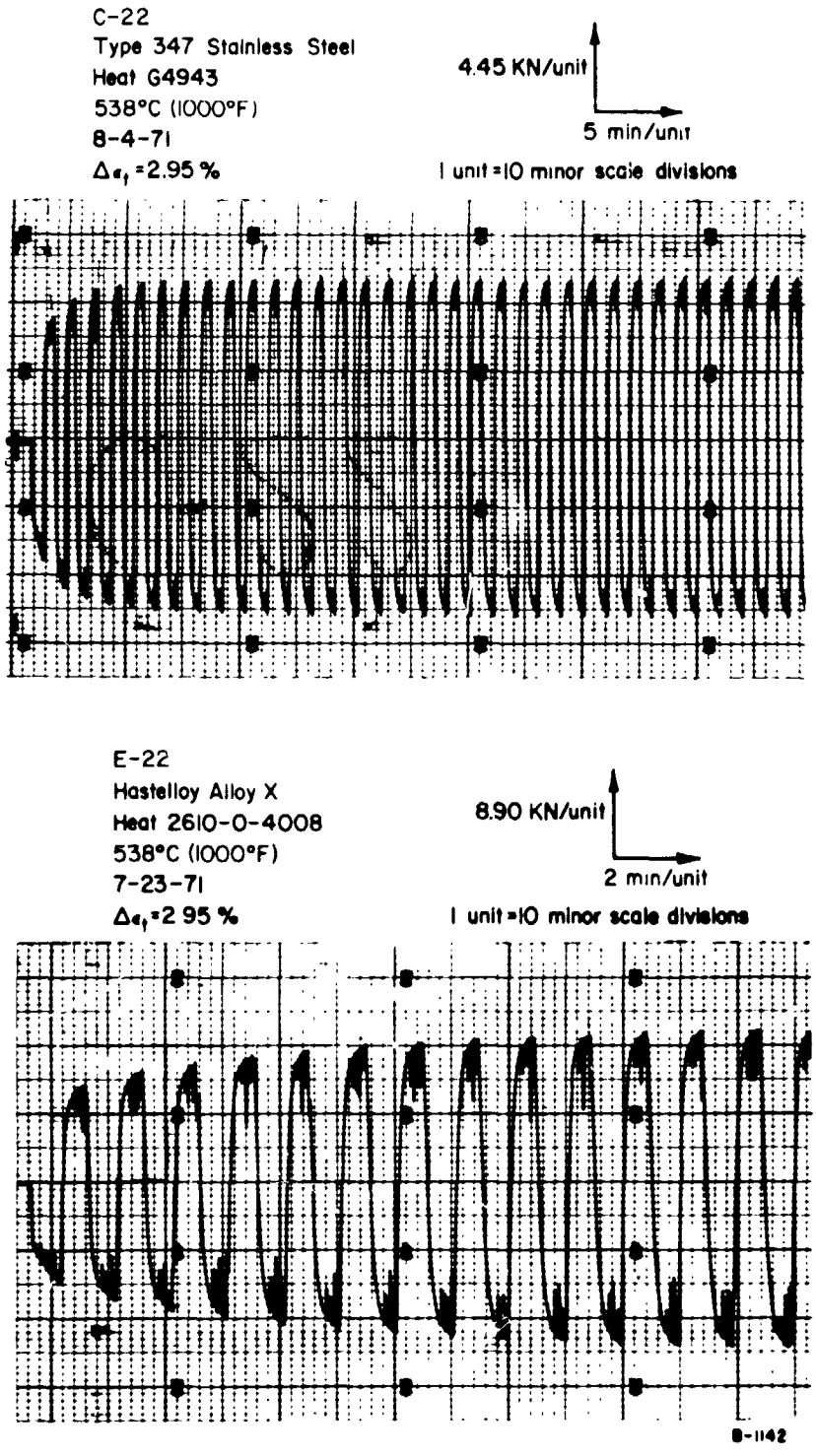

Figure 16. – Load-time histories of Type 347 stainless steel and Hastelloy Alloy X at 538° C (1000° F).

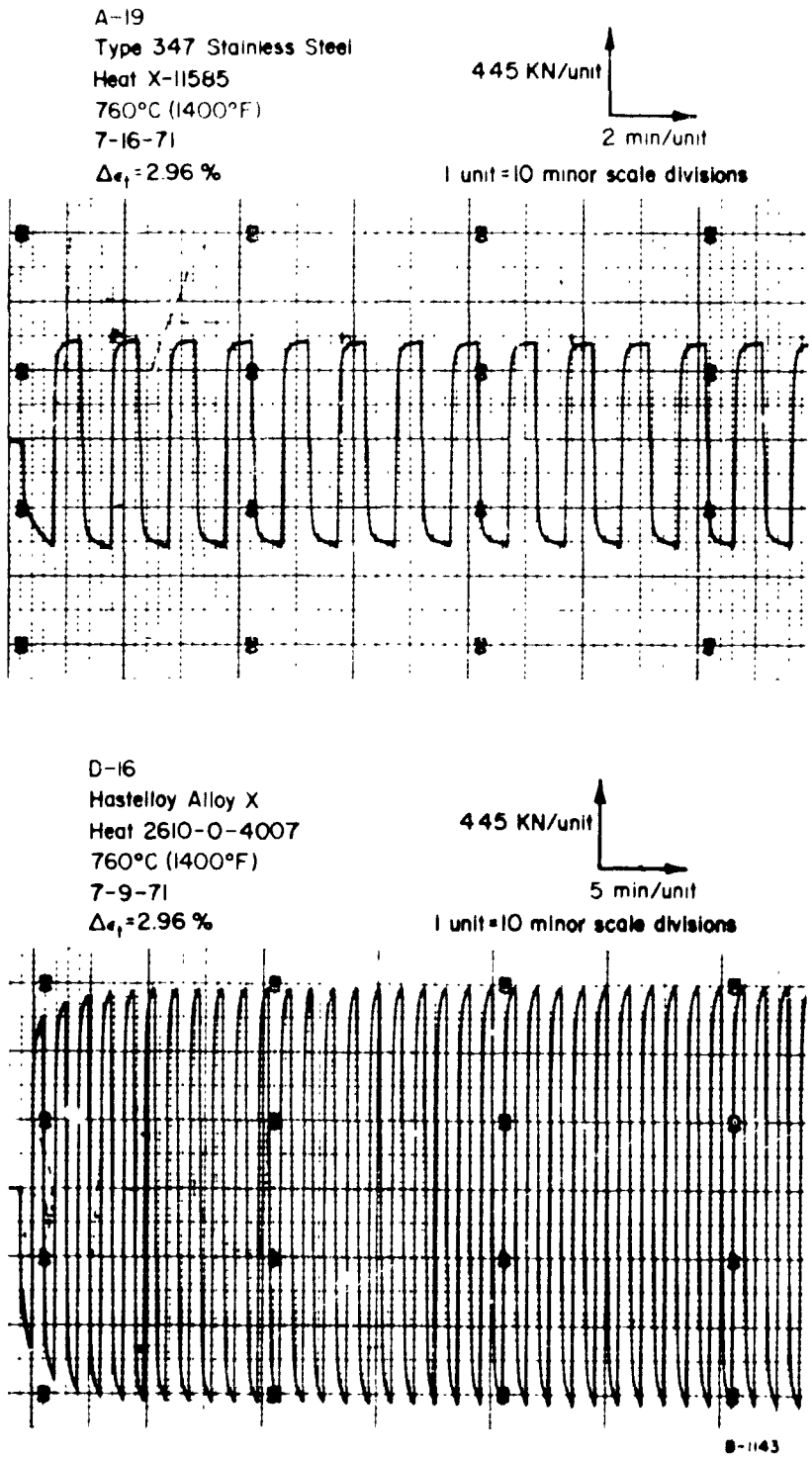

Figure 17. – Load-time histories of Type 347 stainless steel and Hastelloy Alloy X at 760°C (1400°F).

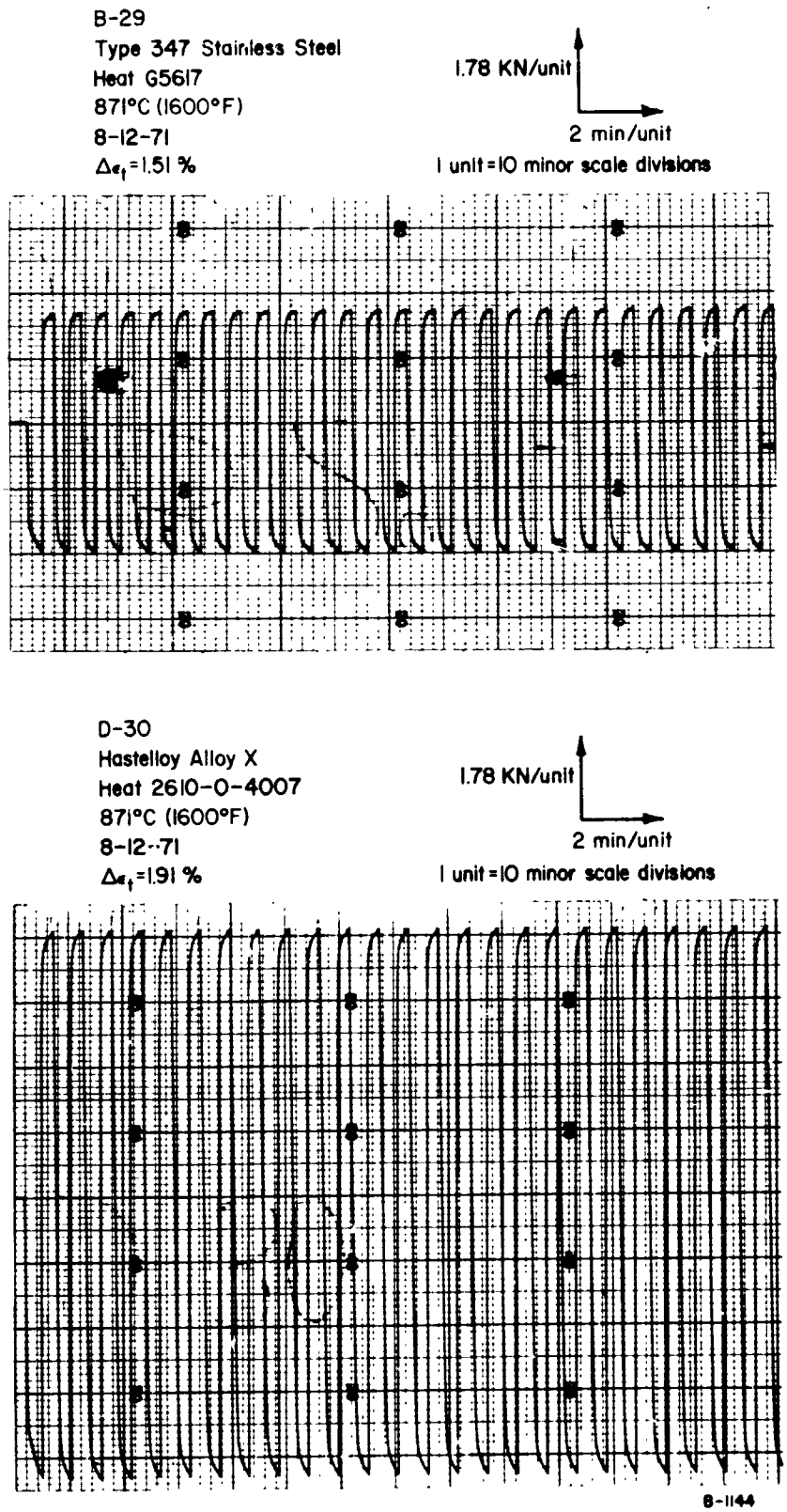

Figure 18. – Load-time histories of Type 347 stainless steel and Hastelloy Alloy X at 871°C (1600°F).

REPRODUCIBILITY OF THE
ORIGINAL PAGE IS POOR

changing resistance to load as a function of strain cycles. The value of the stress at stability was determined from the load-time histories by reading the value of the load at $N_f/2$ and then dividing this value by the area of the specimen at the test temperature.

The load versus time histories were also used to determine the fatigue life of each specimen as defined by the following terms:

N_o = number of cycles where tension load started to drop off just before complete fracture occurred

N_5 = number of cycles where tension load dropped off 5 percent just before complete fracture occurred

N_f = number of cycles to complete fracture.

EXPERIMENTAL RESULTS AND DISCUSSION

The experimental results developed in this program fell into four areas — (1) tensile properties in air, (2) cyclic stress-strain response in air and hydrogen gas, (3) fatigue resistance in air and hydrogen gas, and (4) fractographic and limited metallographic studies of Type 347 stainless steel fatigue-cycled in hydrogen gas at 760°C (1400°F). The tensile properties [area (1)] of all 5 heats of material were determined at 21, 538, 649, and 760°C (70, 1000, 1200, and 1400°F). Cyclic stress-strain response and fatigue resistance [areas (2) and (3)] were evaluated for all 5 heats in both hydrogen gas and air under continuous cycling at total axial strain ranges of about 1.5, 3, and 5 percent and at temperatures of 538, 760, and 871°C (1000, 1400, and 1600°F). Additional continuous cycling experiments were conducted on heat A of Type 347 stainless steel in hydrogen gas at temperatures of 593, 649, and 704°C (1100, 1200, and 1300°F) with a total axial strain range of about 3 percent and at 649°C (1200°F) with a total axial strain range of about 1.5 percent. Fatigue experiments at a total strain range of about 3 percent and with 10-minute compressive hold periods were performed on heat A of Type 347 stainless steel and on heat D of Hastelloy Alloy X in hydrogen gas at 760 and 871°C (1400 and 1600°F). The same type of hold-time experiments were also conducted on heat A at total axial strain ranges of about 1.5 and 5 percent at 760°C (1400°F). Comparative fractographic studies were made of specimens from heat A continuous cycling (no-hold) versus hold-time experiments at total axial strain ranges of about 1.5, 3.0, and 5.0 percent in hydrogen gas at 760°C (1400°F). One specimen from each type of experiment at 1.5 percent strain range was then metallographically examined. Each of the four above areas are discussed separately in the ensuing subsections of this report.

Tensile Properties

The room- and elevated-temperature tensile properties determined in this program are presented in tables V and VI. Table V contains data obtained from the Type 347 stainless steel specimens; at room temperature, data were obtained both before and after heat treatment as listed. Table VI presents data from tests of Hastelloy Alloy X; data before and after heat treatment were obtained at both room temperature and 649°C (1200°F). The tables are arranged to show the results of each test and an average value for all the tests at a given temperature. An overall comparison of the effect of temperature on the tensile properties of Type 347 stainless steel and Hastelloy Alloy X is shown in figure 19.

As can be seen from table V and from figure 19(a), the heat treatment significantly lowered the room temperature yield strength of the Type 347 stainless steel. Also, it slightly lowered the ultimate strength and slightly increased the reduction of area. These trends indicate that prior cold work was annealed out during heat treatment. As seen from table VI and figure 19(a), the heat treatment had little effect on room temperature tensile strength of Hastelloy Alloy X. However, at 649°C (1200°F), the ultimate strength was lowered by the heat treatment, although yield strength was unaffected. In general, the ultimate and yield strength values after heat treatment were close to or just slightly lower than normally expected for both alloys. The lower values were related to the fact that the alloys were subjected to the simulated brazing heat treatment. The influence of temperature on the above-mentioned strength properties was close to that usually seen for these alloys.

The fracture ductility (as measured by both elongation and reduction of area) of both alloys was close to the typical values at room temperature [see fig. 19(b)]. At 538°C (1000°F), the ductility of Type 347 stainless steel dropped slightly below the value recorded for room temperature; at 649°C (1200°F), it was about the same as the value at room temperature; and at 760°C (1400°F), it was a little higher than normal for this alloy. The Hastelloy Alloy X had much higher than normal ductility at 649° and 760°C (1200° and 1400°F), while its ductility at 538°C (1000°F) was similar to that at room temperature. This high fracture ductility was related to the heat treatment. The typical values in figure 19(b) are for solution-treated material. It is normally expected that aging by exposure at elevated temperatures, such as done in the simulated brazing operation, will improve the high-temperature tensile ductility of Hastelloy Alloy X (ref. 6). Also, note that the heat treatment increased tensile ductility at 649°C (1200°F).

TABLE V. — TENSILE PROPERTIES OF TYPE 347 STAINLESS STEEL AT A STRAIN RATE OF 0.005 MIN^{-1}

Temperature, °C (°F)	Vendor heat number	Specimen	Modulus of elasticity		0.2 percent offset yield strength		Ultimate strength		Elongation in 2 inches, percent	Reduction of area, percent	True fracture ductility
			GN/m^2	ksi	MN/m^2	ksi	MN/m^2	ksi			
Before simulated brazing heat treatment[a]											
21 (70)	X-11585	---	---	---	396	57.5	655	95.0	45	66	1.09
	G5617	---	---	---	517	75.0	703	102	39	67	1.10
	G4943	---	---	---	503	73.0	696	101	37	66	1.11
	Average		---	---	472	68.5	685	99.3	40	66	1.10
After simulated brazing heat treatment											
21 (70)	X-11585	AT1	170	24,700	224	32.5	609	88.3	54	71	1.24
	X-11585	AT2	176	25,500	216	31.3	600	87.0	53	71	1.22
	G5617	BT5	167	24,200	219	31.7	604	87.6	54	72	1.26
	G5617	BT6	172	24,900	216	31.3	608	88.2	56	72	1.26
	G4943	CT9	159	23,000	232	33.7	607	88.0	52	72	1.28
	G4943	CT10	157	22,800	230	33.3	607	88.0	52	72	1.27
	Average		167	24,200	223	32.3	[illegible]5	87.8	53	72	1.25
538 (1000)	X-11585	AT13	148	21,500	134	19.5	393	57.0	36	64	1.03
	G5617	BT15	--	--	136	19.7	387	56.2	37	66	1.09
	G4943	CT17	170	24,600	139	20.1	383	55.5	36	65	1.05
	Average		159	23,000	137	19.8	387	56.2	36	65	1.06
649 (1200)	X-11585	AT14	157	22,800	130	18.8	310	45.0	46	72	1.26
	G5617	BT16	143	20,700	133	19.3	299	43.3	51	74	1.35
	G4943	CT18	172	25,000	132	19.1	301	43.7	49	72	1.27
	Average		157	22,800	132	19.1	303	44.0	49	73	1.29
760 (1400)	X-11585	AT3	155	22,500	112	16.3	199	28.9	59	82	1.69
	X-11585	AT4	137	19,800	115	16.7	197	28.6	58	81	1.64
	G5617	BT7	142	20,600	110	16.0	188	27.3	63	86	1.97
	G5617	BT8	119	17,200	110	15.9	187	27.1	64	86	1.93
	G4943	CT11	121	17,600	116	16.8	179	26.0	66	87	2.00
	G4943	CT12	130	18,800	115	16.7	181	26.3	66	87	2.00
	Average		134	19,400	113	16.4	189	27.4	63	85	1.87

[a]Reported by ANSC.

TABLE VI. – TENSILE PROPERTIES OF HASTELLOY ALLOY X AT A STRAIN RATE OF 0.005 MIN^{-1}

Temperature, °C	Temperature, (°F)	Vendor heat number	Specimen	Modulus of elasticity		0.2 percent offset yield strength		Ultimate strength		Elongation in 2 inches, percent	Reduction of area, percent	True fracture ductility
				GN/m^2	ksi	MN/m^2	ksi	MN/m^2	ksi			
Before simulated brazing heat treatment[a]												
21	(70)	2610-0-4007	--	--	--	363	52.6	793	115	38	60	0.93
		2610-0-4008	--	--	--	367	52.3	793	115	41	64	1.03
		Average		--	--	365	52.4	793	115	39	62	0.98
649	(1200)	2610-0-4007	--	--	--	259	37.6	625	90.7	40	54	0.77
		2610-0-4008	--	--	--	264	38.3	627	90.9	42	55	0.79
		Average		--	--	261	37.9	626	90.8	41	54	0.78
After simulated brazing heat treatment												
21	(70)	2610-0-4007	DT1	181	26,300	356	51.7	793	115	42	52	0.73
		2610-0-4007	DT2	220	31,900	345	50.0	786	114	42	52	0.74
		2610-0-4008	ET5	199	28,900	349	50.6	793	115	42	52	0.73
		2610-0-4008	ET6	207	30,000	346	50.2	793	115	42	51	0.72
		Average		202	29,300	349	50.6	793	115	42	52	0.73
538	(1000)	2610-0-4007	DT9	181	26,300	261	37.8	665	96.5	42	51	0.71
		2610-0-4008	ET11	196	28,500	261	37.8	672	97.4	41	52	0.74
		Average		189	27,400	261	37.8	668	96.9	41	51	0.72
649	(1200)	2610-0-4007	DT10	163	23,600	257	37.3	576	83.5	59	72	1.27
		2610-0-4008	ET12	168	24,300	245	35.6	585	84.8	54	61	0.98
		Average		165	23,900	252	36.5	580	84.1	57	67	1.12
760	(1400)	2610-0-4007	DT3	141	20,400	226	32.8	365	52.9	84	86	1.97
		2610-0-4007	DT4	139	20,200	228	33.0	380	55.1	102	90	2.24
		2610-0-4008	ET7	153	22,200	224	32.5	393	57.0	82	75	1.37
		2610-0-4008	ET8	153	22,200	228	33.0	390	56.5	78	77	1.46
		Average		146	21,200	226	32.8	382	55.4	87	82	1.76

[a]Reported by Tackett (ref. 6).

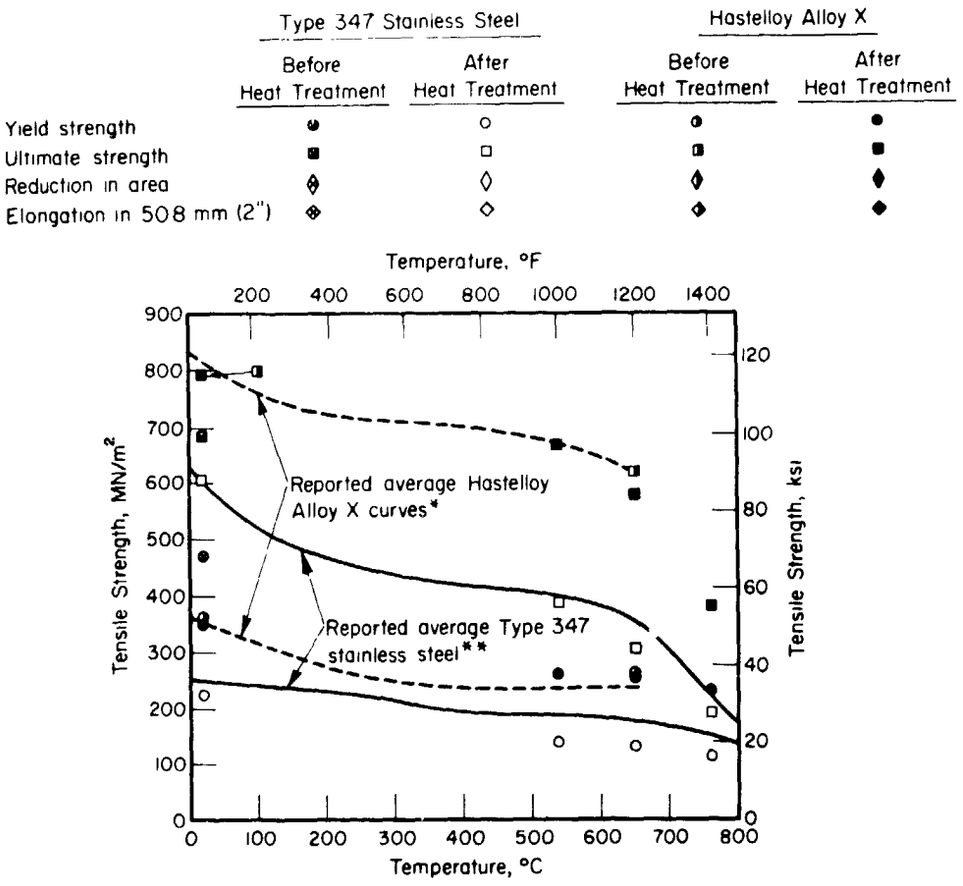

(a) Strength properties.

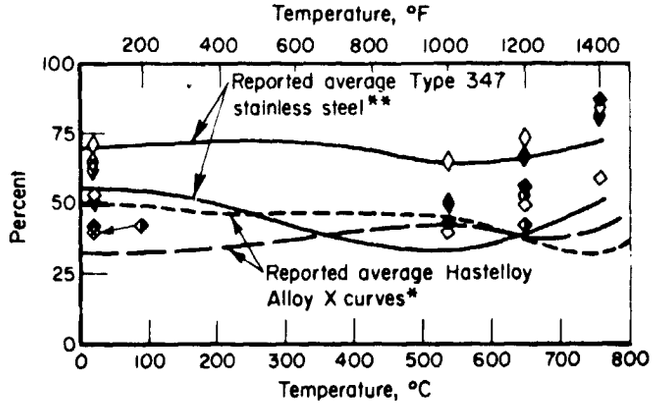

(b) Ductility properties.

Figure 19. – Effect of temperatures on average material properties of Type 347 stainless steel and Hastelloy Alloy X.

* Data from ref. 10 (Vol. II., p 264).
** Data from ref. 10 (Vol. I-A, p 191).

Stress-strain curves from the tensile tests are presented in figures 20 and 21. All curves, except those for Hastelloy Alloy X at 538°C (1000°F) [see figure 21(b)] and Type 347 stainless steel at 538° and 649°C (1000° and 1200°F) [see figures 20(b) and 20(c)], are average curves for the conditions indicated. The tensile stress-strain curves were combined where duplicate tests of the same heat exhibited little variation. For Type 347 stainless steel at 649°C (1200°F), the curves [see figure 20(c)] were not combined because at this temperature tensile tests were not duplicated within each heat. Both materials exhibited some instability in stress-strain response at 538°C (100C°F). This instability is defined as large decreases and increases in stress for small increases in strain in the inelastic deformation regime of the material (serrated flow). The 538°C (1000°F) curve for Hastelloy Alloy X [see figure 21(b)] was from one specimen to show this type of stress-strain behavior. Both specimens (DT9 and DT11) gave similar curves until yielding started to occur. Figure 20(b) shows the same type of material instability for Type 347 stainless steel (the curves from all three of the specimens — AT13, BT15, and CT17 — are shown because they differed too much to be combined).

Cyclic Stress-Strain Response

The stress response of Type 347 stainless steel and Hastelloy Alloy X was evaluated at temperatures ranging from 538°C (1000°F) to 871°C (1600°F) under both continuous strain cycling and strain cycling with 10-minute compressive hold times. The majority of experiments were conducted in a purified hydrogen gas environment, but a selected number of specimens were also evaluated in a laboratory air environment.

Continuous Cycling.—Figures 22 through 24 illustrate representative stress amplitude material response for continuous cycling tests conducted in hydrogen gas. Figures 22(a) and (b) show the substantial cyclic hardening which occurred for Type 347 stainless steel and Hastelloy Alloy X, respectively, at 538°C (1000°F). At this temperature, both materials hardened regardless of strain range; however, Hastelloy Alloy X hardened considerably more than Type 347 stainless steel.

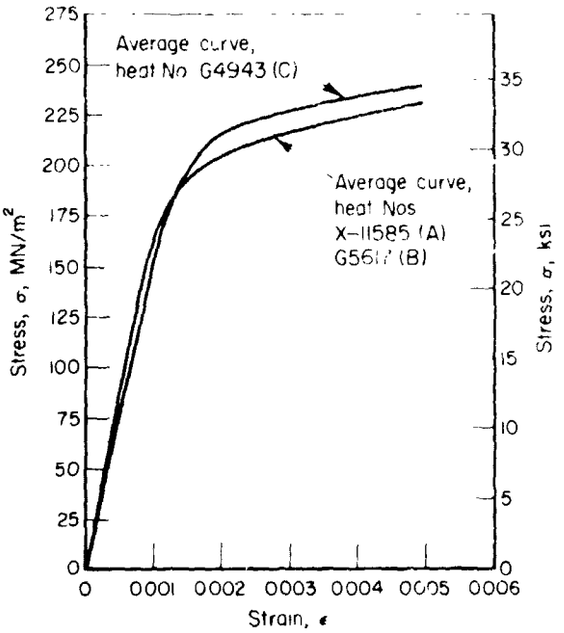

(a) Room temperature, 21°C (70°F).

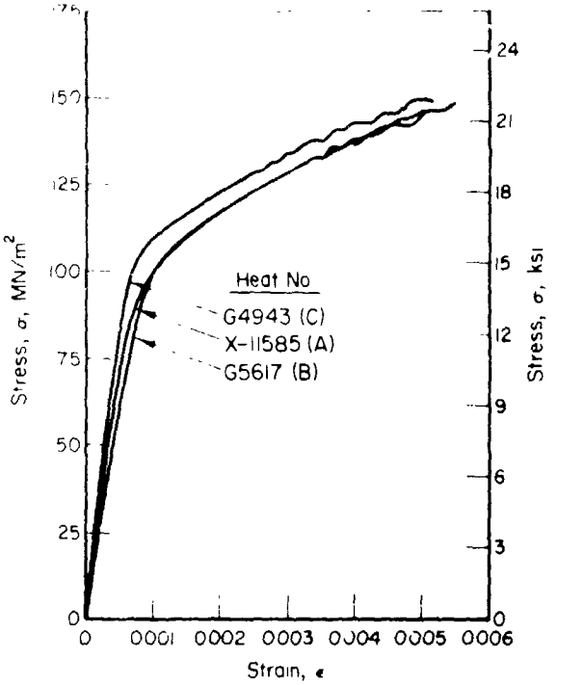

(b) 538°C (1000°F).

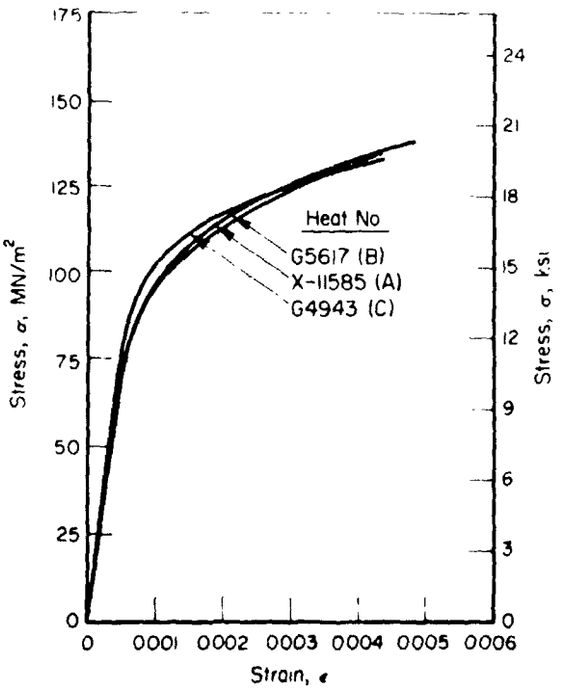

(c) 649°C (1200°F).

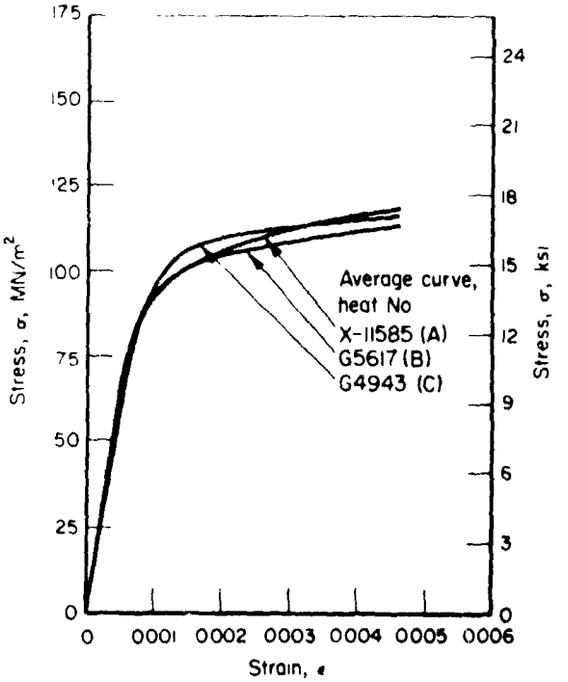

(d) 760°C (1400°F).

Figure 20. – Monotonic stress-strain curves for Type 347 stainless steel.

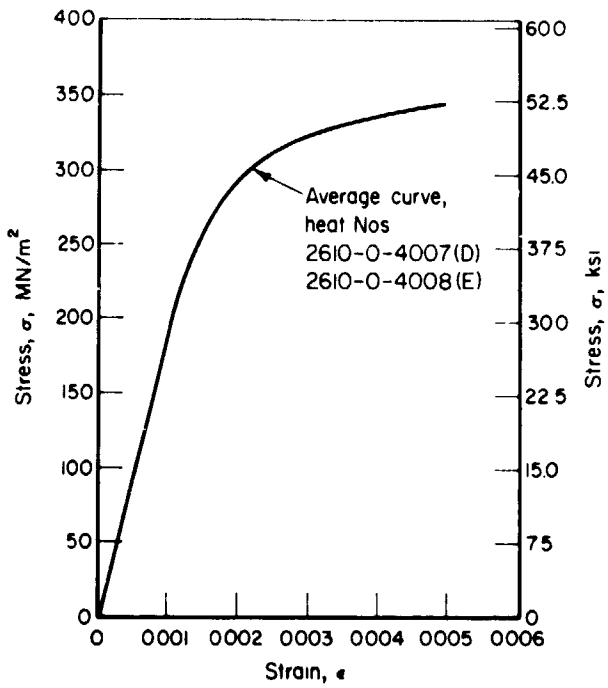

(a) Room temperature, 21°C (70°F).

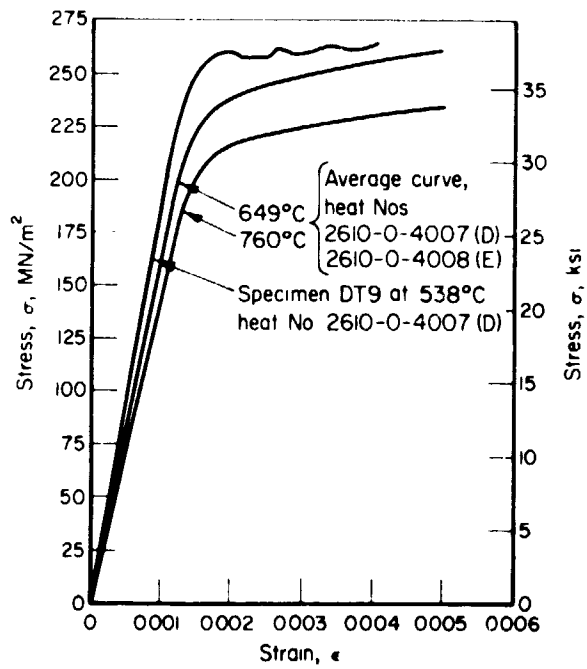

(b) 538°, 649°, and 760°C (1000°, 1200°, and 1400°F).

Figure 21. – Monotonic stress-strain curves for Hastelloy Alloy X.

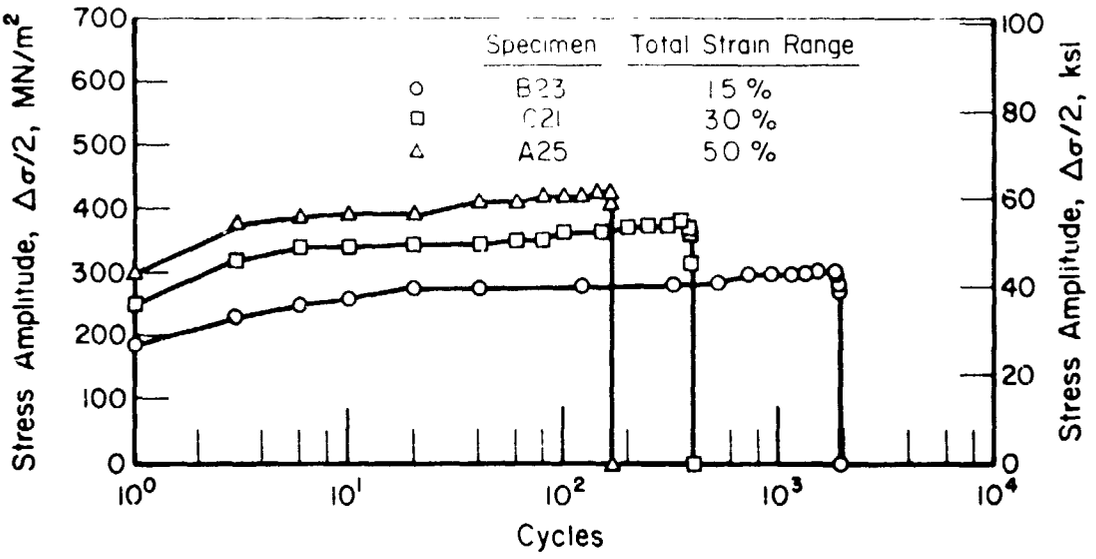

(a) Type 347 stainless steel.

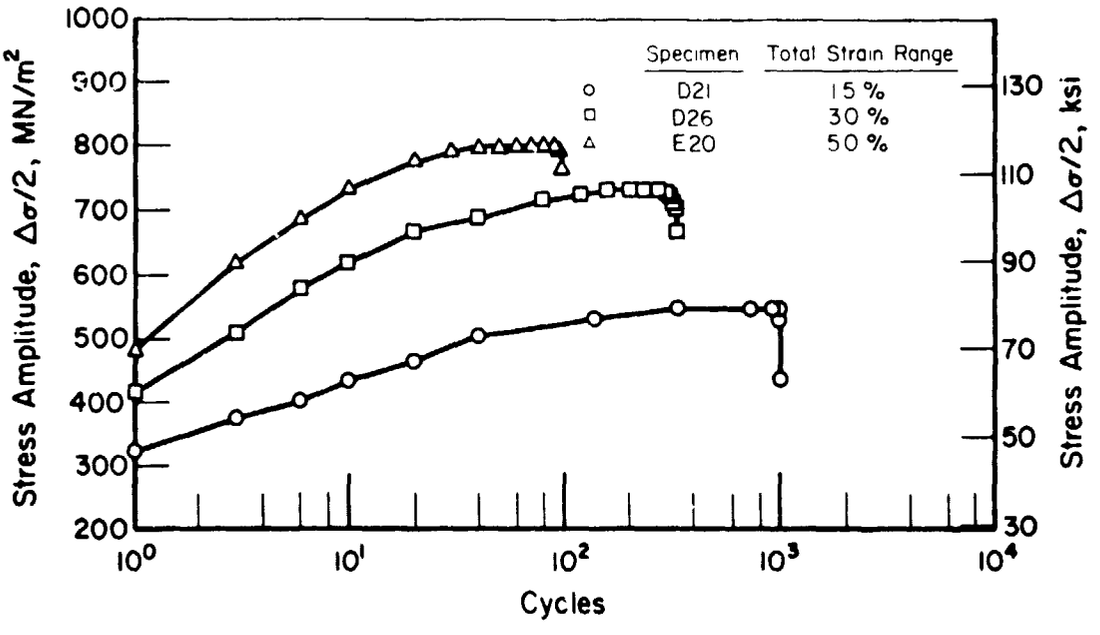

(b) Hastelloy Alloy X.

Figure 22. – Stress amplitude versus fatigue cycles for Type 347 stainless steel and Hastelloy Alloy X in hydrogen gas at 538°C (1000°F).

REPRODUCIBILITY OF THE
ORIGINAL PAGE IS POOR

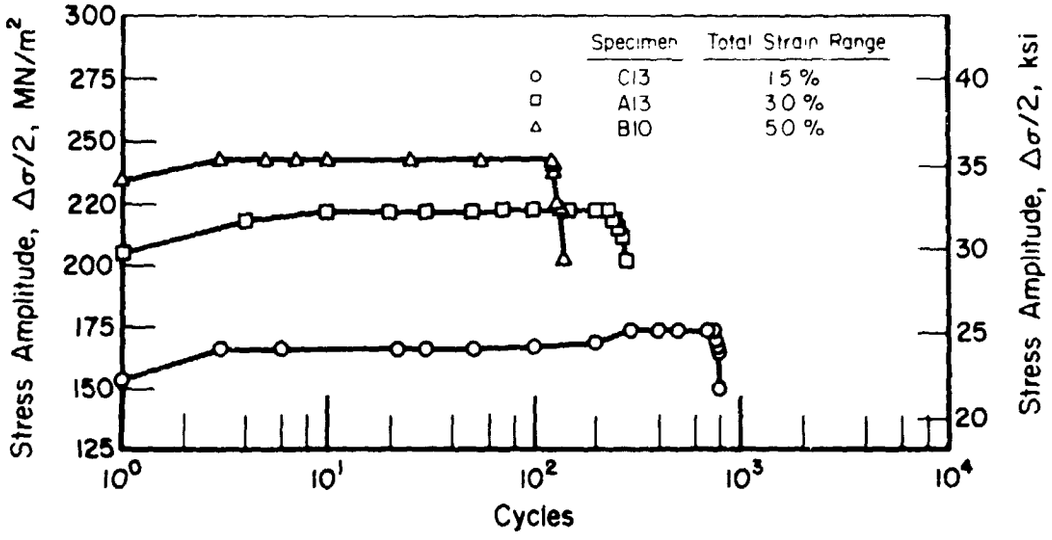

(a) Type 347 stainless steel.

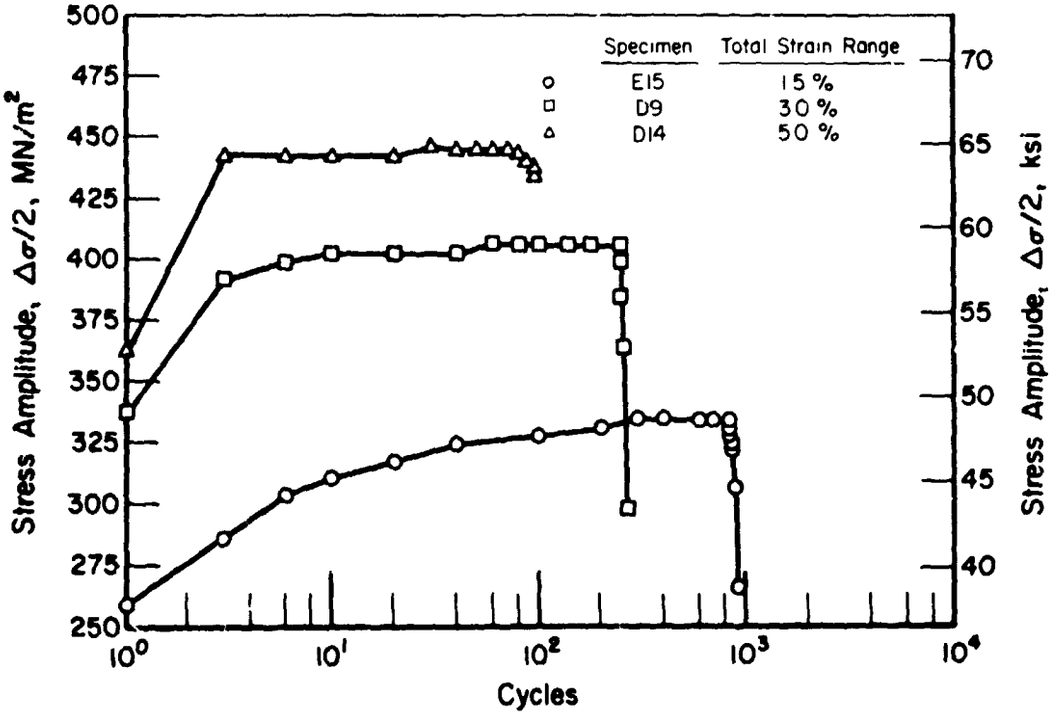

(b) Hastelloy Alloy X.

Figure 23. – Stress amplitude versus fatigue cycles for Type 347 stainless steel and Hastelloy Alloy X in hydrogen gas at 760°C (1400°F).

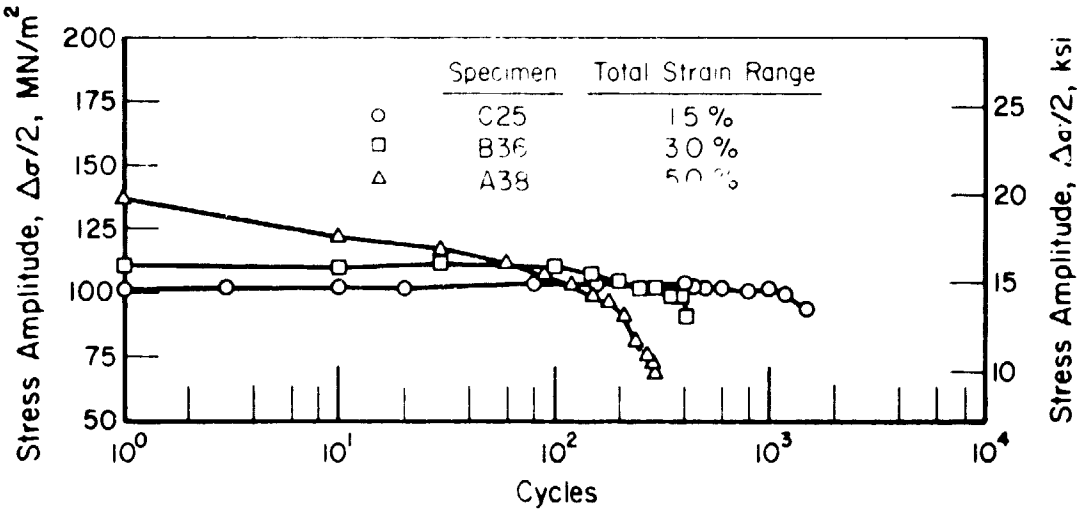

(a) Type 347 stainless steel.

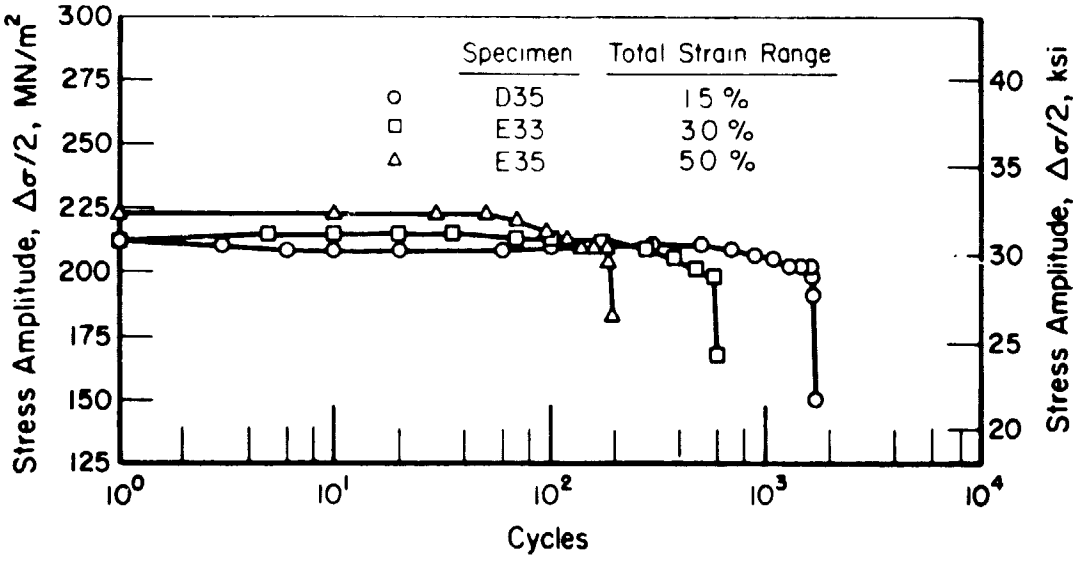

(b) Hastelloy Alloy X.

Figure 24. – Stress amplitude versus fatigue cycles for Type 347 stainless steel and Hastelloy Alloy X in hydrogen gas at 871°C (1600°F).

At 760°C (1400°F), as shown in figures 23(a) and 23(b), the stainless steel showed only a slight tendency to cyclically harden, while Hastelloy Alloy X still cyclically hardened. Figure 23(a) also shows that Hastelloy Alloy X hardened very rapidly at the 5.0 percent total axial strain range, but very gradually at the 1.5 percent strain range.

Figures 24(a) and 24(b) show that neither material cyclically hardened at 871°C (1600°F). The Type 347 stainless steel displayed relatively constant stress response at the 1.5 and 3.0 percent strain ranges; however, at the 5.0 percent axial strain level, the material cyclically softened. Hastelloy Alloy X displayed almost constant stress response for this temperature at all three strain ranges.

The overall effect of temperature on the continuous cycling stress response of Type 347 stainless steel and Hastelloy Alloy X for the intermediate total axial strain range of 3.0 percent is shown in figures 25(a) and (b). Experiments completed at six temperatures ranging from 538°C (1000°F) to 871°C (1600°F) are shown for the Type 347 stainless steel material in figure 25(a). A continuous decline in the amount of cyclic hardening and maximum stable stress was apparent for increasing temperatures. The same general behavior also evident for the Hastelloy Alloy X in figure 25(b) over the same temperature range. In general, the maximum stable stress for both materials at 538°C (1000°F) was about 3 to 4 times that observed at 871°C (1600°F) – regardless of the strain range.

A comparison between the monotonic and cyclic stress response of both materials in hydrogen gas is given in Figure 26. All continuous cycling data generated in the hydrogen gas environment are shown in this figure to demonstrate the relative uniformity in stress response for particular conditions and also to demonstrate the difference in stress response between the Type 347 stainless steel and the Hastelloy Alloy X at the investigated temperatures.

The stress response of both materials tested in air at 538°, 760°, and 871°C (1000°, 1400°, and 1600°F) is shown in figure 27. Again, the curves presented for each condition are typical of generally observed material response. The amount of cycling hardening in air of both materials at each temperature was similar to that observed in the hydrogen gas environment. In most cases, however, the peak stress level was attained in somewhat fewer cycles and the ultimate cycles to failure were correspondingly less. Figure 28 displays all continuous cycling stress response data generated in air for both materials.

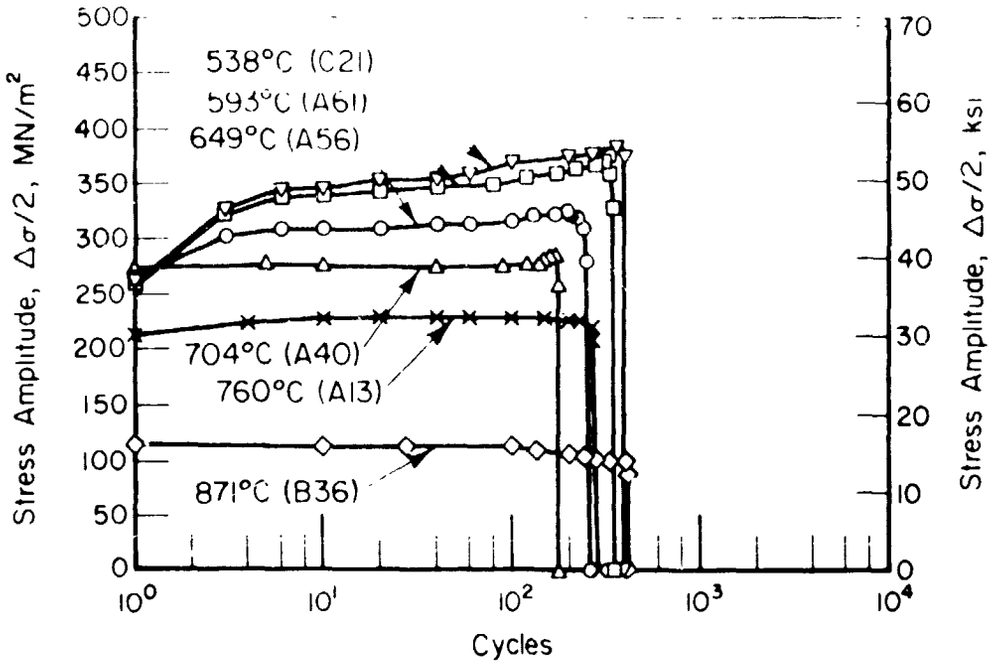

(a) Type 347 stainless steel.

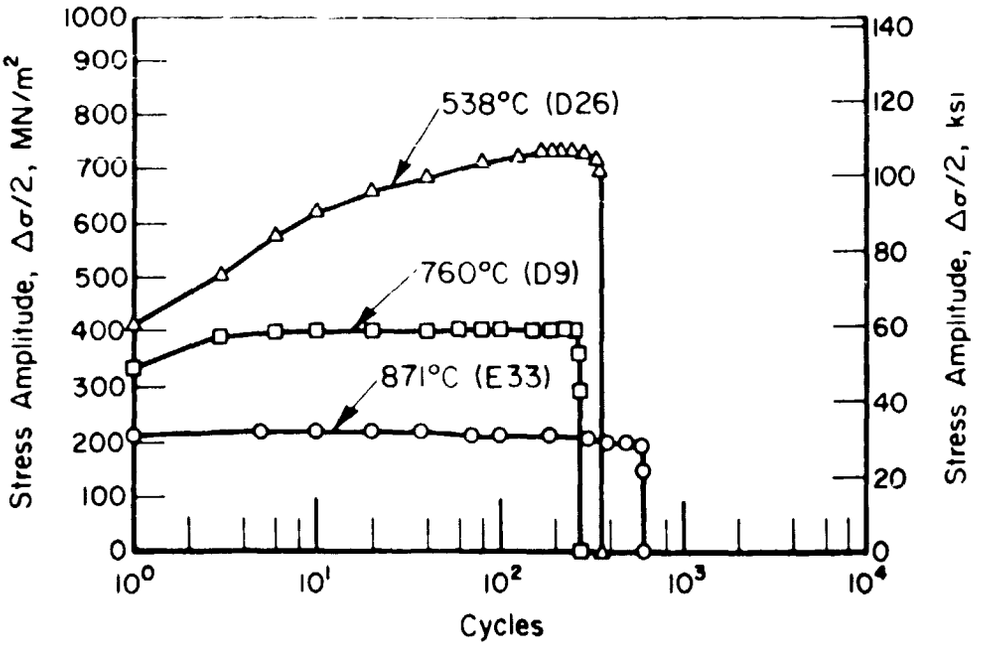

(b) Hastelloy Alloy X.

Figure 25. – Effect of temperature on stress response in hydrogen gas and at a total axial strain range of 3 percent.

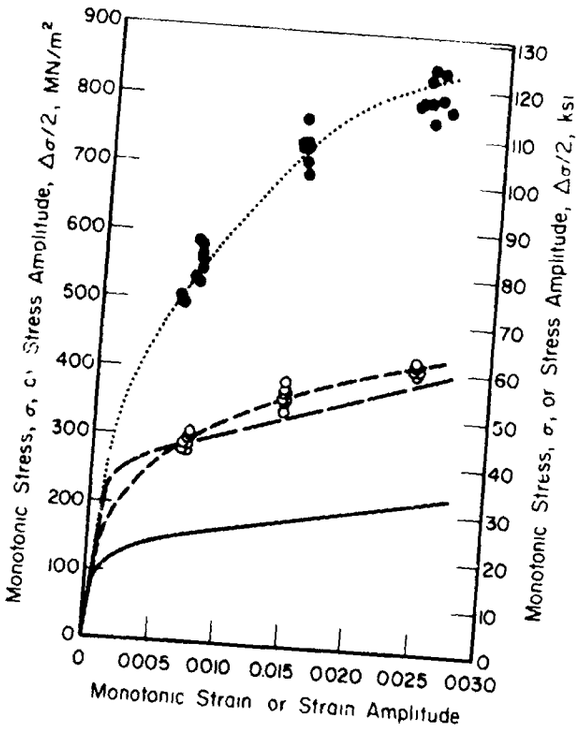

(a) 538°C (1000°F).

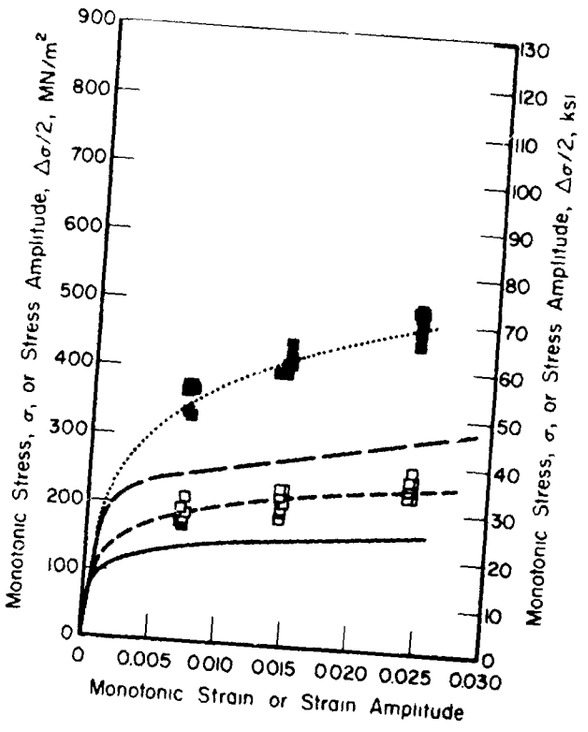

(b) 760°C (1400°F).

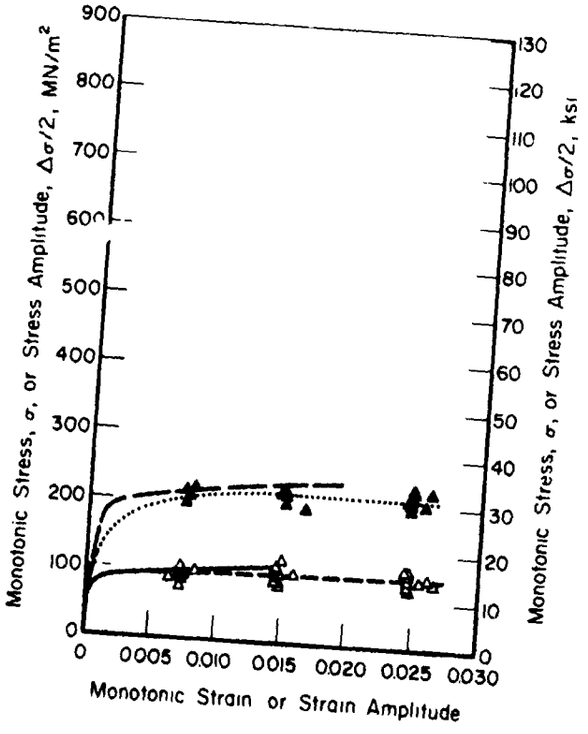

(c) 871°C (1600°F).

Cyclic
Monotonic

Note: Open symbols are cyclic data for Type 347 stainless steel, and solid symbols are cyclic data for Hastelloy Alloy X.

REPRODUCIBILITY OF THE
ORIGINAL PAGE IS POOR

Figure 26. – Monotonic and stabilized cyclic (at $N_f/2$) stress response of Type 347 stainless steel and Hastelloy Alloy X in hydrogen gas.

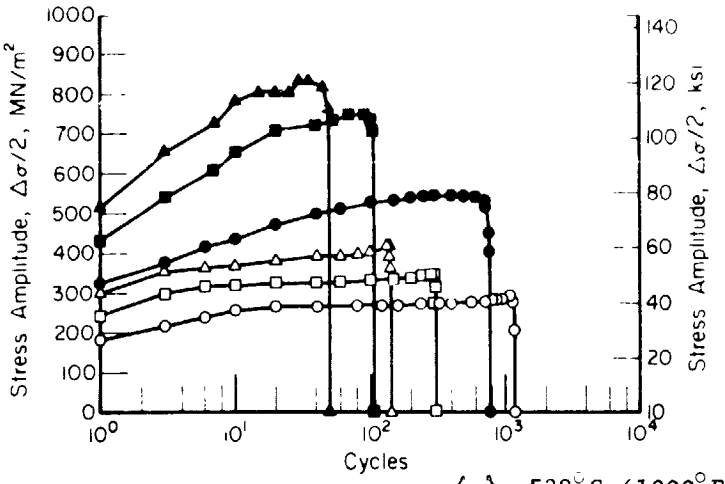

Specimen		
Type 347 Stainless Steel	Hastelloy Alloy X	Total Axial Strain Range
○ A69	● D59	15%
□ A68	■ D51	30%
△ A67	▲ D50	50%

(a) 538°C (1000°F).

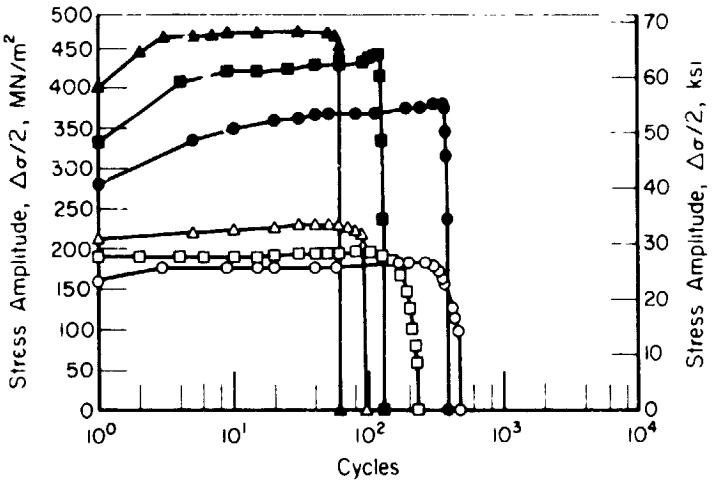

Specimen		
Type 347 Stainless Steel	Hastelloy Alloy X	Total Axial Strain Range
○ B9	● E5	15%
□ B2	■ E2	30%
△ A4	▲ E1	50%

(b) 760°C (1400°F).

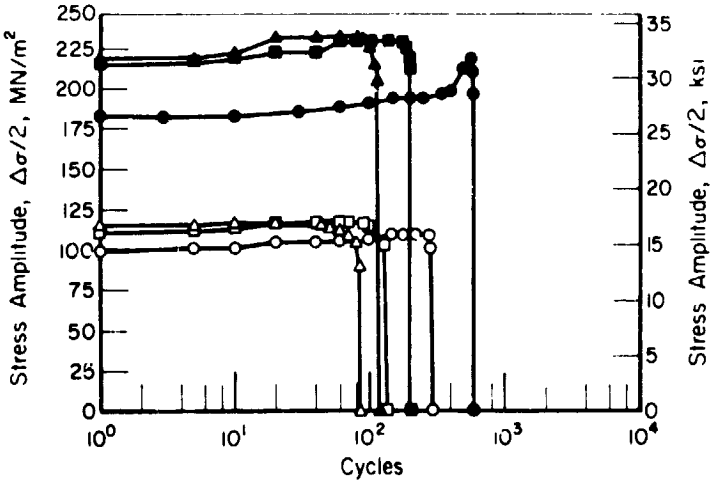

Specimen		
Type 347 Stainless Steel	Hastelloy Alloy X	Total Axial Strain Range
○ A72	● D57	15%
□ A71	■ D52	30%
△ A70	▲ D50	50%

(c) 871°C (1600°F).

Figure 27. — Stress amplitude versus fatigue cycles for Type 347 stainless steel and Hastelloy Alloy X in air.

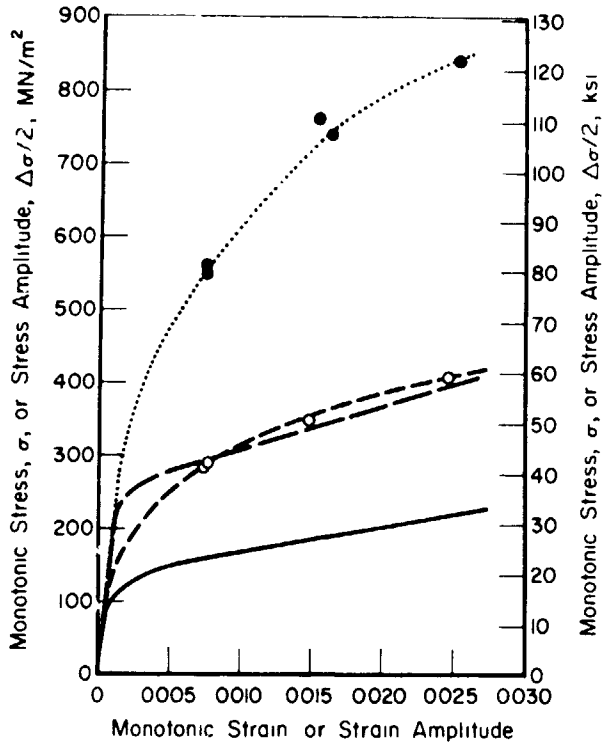

(a) 538°C (1000°F).

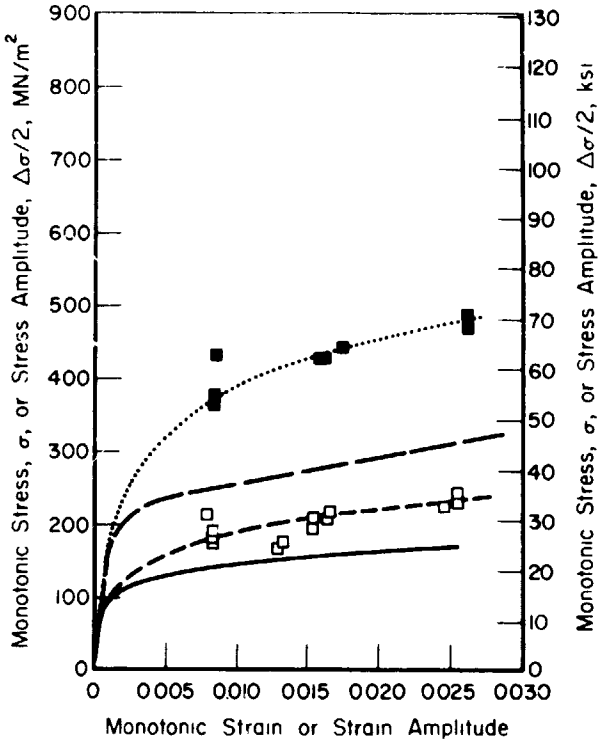

(b) 760°C (1400°F).

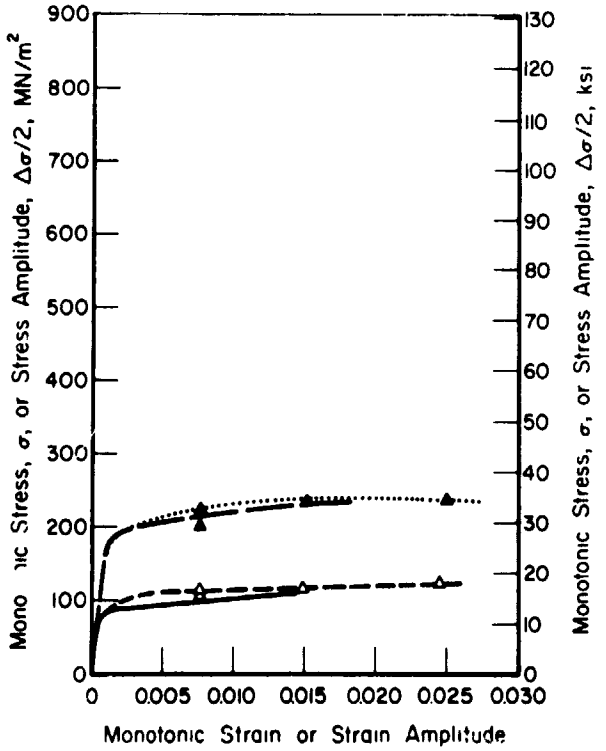

(c) 871°C (1600°F).

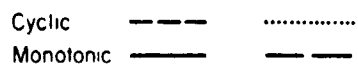

Note: Open symbols are cyclic data for Type 347 stainless steel, and solid symbols are cyclic data for Hastelloy Alloy X.

Figure 28. – Monotonic and stabilized cyclic (at $N_f/2$) stress response of Type 347 stainless steel and Hastelloy Alloy X in air.

The fatigue behavior of Type 347 stainless steel and Hastelloy Alloy X in the hydrogen gas and laboratory air environments will be discussed further in the next major section.

Compressive hold times.—In addition to the continuous cycling experiments, a series of elevated-temperature, compressive-strain, hold-time experiments were conducted. Ten-minute hold times at peak compressive strains were employed on a limited number of specimens tested at 760°C (1400°F) and 871°C (1600°F). All but two of the specimens tested were from heat A of Type 347 stainless steel.

Examples of the cyclically stable stress relaxation characteristics of both materials are shown in figures 29 through 31. Figure 29 illustrates typical stress relaxation response at 760°C (1400°F) for Type 347 stainless steel specimens cycled at total axial strain ranges of 1.5, 3.0, and 5.0 percent. Figure 30 presents additional relaxation data on Type 347 stainless steel at 871°C (1600°F), while figure 31 shows results of both stress relaxation experiments on the Hastelloy Alloy X material. Some scatter in relaxation response is evident, especially for those specimens tested at the highest strain range.

Comparison of figure 29(b) with figure 30 and comparison of figure 31(a) with figure 31(b) provides an illustration of the effect of temperature on the cyclically stable stress relaxation behavior of Type 347 stainless steel and Hastelloy Alloy X, respectively. These figures show relaxation data for tests conducted with a 10-minute hold period at 3.0 percent compressive axial strain. The difference in relaxation response between 760°C (1400°F) and 871°C (1600°F) was substantial for both materials, but it was especially pronounced with the Hastelloy Alloy X where compressive stresses reduced rapidly to near zero at the 871°C (1600°F) temperature.

The curves drawn in figures 29 through 31 represent best-fit lines for the following analytical expression (ref. 11):

$$\ell n \left(\frac{\sigma_o}{\sigma}\right) = \frac{A}{1+M} t^{1+M} \quad , \tag{2}$$

where σ_o = initial stress value

σ = instantaneous stress

t = instantaneous time (in minutes), and

A,M = optimized constants.

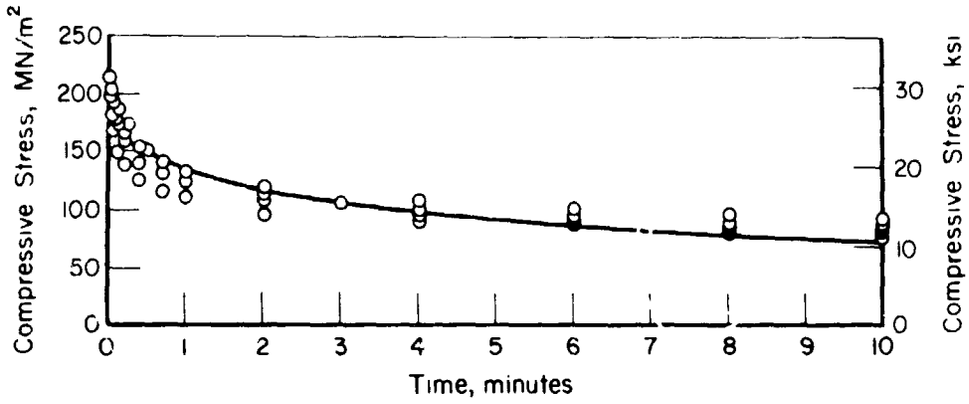

(a) Total axial strain range, $\Delta\varepsilon_t$ – 1.5%.

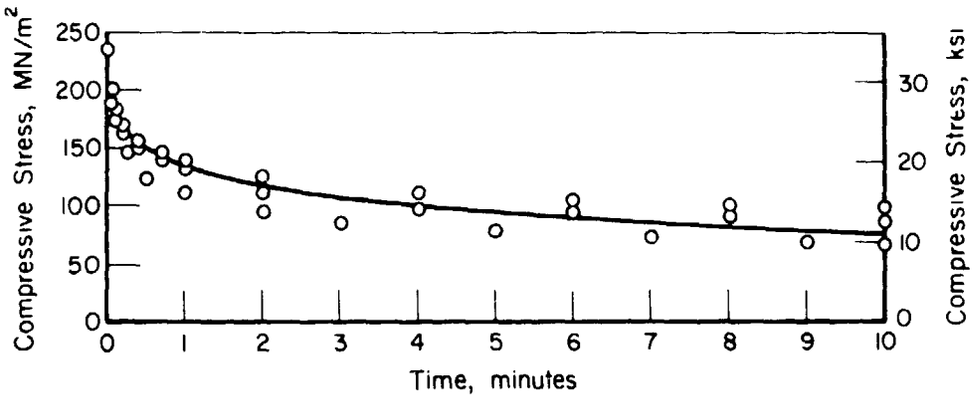

(b) Total axial strain range, $\Delta\varepsilon_t$ – 3.0%.

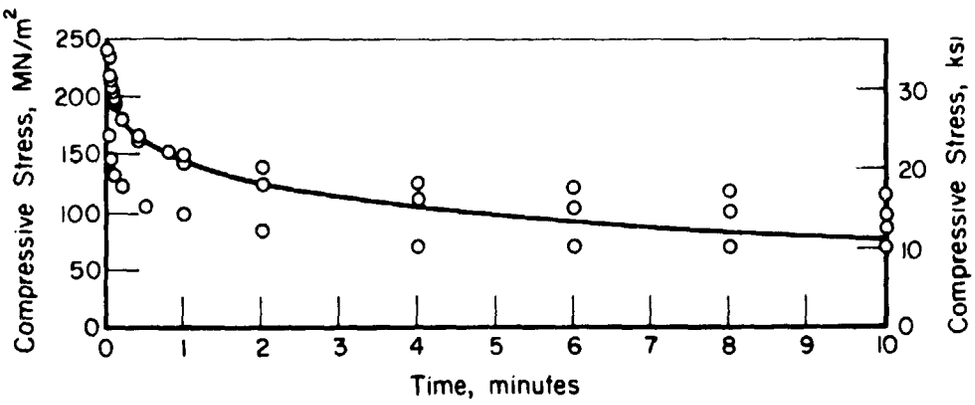

(c) Total axial strain range, $\Delta\varepsilon_t$ – 5.0%.

Figure 29. – Relaxation stress response for Type 347 stainless steel in hydrogen gas at 760°C (1400°F).

REPRODUCIBILITY OF THE
ORIGINAL PAGE IS POOR

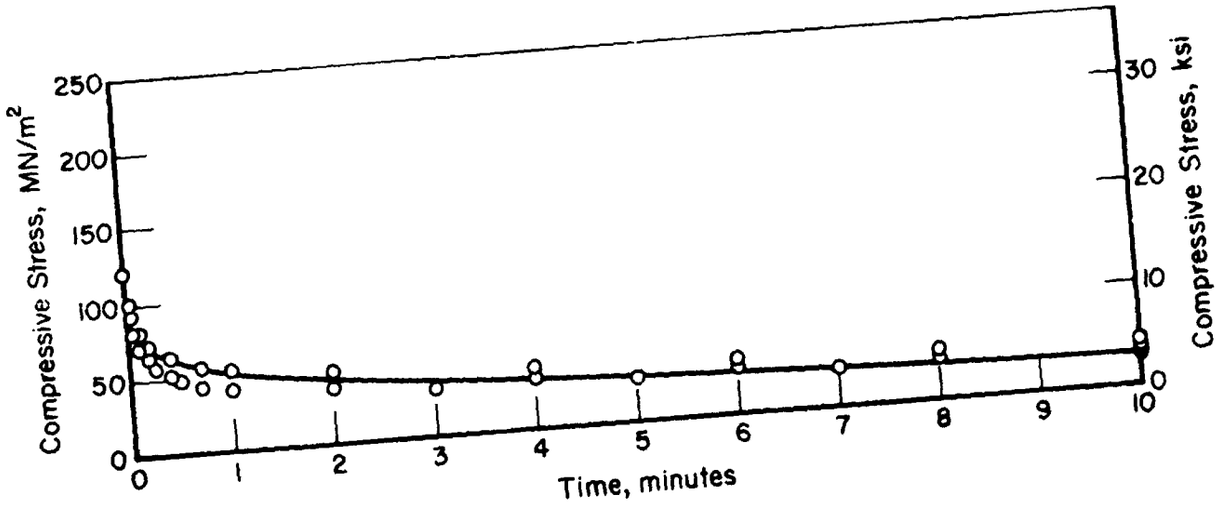

Figure 30. – Relaxation stress response for Type 347 stainless steel in hydrogen gas at 871°C (1600°F) and at a total axial strain range of 3 percent.

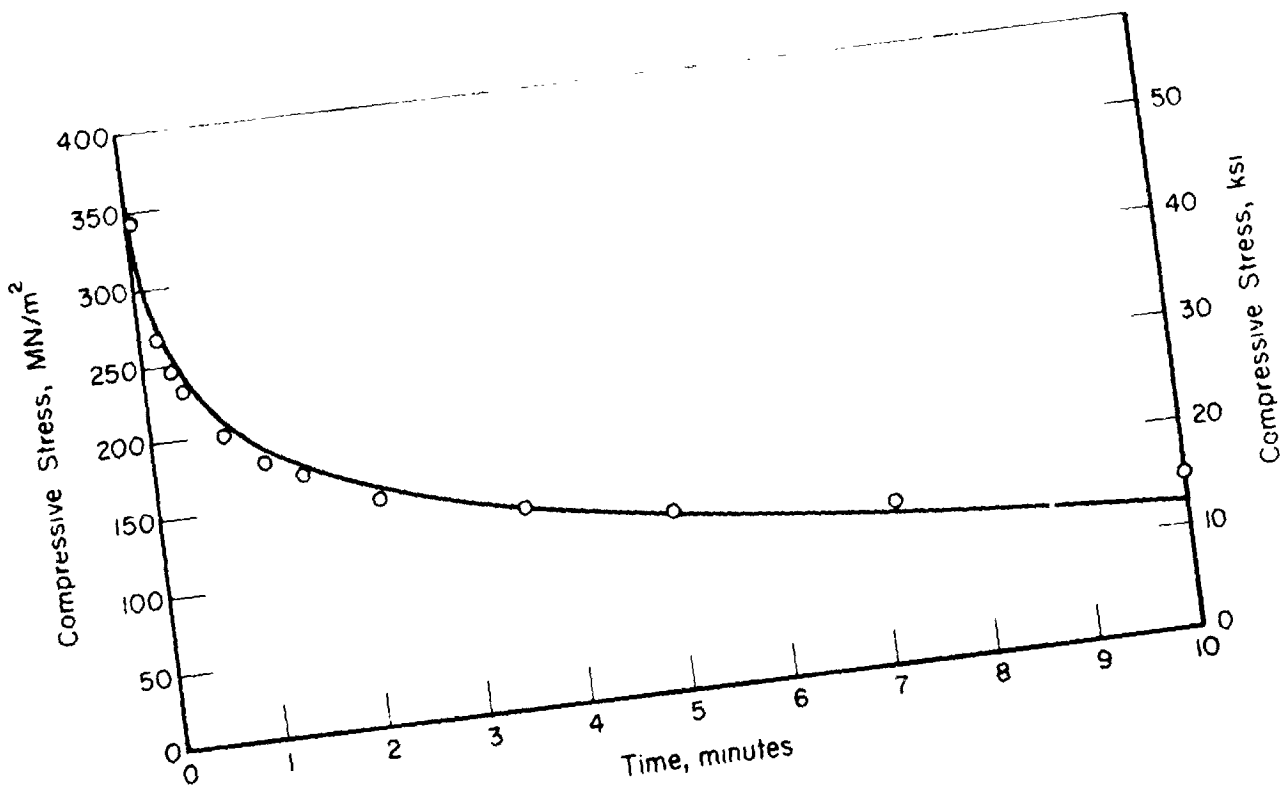

(a) At 760° C (1400° F).

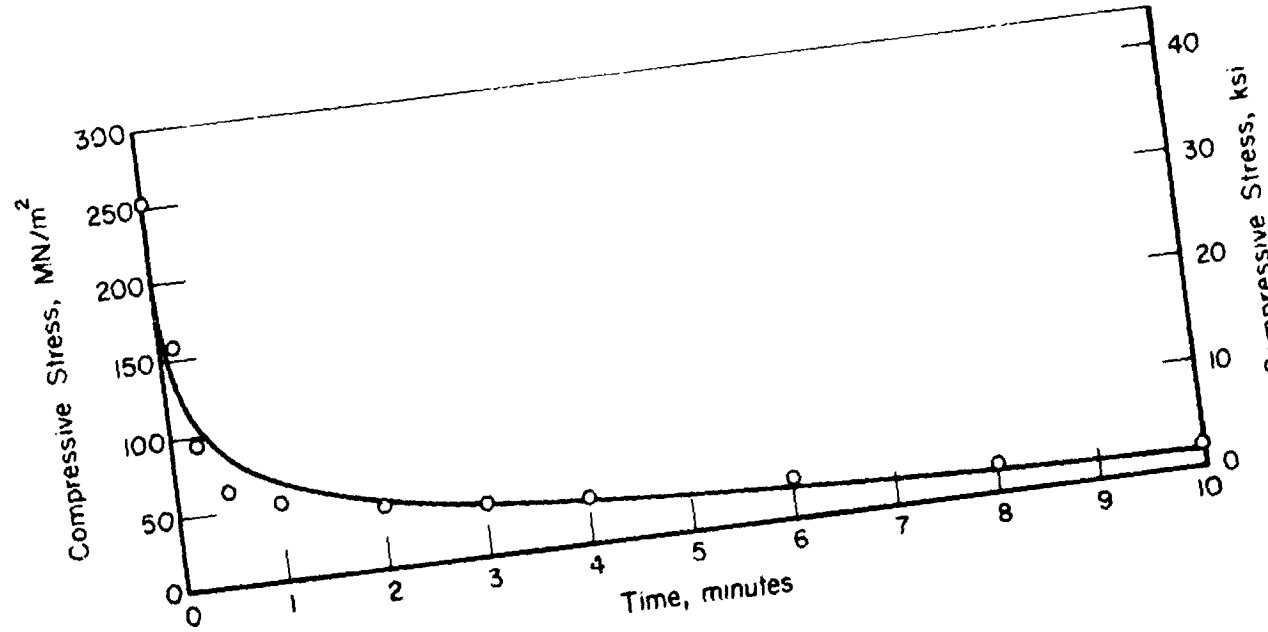

(b) At 871° C (1600° F).

Figure 31. – Relaxation stress response for Hastelloy Alloy X in hydrogen gas and at a total axial strain range of 3 percent.

To find the optimum values of A and M for each collection of data, a least-squares regression was performed on a transformation of Equation (2), which was written as follows:

$$\log\left(\ell n \frac{\sigma_o}{\sigma}\right) = \log\left(\frac{A}{1+M}\right) + (1+M)\log t \quad . \qquad (3)$$

Since Equation (3) was a linear expression, it was straightforward to find the equation coefficients and the associated values of A and M. The resultant fit of the curve to the data was good where the scatter was small, and only fair in cases where substantial data scatter was present. A summary of the stress-relaxation data and optimized constants for Equation (2) are given in table VII. Individual data for each stress-relaxation experiment are listed in Appendix A.

Fatigue Resistance

All fatigue specimens evaluated in this program were cycled to failure under axial-strain control at a constant strain rate of 10^{-3} sec^{-1}. As mentioned previously, these experiments included laboratory air and hydrogen gas environments in the 538° to 871°C (1000° to 1600°F) temperature range and both continuous cycling and compressive strain hold times. The observed fatigue life trends for all continuous cycling experiments are discussed in the following paragraphs, followed by a similar and comparative discussion of the hold-time fatigue-life results.

Continuous cycling in air and hydrogen gas.—The results of all Type 347 stainless steel and Hastelloy Alloy X continuous cycling fatigue experiments are presented in the summary tables and figures of this section. The figures include plots of the number of cycles to failure versus total, inelastic, and elastic strain range for specific environments, temperatures, and/or lots of material. In addition, individual tabular data for specific axial strain ranges are presented in Appendix B. These tabulated data are arranged according to fatigue life, with the shortest specimen life listed first, so that a comparison can be made between the fatigue performance of specific material lots. Each table in Appendix B also includes tabulated values of total, inelastic, and elastic strain range; stress range; and fatigue life (using the 3 fatigue failure criteria previously defined).

TABLE VII. – SUMMARY OF STRESS RELAXATION DATA FOR COMPRESSIVE-STRAIN HOLD-TIME EXPERIMENTS ON TYPE 347 STAINLESS STEEL AND HASTELLOY ALLOY X

Specimen numbers	Temperature °C (°F)	Total axial strain range[a], $\Delta\epsilon_t$	Peak compressive stress at $N_f/2$,				Optimized fitting constants	
			Before hold[a]		After hold[a]			
			MN/m^2	ksi	MN/m^2	ksi	A	M
Type 347 stainless steel								
A42, A45, A47, A49	760 (1400)	1.54	210	30.5	82.1	11.0	0.174	-0.625
A46, A50, A51	760 (1400)	3.06	236	34.2	83.4	12.1	0.173	-0.693
A43, A44, A48	760 (1400)	4.97	239	34.6	93.1	13.5	0.180	-0.649
A52, A53, A63	871 (1600)	3.01	118	17.1	25.7	3.73	0.252	-0.713
Hastelloy alloy X								
D48	760 (1400)	3.05	499	72.4	259	37.6	0.257	-0.714
D49	871 (1600)	3.08	263	38.1	13.8	2.00	0.478	-0.657

[a] Average values of all specimens tested for that material, temperature, and strain range.

The continuous cycling data generated in laboratory air for Type 347 stainless steel and Hastelloy Alloy X are presented in figure 32, and tables B1 and B2 of Appendix B contain the corresponding tabular data.

The laboratory air data generated at 538°C (1000°F) are shown in figure 32(a). Similar data generated at 760° and 871°C (1400° and 1600°F) are illustrated in figures 32(b) and 32(c), respectively. Each plot contains data for both materials at strain ranges of about 1.5, 3.0, and 5.0 percent; the Type 347 stainless steel data are indicated by solid points and the Hastelloy Alloy X data are shown as open points.

It was found that the inelastic strain range fatigue curves in figure 32 could be approximated by the Manson-Coffin relation,

$$\Delta\epsilon_{in} = AN_f^a$$

and that the elastic strain range fatigue curves could be approximated by the Basquin-type relation,

$$\Delta\epsilon_e = BN_f^b \quad .$$

Values of the exponents and coefficients in these two expressions were determined graphically and are summarized in table VIII.

The overall trends of fatigue life versus temperature for both materials tested in laboratory air are shown in figure 33. The Type 347 stainless steel displayed higher fatigue resistance in air than Hastelloy Alloy X at 538° and 760°C (1000° and 1400°F) but the difference was relatively small at 760°C (1400°F), especially at the lowest axial strain range. Fatigue resistance of the Hastelloy Alloy X exceeded that of the Type 347 stainless steel in air at 871°C (1600°F). Except at the lowest axial strain range, the fatigue resistance of the Hastelloy Alloy X increased with increasing temperature, while in all cases the fatigue resistance decreased with increasing temperature for the Type 347 stainless steel.

The increased ductility (see fig. 19) and good oxidation resistance of the Hastelloy Alloy X at higher temperatures enhanced that material's low-cycle fatigue resistance at increasing temperatures for the two higher strain ranges where total test times were relatively short. At the lowest strain range, both ductility and strength became important and total test times increased; thus, the minimum fatigue resistance was observed at 760°C (1400°F) and the maximum was at 528°C (1000°F). In contrast, higher temperatures in air increased the susceptibility of the Type 347 stainless steel to oxidation, which caused a reduction in high temperature

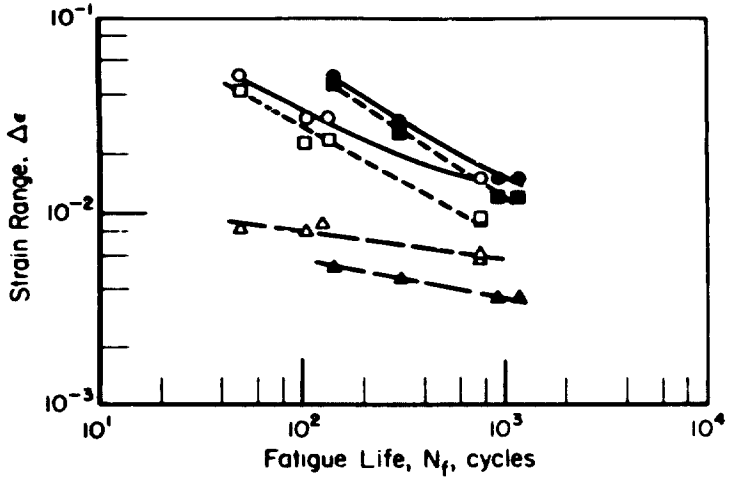

(a) 538°C (1000°F), Heats A and D.

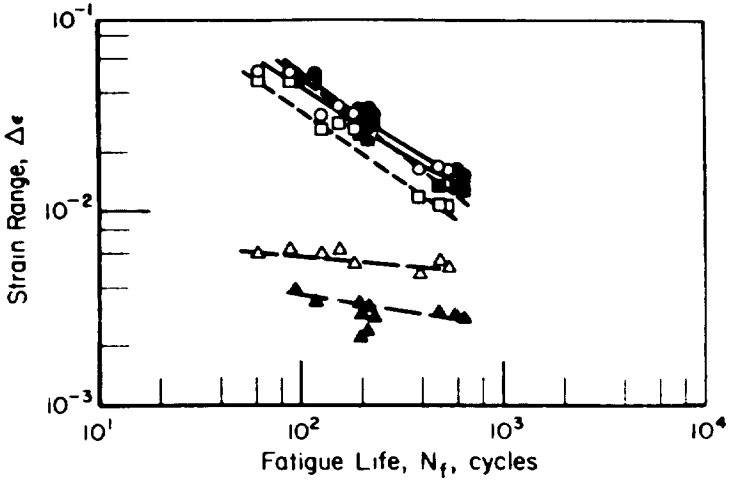

(b) 760°C (1400°F), Heats A, B, C, D, and E.

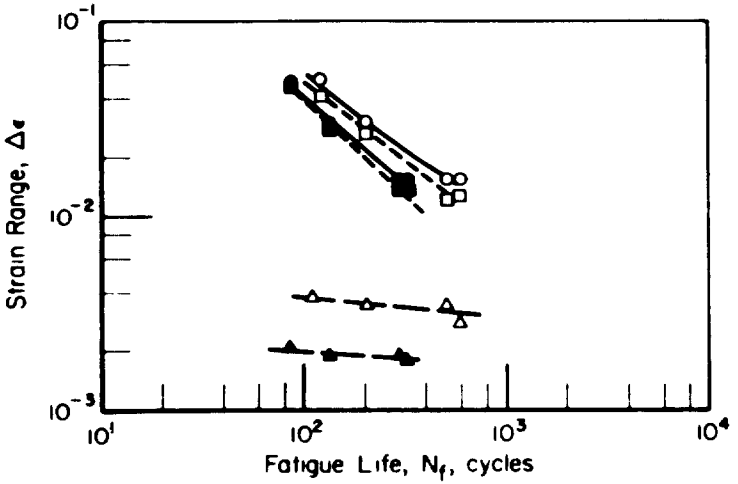

(c) 871°C (1600°F), Heats A and D.

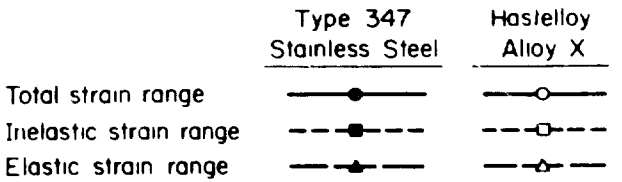

Figure 32. – Fatigue life as a function of strain range for Type 347 stainless steel and Hastelloy Alloy X in air and at an axial strain rate of 10^{-3} sec^{-1}.

TABLE VIII. – SUMMARY OF ELASTIC AND INELASTIC SLOPE AND INTERCEPT VALUES FOR CONTINUOUS CYCLING FATIGUE TESTS ON TYPE 347 STAINLESS STEEL AND HASTELLOY ALLOY X IN AIR AND HYDROGEN GAS

Temperature, °C	(°F)	Material	Heat	Slope		Intercept	
				Elastic b	Inelastic a	Elastic B	Inelastic A
Continuous cycling fatigue tests in air							
538	(1000)	Type 347 Stainless Steel	A	-0.20	-0.66	1.44×10^{-2}	1.15×10^{0}
760	(1400)	Type 347 Stainless Steel	A,B,C	-0.15	-0.77	7.13×10^{-3}	1.66×10^{0}
871	(1600)	Type 347 Stainless Steel	A	-0.074	-0.95	2.76×10^{-3}	3.03×10^{0}
538	(1000)	Hastelloy Alloy X	D	-0.15	-0.57	1.55×10^{-2}	3.90×10^{-1}
760	(1400)	Hastelloy Alloy X	D,E	-0.093	-0.71	8.80×10^{-3}	8.55×10^{-1}
871	(1600)	Hastelloy Alloy X	D	-0.11	-0.80	6.25×10^{-3}	1.93×10^{0}
Continuous cycling fatigue tests in hydrogen gas							
538	(1000)	Type 347 Stainless Steel	A	-0.17	-0.56	1.41×10^{-2}	7.11×10^{-1}
			B	-0.15	-0.55	1.20×10^{-2}	6.43×10^{-1}
			C	-0.18	-0.59	1.40×10^{-2}	8.54×10^{-1}
760	(1400)	Type 347 Stainless Steel	A	-0.096	-0.80	5.51×10^{-3}	2.29×10^{0}
			B	-0.091	-0.72	5.19×10^{-3}	9.92×10^{-1}
			C	-0.12	-0.79	6.15×10^{-3}	2.36×10^{0}
871	(1600)	Type 347 Stainless Steel	A	-0.27	-0.65	1.29×10^{-2}	1.68×10^{0}
			B	-0.089	-0.56	2.79×10^{-3}	9.64×10^{-1}
			C	-0.077	-0.64	2.67×10^{-3}	1.51×10^{0}
538	(1000)	Hastelloy Alloy X	D	-0.12	-0.49	1.52×10^{-2}	3.08×10^{-1}
			E	-0.16	-0.50	1.89×10^{-2}	3.54×10^{-1}
760	(1400)	Hastelloy Alloy X	D	-0.10	-0.75	9.68×10^{-3}	1.59×10^{0}
			E	-0.12	-0.64	1.07×10^{-2}	7.05×10^{-1}
871	(1600)	Hastelloy Alloy X	D	-0.064	-0.62	4.79×10^{-3}	1.25×10^{0}
			E	-0.053	-0.60	4.28×10^{-3}	1.06×10^{0}

REPRODUCIBILITY OF THE ORIGINAL PAGE IS POOR

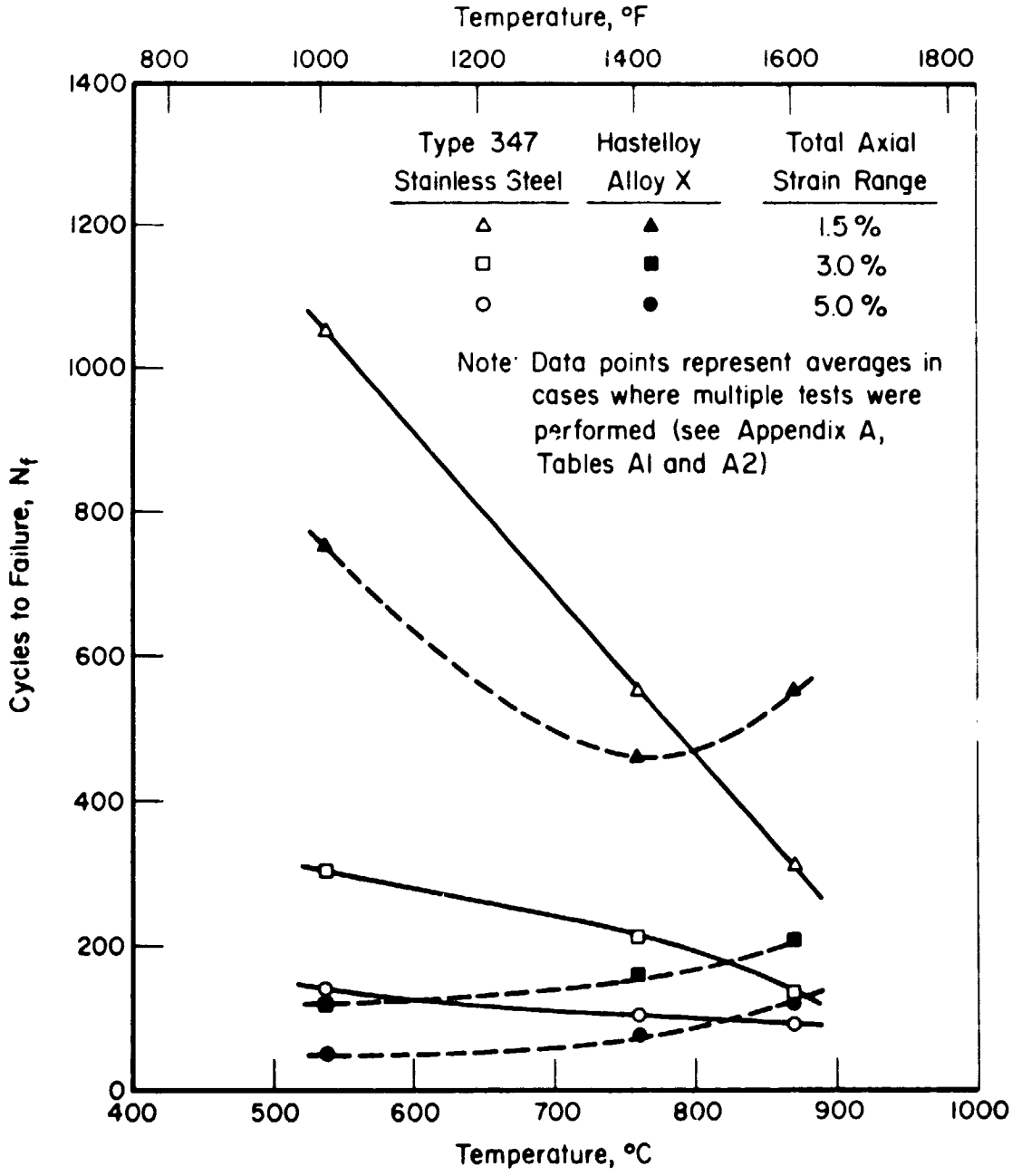

Figure 33. – Fatigue life as a function of temperature and total axial strain range for Type 347 stainless steel and Hastelloy Alloy X in air.

fatigue resistance. This second point was further substantiated by the comparative fatigue performance of the two alloys at different temperatures in an oxidation-inhibiting hydrogen gas environment, as discussed subsequently in this report.

The continuous cycling data generated in hydrogen gas for Type 347 stainless steel and Hastelloy Alloy X are illustrated in figures 34 through 36, and tables B3 through B8 of Appendix B contain the corresponding tabular data.

Figure 34 shows fatigue curves for all 5 heats of material at 538 C (1000° F) in hydrogen gas. Each plot displays total, elastic and inelastic axial strain values as a function of specimen fatigue life. A mean curve is drawn through the total axial strain range data and straight line approximations to the elastic and inelastic axial strain range data are also shown. As for the data in air, these curves were approximated by the Manson-Coffin and Basquin relations with the coefficients and exponents listed in table VIII. Similar data displays are given in Figures 35 and 36 for the continuous cycling fatigue data generated in hydrogen gas at 760 and 871°C (1400 and 1600°F), respectively.

Figures 37(a), (b), and (c) are composite plots of total axial strain range versus fatigue life for the temperatures of 538, 760, and 871°C (1000, 1400 and 1600°F), respectively. Each of these figures was compiled from the average fatigue life curves shown in the previous three figures (figs. 34, 35, and 36) so that direct comparisons between the 2 materials and 5 heats could be made.

In figure 37(a), it can be seen that no large differences in fatigue life occurred among or between heats of the same alloy at the 538°C (1000°F) temperature, but large differences in fatigue life developed between the two alloys. The difference is especially apparent at the 5.0 strain range, where the Type 347 stainless steel displayed fatigue lives almost twice those of Hastelloy Alloy X. This trend was related to the lower ductility of Hastelloy Alloy X at 538°C (1000°F) [see fig. 19(b)], since ductility is a primary factor in fatigue resistance at large strain ranges.

As at 538°C (1000°F), the Type 347 stainless steel material showed little heat-to-heat variation at 760°C (1400°F) [see fig. 37(b)].

In contrast, heat E of Hastelloy Alloy X exhibited significantly lower fatigue lives than heat D at the 5.0 percent total axial strain range. However, this trend was not observed at the 3.0 percent strain range and was only

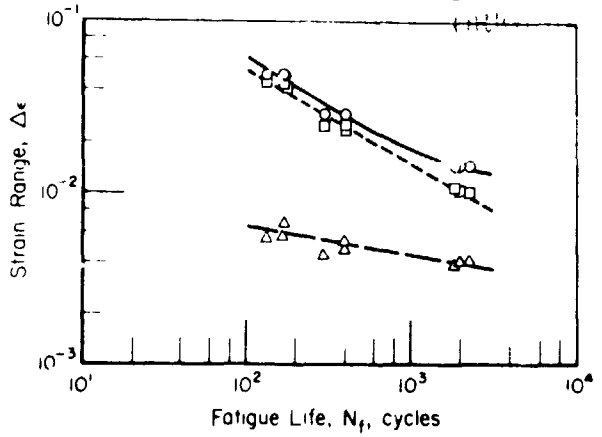

(a) Type 347 stainless steel, Heat A

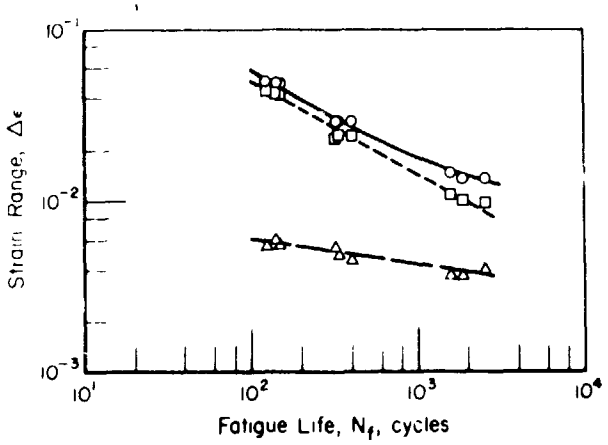

(b) Type 347 stainless steel, Heat B

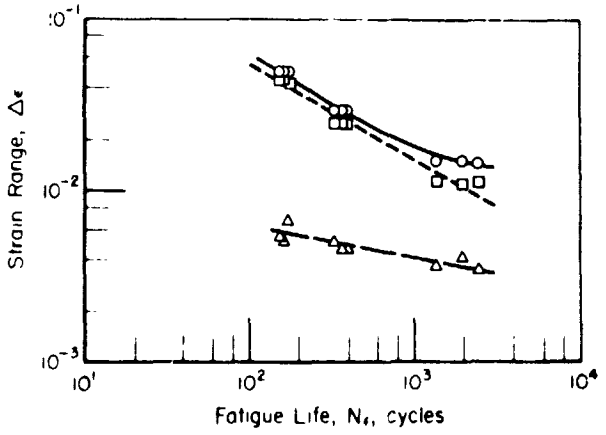

(c) Type 347 stainless steel, Heat C

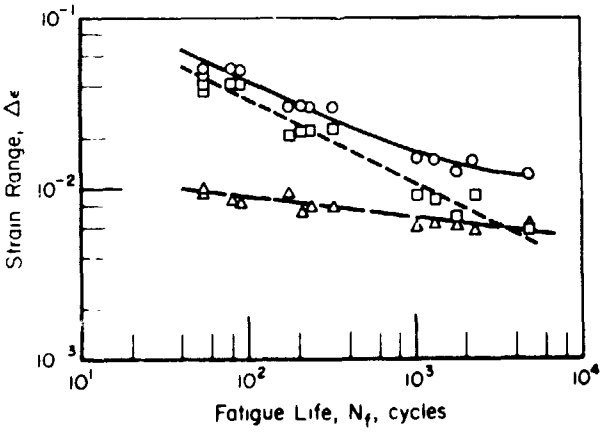

(d) Hastelloy Alloy X, Heat D

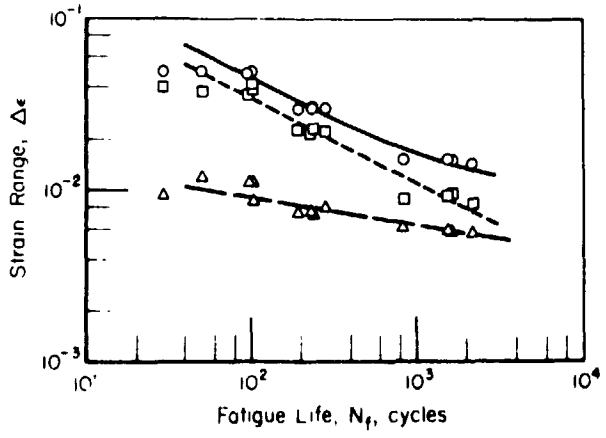

(e) Hastelloy Alloy X, Heat E

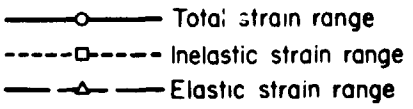

Figure 34. – Fatigue life as a function of strain range for Type 347 stainless steel and Hastelloy Alloy X in hydrogen gas at 538°C (1000°F) and at a strain rate of 10^{-3} sec^{-1}.

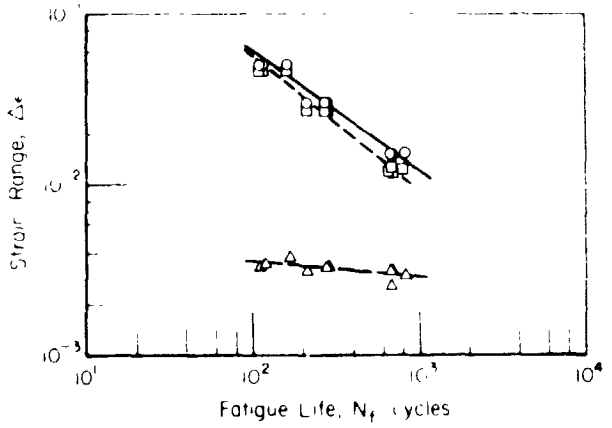

(a) Type 347 stainless steel, Heat A

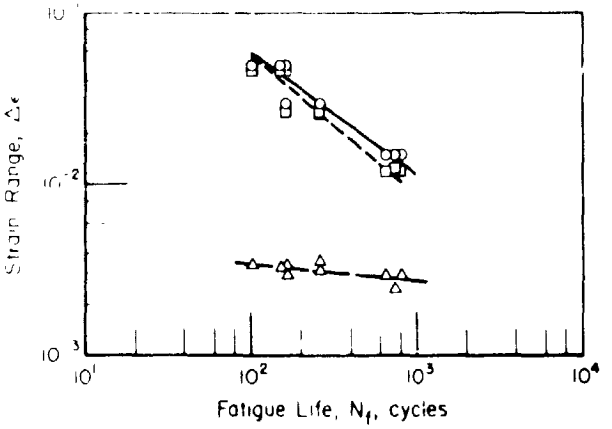

(b) Type 347 stainless steel, Heat B

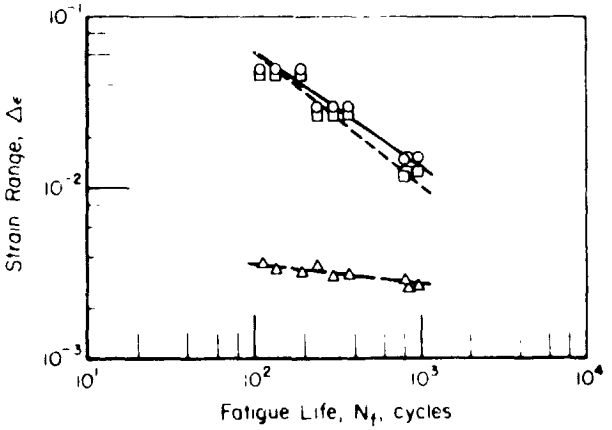

(c) Type 347 stainless steel, Heat C

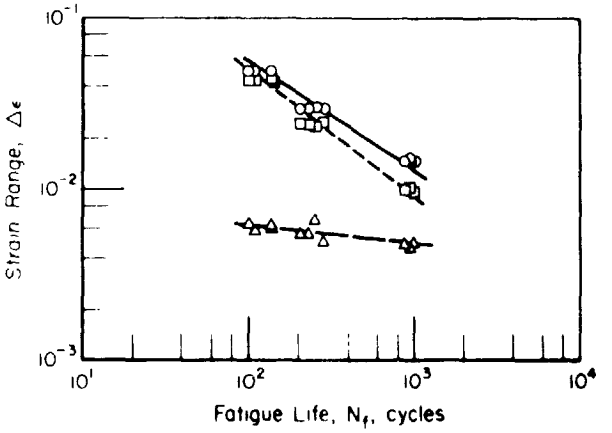

(d) Hastelloy Alloy X, Heat D

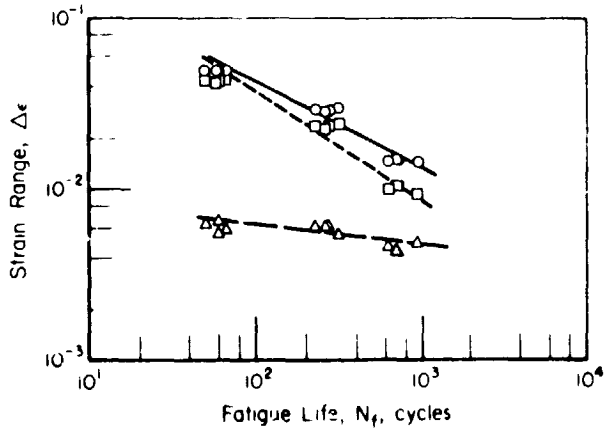

(e) Hastelloy Alloy X, Heat E

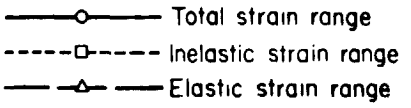

Figure 35. – Fatigue life as a function of strain range for Type 347 stainless steel and Hastelloy Alloy X in hydrogen gas at 760°C (1400°F) and at a strain rate of 10^{-3} sec^{-1}.

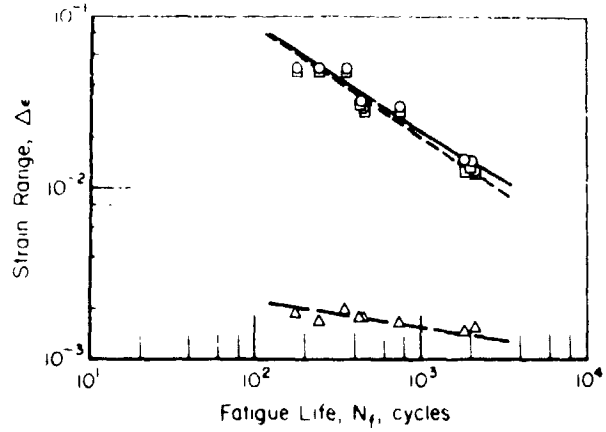

(a) Type 347 stainless steel, Heat A

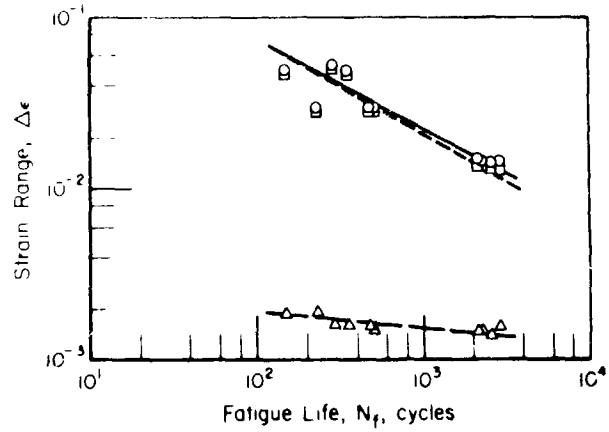

(b) Type 347 stainless steel, Heat B

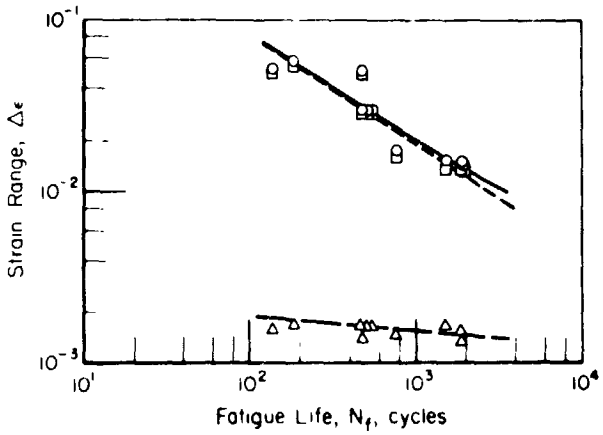

(c) Type 347 stainless steel, Heat C

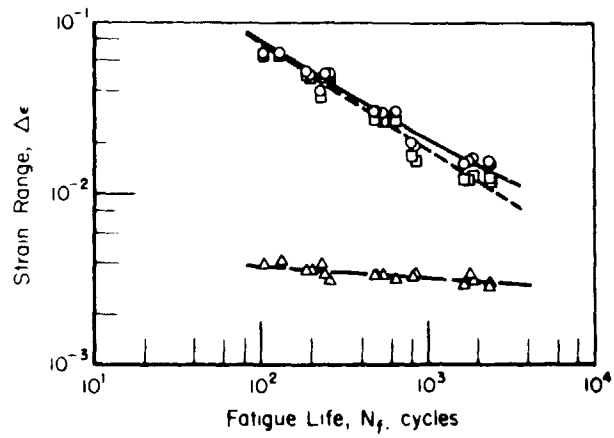

(d) Hastelloy Alloy X, Heat D

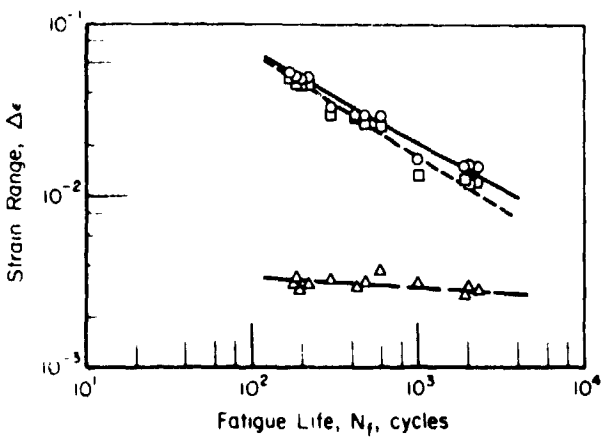

(e) Hastelloy Alloy X, Heat E

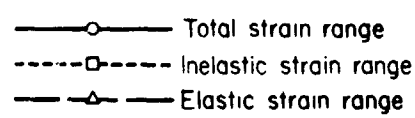

Figure 36. – Fatigue life as a function of strain range for Type 347 stainless steel and Hastelloy Alloy X in hydrogen gas at 871°C (1600°F) and at a strain rate of 10^{-3} sec^{-1}.

ORIGINAL PAGE IS POOR

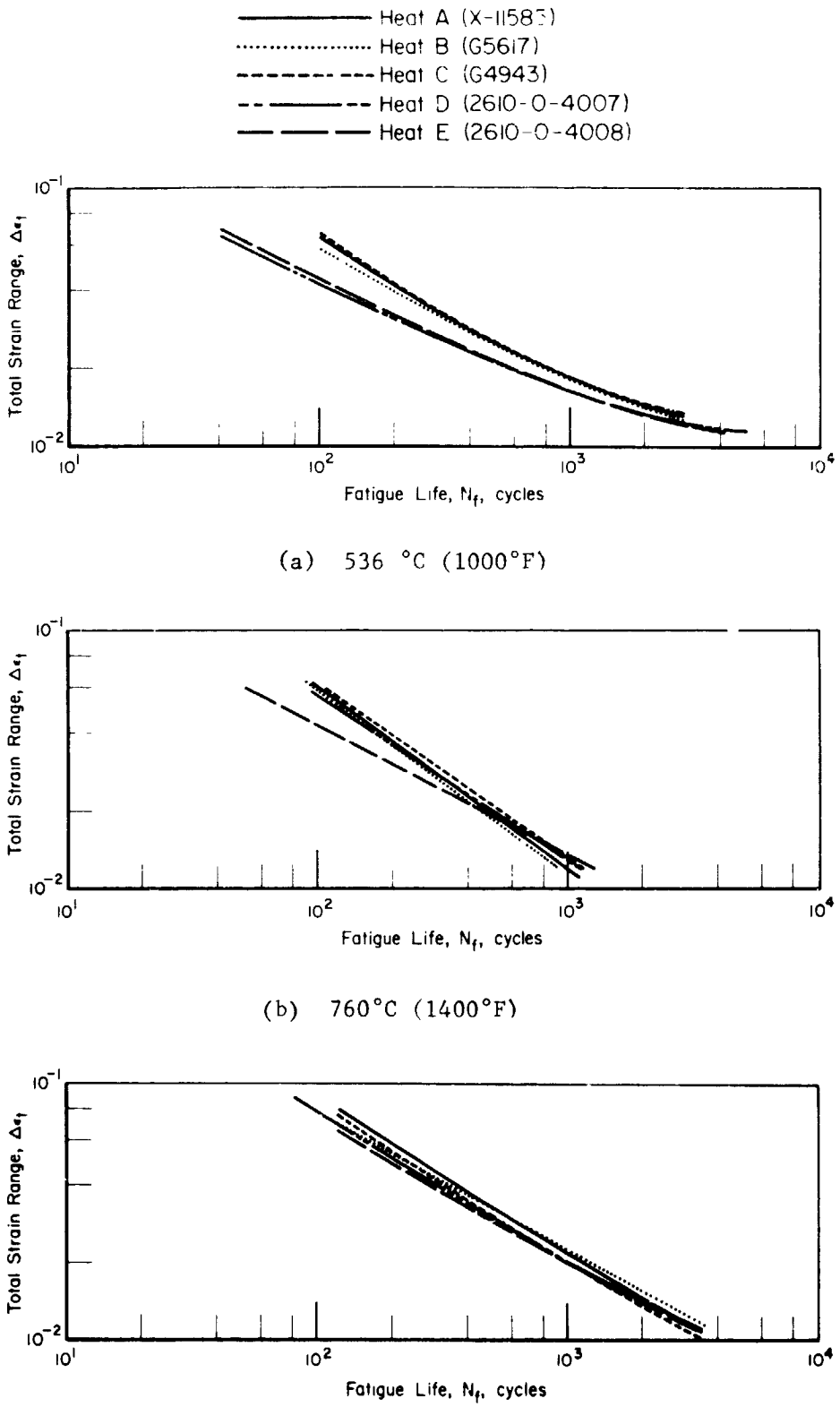

Figure 37. – Fatigue life versus total strain range for Type 347 stainless steel and Hastelloy Alloy X in hydrogen gas at elevated temperature and at strain rate of 10^{-3} sec^{-1}.

slightly evident at the 1.5 percent strain range. This heat-to-heat variation in fatigue life was related to the difference in true fracture ductility of the two heats. The true fracture ductility of the heat D material was higher than that of the heat E material; hence, the material with greater ductility showed better fatigue resistance at high strain ranges. This behavior is in contrast to that at 538°C (1000°F) where the two heats of Hastelloy Alloy X had similar true fracture ductilities, and as a result, the fatigue lives of the two heats were almost identical.

As figure 37(c) illustrates, there was minimal heat-to-heat variation in fatigue life for Hastelloy Alloy X at 871°C (1600°F). However, the Type 347 stainless steel displayed a slight heat-to-heat difference in fatigue life at the lowest strain range (1.5 percent). Specimens from heat B had longer lives than specimens from both heats C and A. Specimens from heat C displayed the shortest fatigue lives for this alloy at 871°C (1600°F).

The overall trend for all 5 heats of material was toward longer fatigue lives at the intermediate temperature (especially at lower strain ranges). One significant exception to these trends, however, was the low strain range data collection at 538°C (1000°F), which displayed the longest lives of all specimens tested for both materials. This trend is explained by the fact that both materials maintained from 65 to 85 percent of their room-temperature strength at 538°C (1000°F), and that at the lowest strain range, strength as well as ductility played an important role in determining fatigue resistance.

The average trends in hydrogen gas fatigue life for each material (after combining data from different heats, where reasonable) are shown in figure 38. Only for Hastelloy Alloy X at 761°C (1400°F) was it necessary to draw separate average lines; in all other cases, heat-to-heat variations in fatigue life were not significant in comparison to data scatter for a single heat.

The laboratory air data are also shown in figure 38. In all cases, the laboratory air test conditions resulted in slightly reduced average fatigue lives from those obtained in hydrogen gas.

After it was determined that tests conducted at the intermediate temperature of 760°C (1400°F) resulted in the lowest fatigue lives of the 3 temperatures initially tested, additional experiments were completed on the Type 347 stainless steel (heat A) at temperatures between 538°C (1000°F) and 760°C (1400°F) to

REPRODUCIBILITY OF THE
ORIGINAL PAGE IS POOR

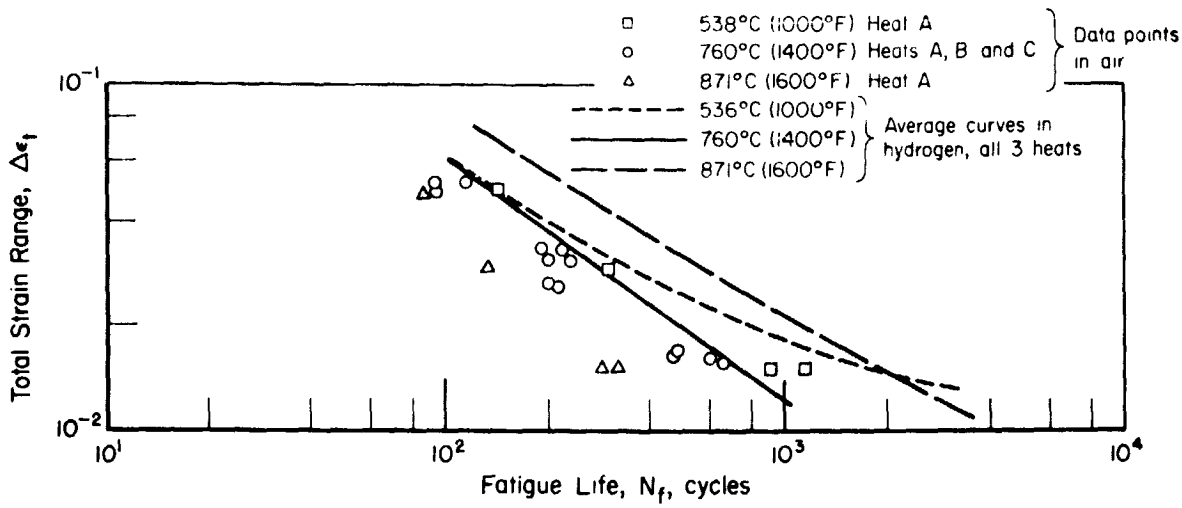

(a) Type 347 stainless steel.

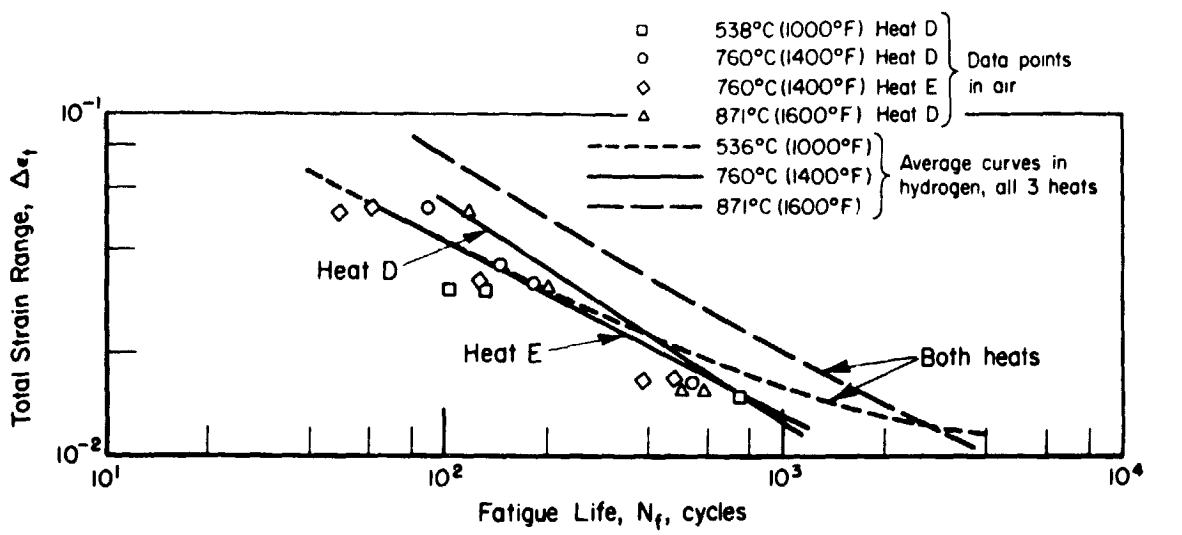

(b) Hastelloy Alloy X.

Figure 38. – Comparison of fatigue life in air with that in hydrogen gas at 538, 760, and 871°C (1000, 1400, and 1600°F) and at a strain rate of 10^{-3} sec^{-1}.

determine the approximate temperature which would produce minimum fatigue lives. The results of those experiments are presented in comparison with previous results in figure 39. The corresponding individual data are given in table B9 of Appendix B. All of these additional experiments were in hydrogen gas at the same axial strain rate (10^{-3} sec^{-1}) that was used before. As figure 39 illustrates, the temperature of 704°C (1300°F) resulted in minimum average fatigue life values over the temperature range of 538°C (1000°F) to 871°C (1600°F). The average fatigue life data for the Type 347 stainless steel (heat A) tests conducted in air are also shown. The difference between fatigue lives in hydrogen gas and air was relatively slight at temperatures below approximately 760°C (1400°F), with the average air data falling approximately 10 to 20 percent below the hydrogen gas data in fatigue life. The difference became very significant at the highest temperature of 871°C (1600°F), however, where results generated in air were highly influenced by oxidation and fatigue lives were less than one-fourth of the average fatigue life in the oxidation-inhibiting hydrogen gas environment. Data in air reported by Berling and Slot (ref. 4) and Baldwin (ref. 2) are also shown in figure 39; close agreement with present results is apparent at all temperatures where data are available.

Hold-time cycling.—The limited number of hold-time experiments were designed to be exploratory in nature. Only heat A of Type 347 stainless steel and heat D of Hastelloy X were included in this work. Test conditions were selected to simulate the worst case expected in service — 10-minute hold periods at peak compressive strain. Hold-time studies of other austenitic alloys (Types 304 and 316 stainless steel and Alloy 800) in air (for example, see refs. 12 through 17) have shown that fatigue life decreases with increasing length of hold time and that tension hold periods are much more damaging than compressive ones. However, for the intended application to rocket engine nozzles, it was anticipated that only compressive hold periods of less than 10 minutes would be encountered; thus, no other types and lengths of hold periods that might be more damaging were investigated in this program.

The hold-time fatigue results are summarized in table B10 of Appendix B. Ten of the 15 hold-time experiments were on heat A at 760°C (1400°F); all three strain ranges — 1.5, 3.0, and 5.0 percent — were investigated at this temperature. In addition, there were three experiments on heat A at 871°C (1600°F)

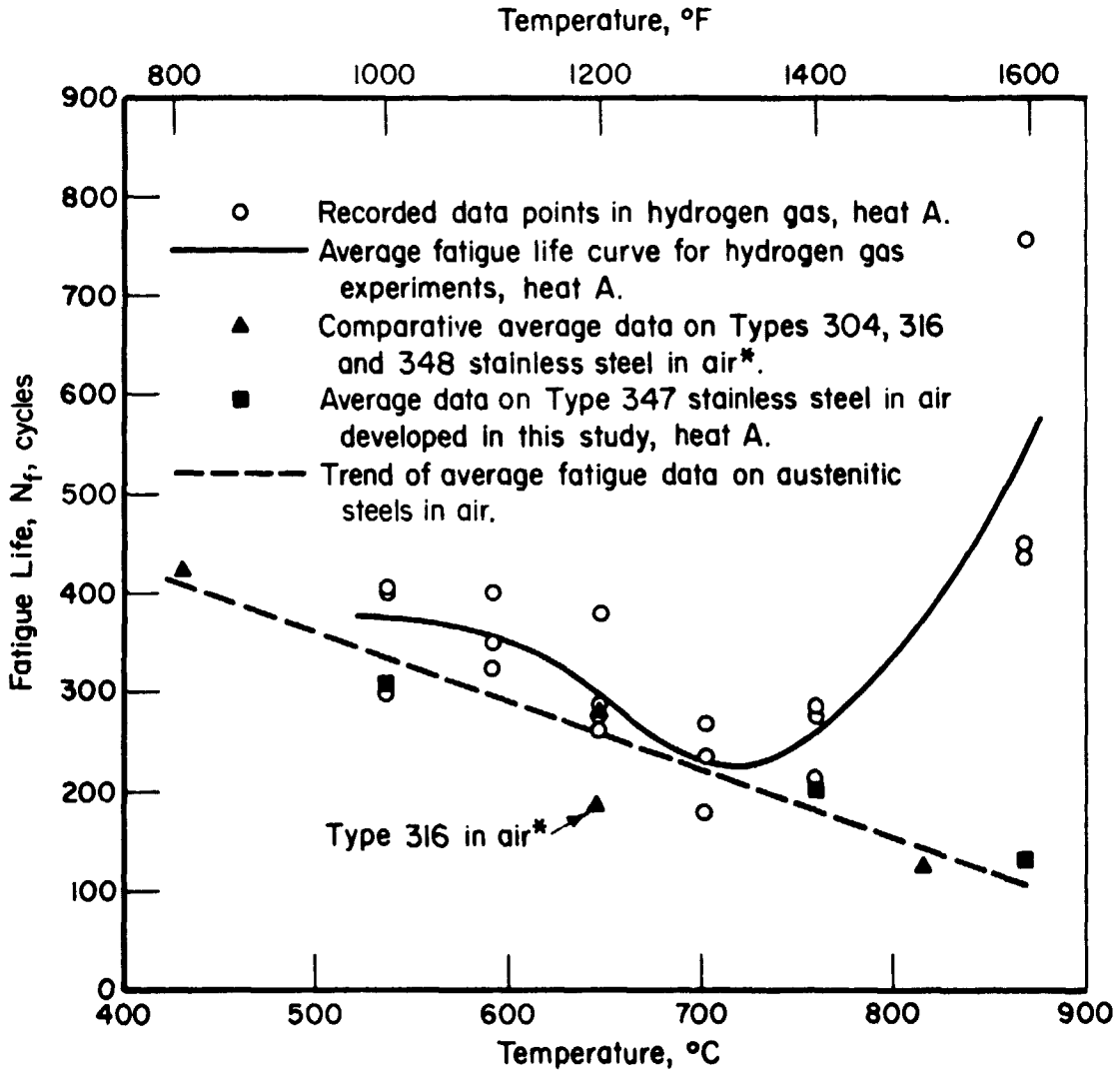

Figure 39. – Fatigue life as a function of temperature for Type 347 stainless steel at 3 percent total axial strain range.

Note. – * Data from Berling and Slot (ref. 7).

and at 3.0 percent strain range and two experiments on heat D at 3.0 percent strain range and at 760 and 871°C (1400 and 1600°F). Average fatigue life and stress range data from comparable hold-time and continuous cycling data are compared in table IX. In general, the effect of compressive hold time was to slightly increase the fatigue life and stress range of Type 347 stainless steel and to slightly decrease the fatigue life and slightly increase the stress range of Hastelloy Alloy X. These trends are discussed in more detail later in this report.

The detailed tabulations of hold-time data in table B10 of Appendix B include two values of elastic strain range, $\Delta\epsilon_{ei}$ and $\Delta\epsilon_{ed}$ (see fig. 10). Using the concepts of strain range partitioning (ref. 17), the difference between $\Delta\epsilon_{ed}$ and $\Delta\epsilon_{ei}$ is equal to the plastic-strain reversed by creep-strain range, $\Delta\epsilon_{pc}$. In other words,

$$\Delta\epsilon_{pc} = \Delta\epsilon_{ed} - \Delta\epsilon_{ei} \quad .$$

The remainder or balanced portion of the inelastic strain range, $\Delta\epsilon_{in}$, was the sum of the reversed plastic strain range, $\Delta\epsilon_{pp}$, and the reversed creep strain range, $\Delta\epsilon_{cc}$, or simply stated

$$\Delta\epsilon_{in} - \Delta\epsilon_{pc} = \Delta\epsilon_{pp} + \Delta\epsilon_{cc} \quad .$$

Unfortunately, experiments were not conducted in such a manner that the relative amounts of $\Delta\epsilon_{pp}$ and $\Delta\epsilon_{cc}$ could be determined. Information developed by Halford, et al (ref. 18) on Type 316 stainless steel in air indicates that for the strain rate (10^{-3} sec^{-1}) used in this study, the balanced part of the inelastic strain range would probably be 100 percent $\Delta\epsilon_{cc}$ at 871°C (1600°F), about 25 to 75 percent $\Delta\epsilon_{cc}$ at temperatures between 649 and 760°C (1200 and 1400°F), and about 0 percent $\Delta\epsilon_{cc}$ at temperatures below 593°C (1100°F). Thus, the continuous cycling fatigue curves presented previously contain varying proportions of $\Delta\epsilon_{cc}$ as a function of temperature.

Hold-time effects on Type 347 stainless steel: Results of the hold time tests on the Type 347 stainless steel at 760 and 871°C (1400 and 1600°F) are compared with corresponding continuous cycling data in figures 40 and 41, respectively. The results showed a definite trend of slightly improved fatigue

TABLE IX. – COMPARISON OF AVERAGE FATIGUE LIFE AND STRESS RANGE VALUES FROM COMPRESSIVE HOLD-TIME TESTS WITH THOSE FROM CONTINUOUS CYCLING TESTS OF TYPE 347 STAINLESS STEEL AND HASTELLOY ALLOY X IN HYDROGEN GAS

Temperature, °C (°F)	Total axial strain range, percent	Average fatigue life, N_f, cycles			Average stress range at $N_f/2$				
		With hold time	With continuous cycling	Ratio of hold time to continuous cycling	With hold time		With continuous cycling		Ratio of hold time to continuous cycling
					MN/m^2	ksi	MN/m^2	ksi	
Type 347 stainless steel, heat A									
760 (1400)	5.0	143	133	1.08	477	69.2	500	72.5	0.95
	3.0	359	260	1.38	472	68.4	439	63.7	1.07
	1.5	842	722	1.17	429	62.2	399	57.9	1.07
871 (1600)	3.0	592	546	1.08	237	34.4	201	29.1	1.18
Hastelloy alloy X, heat D									
760 (1400)	3.0	148	242	0.61	931	135	834	121	1.12
871 (1600)	3.0	429	521	0.82	525	76.2	440	63.8	1.19

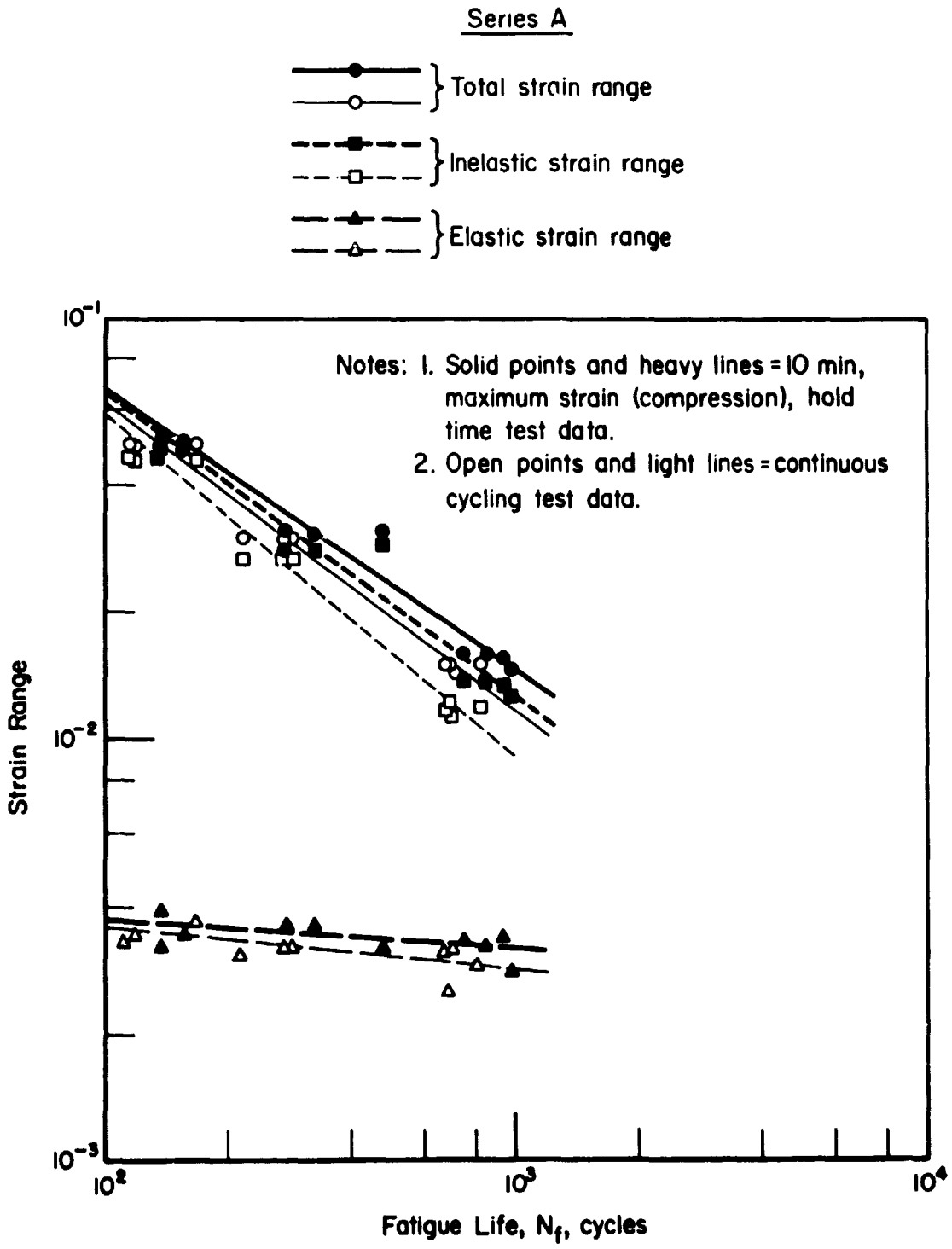

Figure 40. — Comparison of continuous cycling and 10-minute compressive hold time fatigue data for heat A of Type 347 stainless steel in hydrogen gas at 760°C (1400°F) and at an axial strain rate of 10^{-3} sec^{-1}.

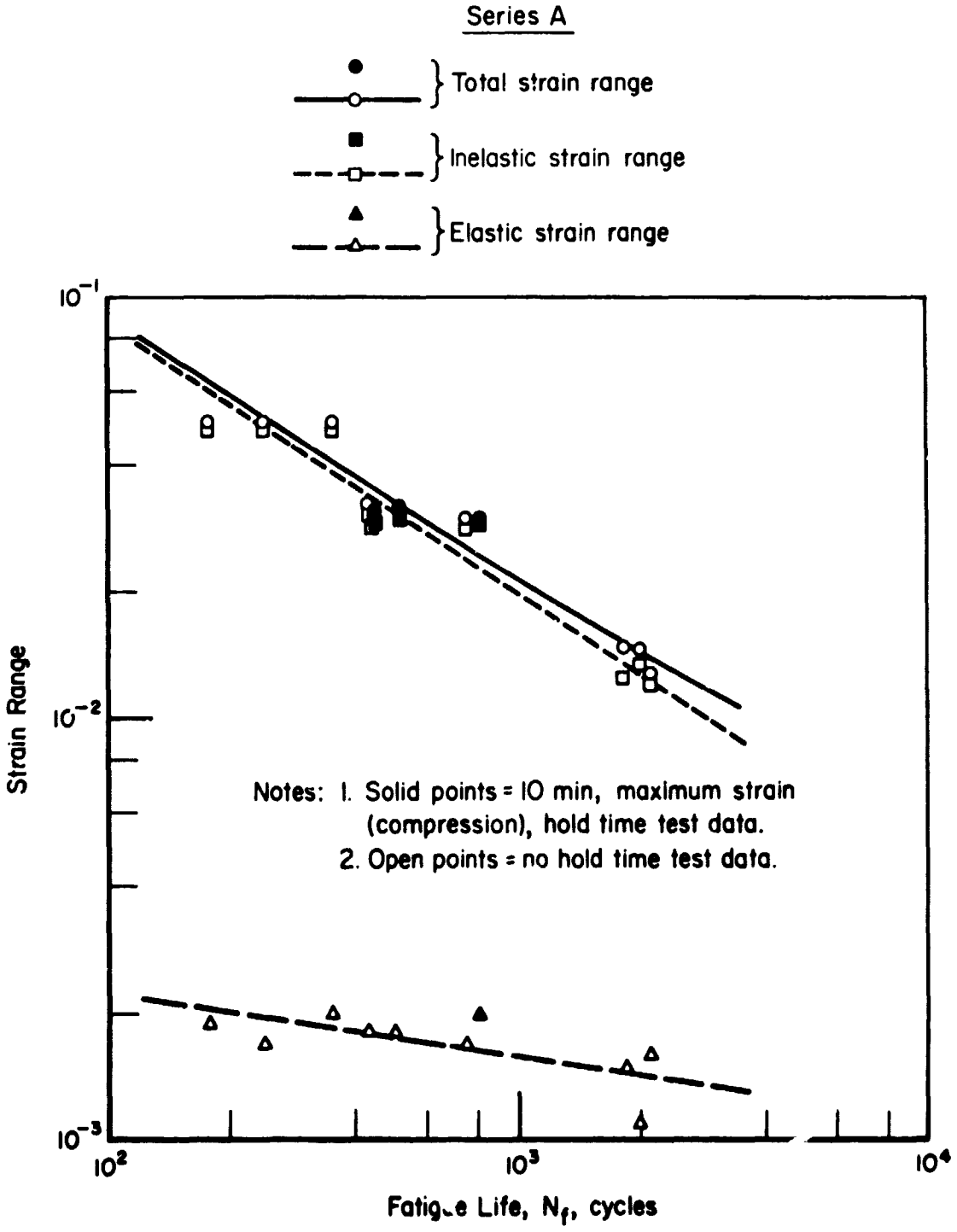

Figure 41. – Comparison of continuous cycling and 10-minute compressive hold time fatigue data for heat A of Type 347 stainless steel in hydrogen gas at 871°C (1600°F) and at an axial strain rate of 10^{-3} sec^{-1}.

resistance with hold time (solid points) as compared to without hold time (open points) at 760°C (1400°F), but no significant effect of hold time at 871°C (1600°F). The improvement at 760°C (1400°F) was slightly larger at the two lower strain ranges than at the highest one.

These trends are qualitatively in agreement with the behavior of Type 316 stainless steel in air at 704°C (1300°F) reported by Manson, et al (ref. 17), where $\Delta\epsilon_{cc}$, $\Delta\epsilon_{pc}$, and $\Delta\epsilon_{pp}$ curves fell close to one another with the $\Delta\epsilon_{cc}$ curve falling slightly below the $\Delta\epsilon_{pc}$ curve and diverging from it with increasing fatigue life. Thus, if in the present case, the continuous cycling data are predominantly of the $\Delta\epsilon_{cc}$ type, then addition of a $\Delta\epsilon_{pc}$ type of component would be beneficial to fatigue resistance. Furthermore, close inspection of the data at 760°C (1400°F) in table B10 of Appendix B shows that the value of $\Delta\epsilon_{pc}$ ($\Delta\epsilon_{ed}$-$\Delta\epsilon_{ei}$) is relatively constant at a value of about 0.12, regardless of total strain range. Therefore, it was a larger portion of $\Delta\epsilon_{in}$ at low strain ranges than at high strain ranges. At 871°C (1600°F), $\Delta\epsilon_{pc}$ was only about 0.08 percent or less and was thus only about 3 percent of the value of $\Delta\epsilon_{in}$. More exact, quantitative correlations using the strain range partitioning approach were not possible because of the lack of relevant and appropriate data.

To investigate possible reasons why the $\Delta\epsilon_{cc}$ type of cycle was more deleterious than the $\Delta\epsilon_{pc}$ type, limited fractographic and metallographic studies were conducted. The results are discussed later in this report.

Hold-time effects on Hastelloy Alloy X: Since only two hold-time tests were conducted on Hastelloy Alloy X, the data were not plotted as were those for the Type 347 stainless steel. The cyclic lives of 148 and 429 are slightly below the average values of 240 and 520 for corresponding continuous cycling tests at 760 and 871°C (1400 and 1600°F), respectively. However, both specimens failed by development of a cyclic deformation instability that resulted in necking in the specimen test section rather than by fatigue cracking. Both Coffin (ref. 19) and Sheffler (ref. 20) have noted that such instabilities are more likely to develop in the absence of severe environmental degradation for fatigue experiments on Type 304 stainless steel in high vacuum at temperatures of 815 and 649°C (1500 and 1200°F), respectively. The stress range at $N_f/2$

for the hold-time tests was about 12 percent greater at 760°C (1400°F) and about 19 percent greater at 871°C (1600 F) than that for comparable (same $\Delta\varepsilon_t$) continuous cycling tests. The relation of this increased stress range to the cyclic instability cannot be explained on the basis of this limited experimental study of hold-time fatigue of Hastelloy Alloy X. Further, hold-time experiments were not carried out on this alloy because it was concluded that the fatigue resistance of the Type 347 stainless steel was better than that of the Hastelloy Alloy X under the particular conditions of this study.

Fractographic and metallographic studies of failed Type 347 stainless steel specimens

The fracture and microstructural characteristics of specimens of Type 347 stainless steel tested with a compressive hold time of 10 minutes during cycling were compared to those tested under conditions of continuous cycling. This work was limited to specimens of heat A that were tested at 760°C (1400°F). Fractographic studies were made on the specimens fatigue tested at strain ranges of 1.5, 3.0, and 5.0 percent. In addition, metallographic studies were conducted on polished and etched sections of a specimen tested at 1.5 percent strain range with no hold time, as well as one with a 10-minute hold period in compression.

Fractographic examinations.—The fracture surfaces were examined using a binocular microscope at magnifications up to 90X. In addition, the surfaces of the specimens adjacent to the fatigue failures were examined for evidence of secondary cracking and upset.

All fracture surfaces exhibited some discoloration (oxidation). In some specimens, the degree of oxidation was considerably greater. In all cases, the fracture surfaces contained more oxidation than did the machined surfaces. This was to be expected, however, since freshly cracked stainless steel surfaces are more active than machined surfaces on which a thin protective oxide has been allowed to form in air at room temperature.

Specimens without compression hold: The amount of oxidation increased with decreasing strain range; i.e., the specimens tested at 1.5 percent strain range oxidized over a larger area of the fracture surface than those tested at 3.0 or 5.0 percent strain range. This suggested that the fatigue cracks

propagated slower and that cracks or fissures were exposed to the environment for a longer period of time prior to final rupture in the low strain-range specimens.

Secondary tearing, after the primary fracture phase, at the sides of the specimens appeared to be greatest in the specimens strained 3.0 percent on each cycle. These specimens showed considerably more secondary tears than the specimens strained 5.0 percent on each cycle. The specimens tested with 1.5 percent axial strain range exhibited somewhat erratic results — two specimens had no secondary tears, while the other two had about the same number of secondary tears as those tested at 3.0 percent strain range.

All specimens tested without a compression hold period during cycling had multiple origins on the fracture surfaces and the fatigue cracks appeared to propagate uniformly from these origins.

Specimens with compression hold: All specimens tested with a 10-minute compression hold exhibited some upset immediately adjacent to the fracture. However, the amount of upset decreased with increased strain, i.e., the specimens tested at 1.5 percent strain range exhibited considerably more upset than the specimens tested at 3.0 or 5.0 percent.

The fracture surfaces of all specimens exhibited some discoloration (oxidation) and, as was the case with the specimens tested without a hold time, the amount of oxidation decreased with increasing strain range.

In contrast to the specimens tested with no hold time, the fracture surfaces of the hold-time specimens exhibited only one or two major crack propagation paths. Although several points of initiation may have formed, only one or two propagated. In addition, the hold-time specimens showed far less secondary cracking or tearing than the no hold-time specimens.

Principal fractographic results: The principal finding of the fractographic examination was that the no-hold specimens had several points of crack initiation which propagated in a fairly uniform manner. The hold specimens also had several local areas of crack initiation, but only one or two of these propagated. The hold specimens exhibited upset at the sides of the specimens a short distance from the fracture surface; the no-hold specimens did not.

Metallographic examinations.—Metallographic studies of polished and etched sections were made on two specimens (A18 and A49). Both specimens

had been tested at a total axial strain range of 1.5 percent, the former with no hold time and the latter with a 10-minute hold period in compression on each cycle.

Specimen without compression hold: The microstructure of a longitudinal section through the fracture of the no-hold specimen is shown in figure 42(a). It was noted that some holes (or voids) existed near the fracture surface, and that some strain lines were faintly evident. The nature of the fracture could not be ascertained because of the fine grain size; i.e., it could not be determined from the metallographic section if the principal fracture was transgranular or intergranular. Careful examination suggested that material existed in these voids. It is believed that this material was an oxide or inclusion, and that the voids formed in or adjacent to an inclusion and opened up during cycling. Similar voids are often observed in tensile creep rupture test specimens that have entered third-stage creep. It was also noted that the strain lines are rather aligned and straight.

The microstructure of a longitudinal section well removed [about 6.35 mm (0.25 inch)] from the fracture is shown in figure 42(b). Strain and voids were not evident.

The microstructure of a secondary crack is shown in figure 42(c). This secondary crack was predominantly intergranular.

Specimen with compression hold: The microstructure of a longitudinal section through the fracture is shown in figure 43(a). Again, it could not be determined from the metallographic section if the failure was intergranular or transgranular. Some voids were observed; however, they were much smaller than in the no-hold specimen. Although strain was evident, there was no directionality to the strain lines and the general microstructure was distorted in all directions.

The microstructure about 6.35 mm (0.25 inch) from the fracture is shown in figure 43(b). The structure is similar to that of the no-hold specimen, shown in figure 42(b). Although not shown by means of photomicrographs, the hold specimen contained little evidence of secondary tears. The one or two secondary cracks observed were only about 0.1 mm (0.004 inch) deep and appeared to be predominantly intergranular.

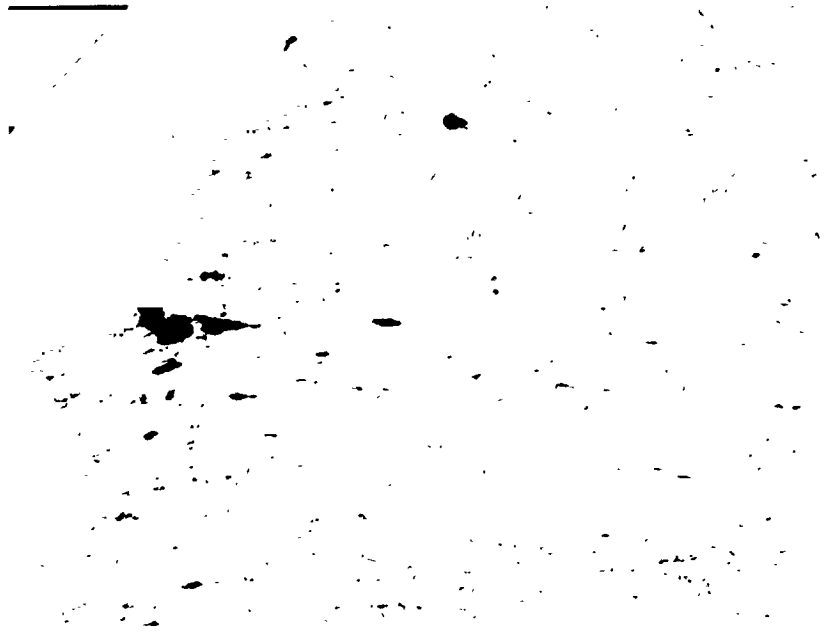

100X Glyceregia Etch 1G011

(a) Longitudinal section through the fracture.

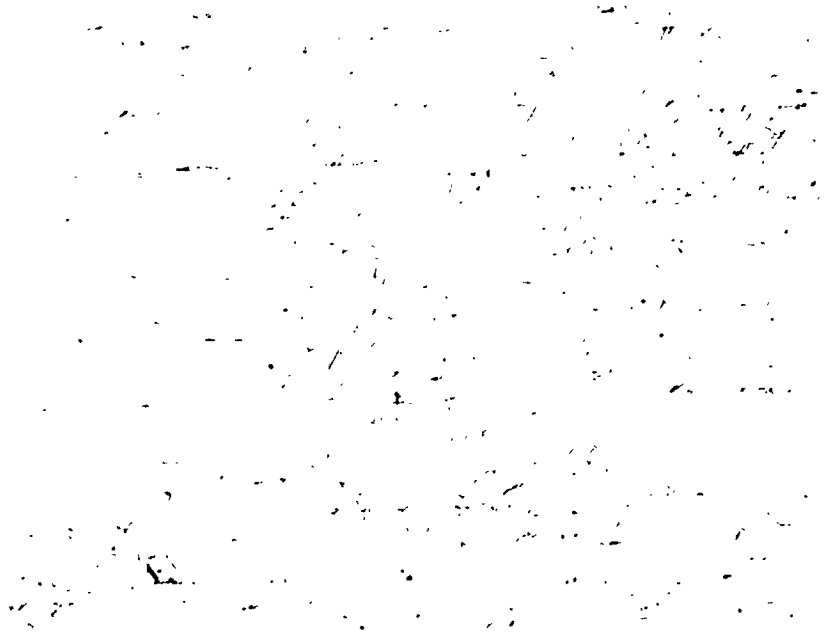

100X Glyceregia Etch 1G010

(b) Longitudinal section through specimen about 6.35 mm (0.25 in.) from fracture.

Figure 42. – Photomicrographs of specimen A18 tested under continuous strain cycling at 1.5 percent total axial strain range and in hydrogen gas at 760°C (1400°F).

REPRODUCIBILITY OF THE ORIGINAL PAGE IS POOR

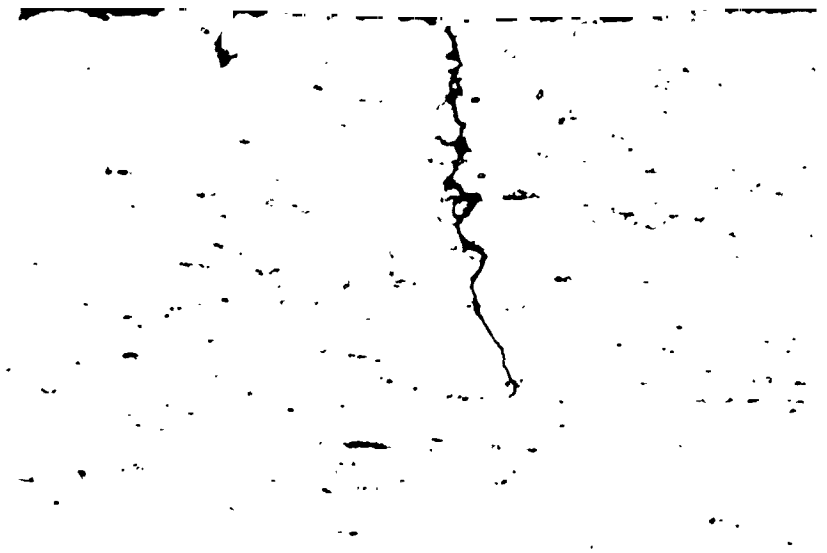

250X Glyceregia Etch 1G012

(c) Longitudinal section through secondary rupture.

Figure 42. – (Continued)

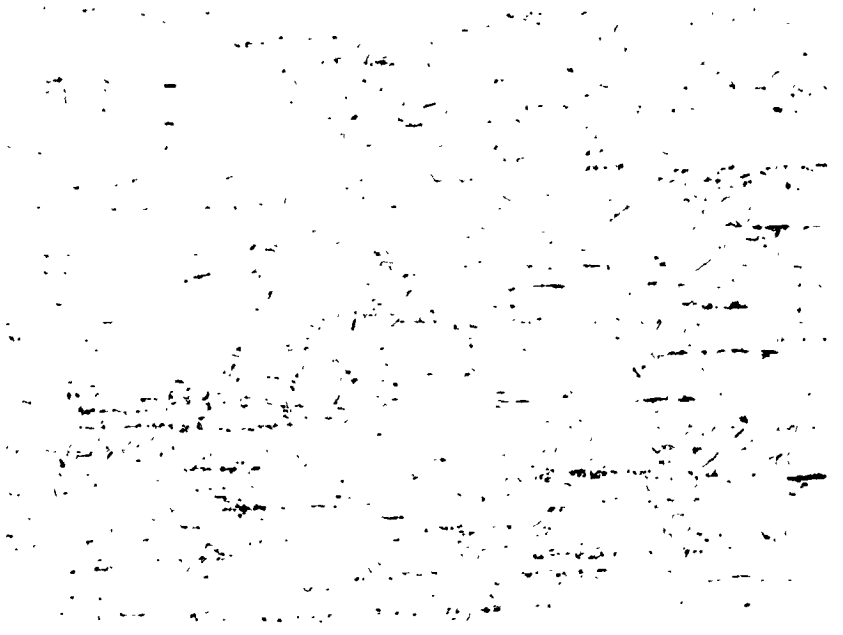

250X Glyceregia Etch 1G108

a. Longitudinal section through the fracture.

100X Glyceregia Etch 1G109

b. Longitudinal section through specimen about 6.35 mm (0.25 in.) from fracture.

Figure 43. – Photomicrographs of specimen A49 tested at 1.5 percent total axial strain range with a 10-minute compressive hold time and in hydrogen gas at 760°C (1400°F).

Principal metallographic results: The metallographic examination revealed that both the hold and no-hold specimens contained some grain-boundary voids adjacent to the fracture. The no-hold specimens had much larger voids, which appeared to have formed at inclusions. In the no-hold specimens, strain was better defined and directionally oriented. In the hold specimens, strain had no directional orientation.

Summary of fractographic and metallographic studies.—The metallographic examinations were too brief to fully substantiate the above findings. However, the observations did indicate that there were both microstructural and fractographic differences in specimens tested without a hold time in compression and with a 10-minute hold in compression. The variation in the size of the voids adjacent to the fracture indicated that the compression hold tended to inhibit void formation or close voids that were formed by tensile creep strain in the material. This may explain the improved fatigue resistance of the specimens tested with a 10-minute hold time at maximum compressive strain.

CONCLUSIONS

In this investigation, the low-cycle-fatigue characteristics of 3 heats of Type 347 stainless steel and 2 heats of Hastelloy Alloy X were evaluated in both hydrogen gas and air at temperatures from 538 to 871°C (1000 to 1600°F) and at total axial strain ranges of 1.5, 3.0, and 5.0 percent. The approximate range in fatigue life for all conditions was from 100 to 2000 cycles. The following conclusions were made:

(1) In hydrogen gas

(a) The cyclic stress-strain behavior of both materials at 538°C (1000°F) was characterized by appreciable cyclic hardening at all strain ranges. At 760°C (1400°F), Type 347 stainless steel was almost stable (showed little cyclic hardening) and Hastelloy Alloy X still exhibited considerable cyclic hardening, especially at the 5.0 percent total axial strain range. At 871°C (1600°F), neither material hardened significantly; in fact, for Type 347

stainless steel at 5.0 percent axial strain range, there was continuous cyclic softening until failure.

(b) The fatigue resistance of Type 347 stainless steel material was somewhat higher than that of Hastelloy Alloy X at all temperatures between 538 and 871°C (1000 and 1600°F) and all total axial strain ranges between 1.5 and 5.0 percent.

(c) The lowest fatigue resistance of the Type 347 stainless steel occurred between 704 and 760°C (1300 and 1400°F). The Hastelloy Alloy X displayed the lowest fatigue resistance at 538°C (1000°F) for the 3.0 and 5.0 percent axial strain range and at 760°C (1400°F) for the 1.5 percent axial strain range.

(d) Little heat-to-heat variation in fatigue resistance was observed for either material at any specific condition, except for the Hastelloy Alloy X at 760°C (1400°F), where heat D exhibited greater fatigue resistance than heat E.

(e) In comparison with continuous cycling, the 10-minute compressive hold time experiments at 760 and 871°C (1400 and 1600°F) resulted in increased fatigue lives for Type 347 stainless steel and decreased fatigue lives for Hastelloy Alloy X. The hold-time effects on fatigue life were qualitatively explained by strain-range partitioning. The stress relaxation behavior of both materials was also analytically described by an exponential decay function.

(f) Fractographic and metallographic studies indicated that both hold-time and continuous-cycling specimens developed some grain boundary voids near fracture. The size of these voids indicated, however, that compressive hold times tended to inhibit the growth of voids or caused some to close.

(2) In air

(a) The data generated in this study compared closely with other data in the literature on similar austenitic alloys.

(b) Both alloys showed slightly lower fatigue resistance in air than in hydrogen gas for temperatures up to 760°C (1400°F).

(c) The fatigue resistance of the Type 347 stainless steel in air was considerably below that in hydrogen gas at 871°C (1600°F), due to oxidation. The Hastelloy Alloy X, which was not appreciably affected by oxidation, showed somewhat better fatigue resistance at 871°C (1600°F) than at 760°C (1400°F).

(d) The Type 347 stainless steel was slightly higher than the Hastelloy Alloy X in fatigue resistance at 538 and 760°C (1000 and 1400°F) but lower at 871°C (1600°F).

RECOMMENDATIONS

On the basis of findings in this study, several areas warrant further investigation. They are, in an approximate order of increasing complexity and involvement,

(a) Additional experimentation at different strain rates to develop $\Delta\epsilon_{pp}$-N_f and $\Delta\epsilon_{cc}$-N_f bounds on the high-temperature continuous-cycling life characteristics of both alloys. This work would involve slower strain rates at 538°C (1000°F), both slower and faster strain rates at 760°C (1400°F), and faster strain rates at 871°C (1600°F). These results would also indicate the sensitivity of these relationships to temperature.

(b) Experiments with longer hold times in both air and hydrogen gas are needed to make the information pertinent for other service applications, such as reactor components.

(c) Laboratory assessment of the severity of $\Delta\epsilon_{cp}$ (tension strain or load holds) loading cycles in hydrogen gas.

(d) Laboratory assessment of both $\Delta\epsilon_{cp}$ and $\Delta\epsilon_{pc}$ types of load cycles in air.

(e) Further work on lower strain range, high-cycle fatigue where Hastelloy Alloy X should have superior fatigue resistance to Type 347 stainless steel because of its superior strength.

(f) Component testing to evaluate the effect of multiaxial stress-strain conditions on the high-temperature fatigue resistance of both alloys.

APPENDIX A

CYCLICALLY STABLE (AT $N_f/2$) STRESS RELAXATION DATA FROM COMPRESSIVE HOLD-TIME TESTS OF TYPE 347 STAINLESS STEEL (HEAT A) AND HASTELLOY ALLOY X (HEAT D) IN HYDROGEN GAS

Specimen A43
at 760°C (1400°F)
and $\Delta\epsilon_t$ = 4.97

Time, min	Compressive stress level	
	MN/m^2	ksi
0	259	37.7
0.025	232	33.7
0.050	212	30.8
0.075	202	29.3
0.10	195	28.3
0.20	178	25.8
0.40	161	23.3
1.0	140	20.3
2.0	123	17.9
4.0	110	15.9
6.0	103	14.9
8.0	99.3	14.4
10.0	95.8	13.9

Specimen A48
at 760°C (1400°F)
and $\Delta\epsilon_t$ = 4.97

Time, min	Compressive stress level	
	MN/m^2	ksi
0	255	37.0
0.025	217	31.5
0.050	207	30.0
0.10	193	28.0
0.20	179	26.0
0.40	166	24.0
0.80	152	22.0
1.0	148	21.5
2.0	138	20.0
4.0	124	18.0
6.0	121	17.5
8.0	117	17.0
10.0	114	16.5

Specimen A44
at 760°C (1400°F)
and $\Delta\epsilon_t$ = 4.97

Time, min	Compressive stress level	
	MN/m^2	ksi
0	203	29.4
0.025	165	23.9
0.050	144	20.9
0.10	130	18.9
0.20	120	17.4
0.50	100	14.5
1.0	95.8	13.9
2.0	82.7	12.0
4.0	68.7	10.0
6.0	68.7	10.0
8.0	68.7	10.0
10.0	68.7	10.0

Specimen A50
at 760°C (1400°F)
and $\Delta\epsilon_t$ = 3.06

Time, min	Compressive stress level	
	MN/m^2	ksi
0	240	34.9
0.05	184	26.7
0.10	172	24.9
0.20	168	23.4
0.40	148	21.4
0.70	137	19.9
1.0	130	18.9
2.0	110	15.9
4.0	95.8	13.9
6.0	93.1	13.5
8.0	88.9	12.9
10.0	86.2	12.5

PRECEDING PAGE BLANK NOT FILMED

Specimen A51
at 760°C (1400°F)
and $\Delta\varepsilon_t$ = 3.06

Time, min	Compressive stress level	
	MN/m^2	ksi
0	235	34.1
0.05	200	29.1
0.10	183	26.6
0.20	169	24.5
0.40	155	22.5
0.70	145	21.0
1.0	138	20.0
2.0	124	18.0
4.0	110	16.0
6.0	103	15.0
8.0	100	14.5
10.0	99.0	14.3

Specimen A46
at 760°C (1400°F)
and $\Delta\varepsilon_t$ = 3.06

Time, min	Compressive stress level	
	MN/m^2	ksi
0	225	32.6
0.25	145	21.0
0.50	121	17.6
1.0	110	16.0
2.0	93.8	13.6
3.0	84.1	12.2
5.0	77.2	11.2
7.0	71.7	10.4
9.0	67.6	9.80
10.0	66.1	9.60

Specimen A47
at 760°C (1400°F)
and $\Delta\varepsilon_t$ = 1.54

Time, min	Compressive stress level	
	MN/m^2	ksi
0	199	28.9
0.025	174	25.3
0.050	165	24.0
0.10	147	21.4
0.20	136	19.8
0.40	123	17.8
0.70	113	16.4
1.0	109	15.8
2.0	93.8	13.6
4.0	88.3	12.8
6.0	85.5	12.4
8.0	80.0	11.6
10.0	74.5	10.8

Specimen A45
at 760°C (1400°F)
and $\Delta\varepsilon_t$ = 1.54

Time, min	Compressive stress level	
	MN/m^2	ksi
0	217	31.5
0.025	196	28.4
0.05	181	26.2
0.10	171	24.8
0.20	159	23.0
0.40	139	20.2
0.70	130	18.8
1.0	122	17.7
2.0	107	15.5
4.0	94.5	13.7
6.0	89.0	12.9
8.0	84.8	12.3
10.0	80.7	11.7

Specimen A49
at 760°C (1400°F)
and $\Delta\varepsilon_t$ = 1.54

Time, min	Compressive stress level	
	MN/m^2	ksi
0	231	33.5
0.025	202	29.3
0.050	190	27.5
0.10	180	26.1
0.20	166	24.1
0.40	152	22.0
0.70	139	20.2
1.0	131	19.0
2.0	117	17.0
4.0	105	15.2
6.0	99.3	14.4
8.0	93.8	13.6
10.0	89.6	13.0

Specimen A42
at 760°C (1400°F)
and $\Delta\varepsilon_t$ = 1.54

Time, min	Compressive stress level	
	MN/m^2	ksi
0	205	29.7
0.125	190	27.5
0.25	175	25.4
0.50	154	22.3
1.0	133	19.3
2.0	115	16.6
3.0	106	15.4
4.0	101	14.6
6.0	93.1	13.5
8.0	88.9	12.9
10.0	86.2	12.5

Specimen A52
at 871°C (1600°F)
and $\Delta\varepsilon_t$ = 3.01

Time, min	Compressive stress level	
	MN/m^2	ksi
0	117	16.9
0.05	81.0	11.7
0.10	70.0	10.1
0.20	63.0	9.07
0.40	51.4	7.46
0.70	41.7	6.05
1.0	40.0	5.65
2.0	36.1	5.24
4.0	33.4	4.84
6.0	30.6	4.44
8.0	27.8	4.03
10.0	26.4	3.83

Specimen A63
at 871°C (1600°F)
and $\Delta\varepsilon_t$ = 3.01

Time, min	Compressive stress level	
	MN/m^2	ksi
0	116	16.8
0.25	55.3	8.02
0.50	47.0	6.81
1.0	[illegible]	5.61
1.5	[illegible]	5.21
2.0	[illegible]	5.01
3.0	[illegible]	4.41
5.0	[illegible]	4.01
7.0	25.0	3.61
10.0	22.1	3.21

Specimen A53
at 871°C (1600°F)
and $\Delta\varepsilon_t$ = 3.01

Time, min	Compressive stress level	
	MN/m^2	ksi
0	128	18.6
0.025	99.3	14.4
0.05	91.0	13.2
0.10	80.0	11.6
0.20	70.3	10.2
0.40	62.1	9.02
0.70	55.3	8.02
1.0	52.5	7.62
2.0	45.6	6.61
4.0	38.7	5.61
6.0	34.5	5.01
8.0	31.8	4.61
10.0	29.0	4.21

Specimen D48
at 760°C (1400°F)
and $\Delta\varepsilon_t$ = 3.05

Time, min	Compressive stress level	
	MN/m^2	ksi
0	476	69.0
0.045	343	49.7
0.18	265	38.5
0.27	245	35.5
0.36	231	33.5
0.45	224	32.5
0.72	200	29.0
1.08	179	26.0
1.44	167	24.3
2.16	146	21.3
3.56	130	18.8
5.00	115	16.7
7.16	105	15.2
10.00	101	14.7

Specimen D49
at 871 °C (1600°F)
and $\Delta\varepsilon_t$ = 3.05

Time, min	Compressive stress level	
	MN/m^2	ksi
0	251	36.5
0.125	157	22.8
0.25	91.0	13.2
0.50	59.4	8.62
1.0	49.0	7.10
2.0	38.6	5.60
3.0	31.4	4.56
4.0	28.0	4.05
6.0	24.4	3.55
8.0	17.4	2.53
10.0	14.0	2.02

APPENDIX B

CONTINUOUS CYCLING AND HOLD-TIME FATIGUE DATA FOR TYPE 347 STAINLESS STEEL AND HASTELLOY ALLOY X

PRECEDING PAGE BLANK NOT FILMED

TABLE B1. – SUMMARY OF CONTINUOUS CYCLING FATIGUE DATA FOR TYPE 347 STAINLESS STEEL IN AIR AND AT AN AXIAL STRAIN RATE OF 10^{-3} SEC^{-1}

Specimen	Temperature, °C (°F)	Total axial strain range, $\Delta\epsilon_t$	Axial strain range at $N_f/2$, percent		Stress range at $N_f/2$, $\Delta\sigma$		Fatigue life, cycles		
			Inelastic, $\Delta\epsilon_{in}$	Elastic, $\Delta\epsilon_e$	MN/m^2	ksi	N_o	N_s	N_f
A67	538 (1000)	4.94	4.42	0.52	821	119	136	138	142
A68		2.97	2.52	0.45	696	101	298	301	304
A73		1.54	1.19	0.35	574	83.2	905	912	925
A69		1.53	1.18	0.35	568	82.4	1129	1146	1170
C2	760 (1400)	4.92	4.54	0.38	446	64.7	81	88	95
A4		5.10	4.73	0.37	461	66.8	60	78	96
B1		5.11	4.77	0.34	487	70.6	80	87	118
B7		3.32	2.99	0.33	438	63.5	120	140	195
C1		2.64	2.42	0.22	352	51.1	137	167	197
A3		3.09	2.80	0.29	418	60.6	125	135	200
A5		2.59	2.35	0.24	331	48.0	148	177	217
B3		3.31	2.99	0.32	421	61.0	140	157	219
B2		3.09	2.81	0.28	390	56.5	130	141	233
B9		1.63	1.35	0.28	367	53.2	280	310	477
B8		1.64	1.34	0.30	376	54.5	300	330	485
C4		1.64	1.32	0.29	355	51.5	400	420	591
A2		1.57	1.29	0.28	431	62.5	430	465	655
A70	871 (1600)	4.90	4.69	0.21	245	35.5	46	65	87
A71		2.98	2.79	0.19	236	34.3	98	107	134
A72		1.53	1.34	0.19	227	32.9	286	288	292
A74		1.54	1.36	0.18	232	33.7	--	--	329

TABLE B2. – SUMMARY OF CONTINUOUS CYCLING FATIGUE DATA FOR HASTELLOY ALLOY X IN AIR AND AT AN AXIAL STRAIN RATE OF 10^{-3} SEC^{-1}

Specimen	Temperature, °C (°F)	Total axial strain range, $\Delta\varepsilon_t$	Axial strain range at $N_f/2$, percent		Stress range at $N_f/2$, $\Delta\sigma$		Fatigue life, cycles		
			Inelastic, $\Delta\varepsilon_{in}$	Elastic, $\Delta\varepsilon_e$	MN/m^2	ksi	N_o	N_5	N_f
D53		5.05	4.22	0 83	1680	243	44	48	49
D54	538 (1000)	3.05	2.27	0.78	1520	221	96	104	105
D58		3.24	2.38	0.86	1480	214	129	131	134
D56		1.50	0.89	0.61	1120	162	676	710	754
D55		1.50	0.93	0.57	1100	160	682	721	760
E1		5.23	4.63	0.60	938	136	56	59	62
D1		5.22	4.58	0.64	972	141	70	81	90
E2		3.22	2.62	0.60	855	124	116	118	128
D3	760 (1400)	3.47	2.83	0.64	882	128	125	131	156
D2		3.18	2.65	0.53	855	124	145	157	184
E5		1.66	1.19	0.47	752	109	363	365	387
E3		1.69	1.14	0.55	862	125	370	415	470
D4		1.66	1.14	0.52	724	105	420	441	540
D50		5.02	4.64	0.38	476	69.0	98	100	120
D52		3.03	2.68	0.35	466	67.6	192	200	206
D51	871 (1600)	1.55	1.21	0.34	445	64.5	--	--	506
D57		1.54	1.26	0.28	405	58.8	575	577	595

REPRODUCIBILITY OF THE
ORIGINAL PAGE IS POOR

TABLE B3. — SUMMARY OF CONTINUOUS CYCLING FATIGUE DATA FOR TYPE 347 STAINLESS STEEL IN HYDROGEN GAS AT 538°C (1000°F) AND AT AN AXIAL STRAIN RATE OF 10^{-3} SEC^{-1}

Specimen	Total axial strain range, $\Delta\varepsilon_t$	Axial strain range at $N_f/2$, percent		Stress range at $N_f/2$, $\Delta\sigma$		Fatigue life, cycles		
		Inelastic, $\Delta\varepsilon_{in}$	Elastic, $\Delta\varepsilon_e$	MN/m^2	ksi	N_o	N_s	N_f
B24[a]	4.94	4.39	0.55	814	118	120	--	124
A21	4.92	4.38	0.54	841	122	121	125	132
B19[a]	4.94	4.34	0.60	841	122	141	--	142
B21	4.92	4.36	0.56	848	123	147	148	150
C15	4.93	4.40	0.53	841	122	153	153	155
C16	4.93	4.42	0.51	841	122	156	157	164
A25	4.97	4.41	0.56	834	121	166	167	170
A22	4.89	4.22	0.67	834	121	165	168	172
C17	4.92	4.25	0.67	841	122	171	172	174
A26	2.92	2.48	0.44	690	100	288	293	300
B26	2.91	2.37	0.54	752	109	307	320	327
C22	2.95	2.44	0.51	724	105	331	332	336
B25	2.92	2.43	0.49	738	107	336	337	339
C19	2.91	2.45	0.46	731	106	361	364	372
C21	2.92	2.46	0.46	738	107	367	373	397
A27[b]	2.92	2.38	0.54	779	113	--	--	401
A28	2.96	2.49	0.47	731	106	385	397	403
B27	2.89	2.44	0.45	731	106	382	389	405
C14	1.50	1.13	0.37	598	86.8	1303	1320	1369
B22	1.48	1.11	0.37	610	88.5	1555	1570	1590
A20	1.49	1.10	0.39	607	88.0	1812	1822	1856
B23	1.38	1.01	0.37	583	84.5	1840	1857	1877
C20	1.49	1.08	0.41	598	86.7	1810	1912	1952
A24	1.48	1.07	0.41	583	84.5	1949	1951	1975
A23	1.46	1.04	0.42	594	86.2	2238	2241	2251
C18	1.47	1.12	0.35	560	81.2	2425	2435	2443
B20	1.39	0.99	0.40	565	82.0	2495	2500	2536

(a) The values of N_o and N_s are not defined for these because the load continued to increase until failure occurred.

(b) The value of N_s is not reported because the tensile load did not drop off 5 percent before failure.

TABLE B4. – SUMMARY OF CONTINUOUS CYCLING FATIGUE DATA FOR HASTELLOY ALLOY X IN HYDROGEN GAS AT 538°C (1000°F) AND AN AXIAL STRAIN RATE OF 10^{-3} SEC^{-1}

Specimen	Total axial strain range, $\Delta\varepsilon_t$	Axial strain range at $N_f/2$, percent		Stress range at $N_f/2$, $\Delta\sigma$		Fatigue life, cycles		
		Inelastic, $\Delta\varepsilon_{in}$	Elastic, $\Delta\varepsilon_e$	MN/m^2	ksi	N_o	N_s	N_f
E23	4.90	3.99	0.91	1709	248	27	28	30
E19	4.85	3.70	1.15	1676	242	48	49	51
D17	4.73	3.76	0.97	1600	232	52	54	56
D28[a]	5.04	4.14	0.90	1703	247	--	--	56
D25	5.02	4.16	0.86	1620	235	76	79	81
D22	4.95	4.13	0.82	1551	225	76	79	93
E20	4.75	3.65	1.10	1607	232	93	96	98
E18	4.86	3.76	1.10	1607	232	90	101	104
E30	4.96	4.12	0.84	1586	230	92	94	104
D18	3.02	2.08	0.94	1386	200	174	177	179
E22	2.95	2.22	0.73	1476	214	171	176	194
D23[b]	3.01	2.28	0.73	1420	206	210	--	212
E25	2.94	2.18	0.76	1462	211	232	233	238
D27	2.96	2.18	0.78	1476	214	233	238	240
E28	3.00	2.26	0.74	1469	212	238	239	241
E29	2.96	2.17	0.79	1482	215	287	288	289
D26	3.00	2.22	0.78	1469	212	303	313	328
E21	1.49	0.88	0.61	1165	168	820	830	846
D21	1.50	0.91	0.59	1096	158	992	1005	1029
D24	1.45	0.85	0.60	1172	170	1312	1313	1315
E27[c]	1.50	0.92	0.58	1138	164	--	--	1589
E24	1.50	0.93	0.57	1124	162	1642	1642	1644
D19	1.26	0.67	0.59	993	144	1756	1763	1775
E26	1.40	0.83	0.57	1069	155	2183	2184	2193
D29	1.46	0.90	0.56	1055	153	2143	2150	2205
D20	1.21	0.58	0.63	1014	147	4694	4696	4750

(a) The values of N_o and N_s are not defined for these because the load continued to increase until failure occurred.

(b) The value of N_s is not reported because the tensile load did not drop off 5 percent before failure.

TABLE B5. – SUMMARY OF CONTINUOUS CYCLING FATIGUE DATA FOR TYPE 347 STAINLESS STEEL IN HYDROGEN GAS AT 760°C (1400°F) AND AT AXIAL STRAIN RATE OF 10^{-3} SEC^{-1}

Specimen	Total axial strain range, $\Delta\varepsilon_t$	Axial strain range at $N_f/2$, percent		Stress range at $N_f/2$, $\Delta\sigma$		Fatigue life, cycles		
		Inelastic, $\Delta\varepsilon_{in}$	Elastic, $\Delta\varepsilon_e$	MN/m^2	ksi	N_0	N_5	N_f
B11[a]	4.88	4.54	0.34	472	68.5	---	---	102
C6	4.92	4.56	0.36	452	65.5	104	105	111
A12	4.89	4.56	0.33	500	72.5	103	108	113
A11	4.88	4.54	0.34	473	68.6	111	113	119
C7	4.87	4.54	0.33	500	72.5	128	128	135
B10[b]	4.88	4.55	0.33	485	70.4	123	127	150
B12	4.87	4.53	0.34	472	68.5	150	155	162
A10[b]	4.89	4.52	0.37	527	76.4	160	160	168
C5[b]	4.85	4.53	0.32	452	65.5	182	185	191
B14[a]	2.94	2.64	0.30	452	65.5	---	---	162
A17	2.96	2.65	0.31	459	66.6	185	193	214
C9	2.95	2.60	0.35	459	66.5	222	227	238
B18	2.94	2.62	0.32	390	56.6	217	250	258
B15	2.95	2.59	0.36	439	63.6	243	246	260
A19	2.96	2.64	0.32	413	59.9	200	225	280
A13	2.94	2.62	0.32	445	64.5	235	260	286
C11	2.95	2.65	0.30	376	54.6	270	271	299
C10	2.95	2.64	0.31	396	57.5	325	327	368
B16[a]	1.49	1.19	0.30	360	52.2	---	---	648
A14	1.49	1.18	0.31	424	61.5	620	650	677
A16	1.49	1.24	0.25	378	54.8	682	683	691
A15	1.45	1.13	0.32	397	57.6	616	650	700
B13	1.49	1.24	0.25	368	53.3	515	520	739
B17	1.50	1.20	0.30	378	54.8	735	740	790
C13	1.46	1.17	0.29	348	50.4	760	760	796
A18	1.49	1.20	0.29	397	57.6	750	775	820
C8[a]	1.49	1.23	0.26	363	52.6	---	---	822
C12	1.50	1.23	0.27	376	54.5	850	879	950

(a) Values of N_0 and N_5 are not reported because before failure occurred, the load began to increase.

(b) These specimens were tested in the "Nix Ox" catalyst purified hydrogen atmosphere; all others were tested in a palladium catalyst purified hydrogen atmosphere.

TABLE B6. – SUMMARY OF CONTINUOUS CYCLING FATIGUE DATA FOR HASTELLOY ALLOY X IN HYDROGEN GAS AT 760° C (1400° F) AND AN AXIAL STRAIN RATE OF 10^{-3} SEC^{-1}

Specimen	Total axial strain range, $\Delta\varepsilon_t$	Axial strain range at $N_f/2$, percent		Stress range at $N_f/2$, [illegible]		Fatigue life, cycles		
		Inelastic, $\Delta\varepsilon_{in}$	Elastic, $\Delta\varepsilon_e$	MN/m^2	ksi	N_c	N_s	N_f
E8 (a)	4.91	4.28	0.63	1010	146	49	49	50
E6 (a)	4.89	4.23	0.66	993	144	58	57	59
E13(b)	4.92	4.36	0.56	952	138	--	53	61
E7 (a)	4.92	4.33	0.59	1000	145	64	64	67
D14	4.92	4.29	0.63	896	130	97	80	99
D5 (a)	4.88	4.31	0.57	1000	145	106	105	108
D7 (a)	4.93	4.34	0.59	931	135	134	132	136
D6 (a)	4.88	4.25	0.63	993	144	134	134	137
D16(b)	2.96	2.41	0.55	885	124	---	201	203
E16	2.92	2.32	0.60	821	119	227	223	228
D15	2.96	2.39	0.57	848	123	228	227	230
D10	2.98	2.32	0.66	821	119	235	232	251
E10	2.84	2.24	0.60	793	115	250	247	262
E17	2.92	2.30	0.62	786	114	265	255	275
D9	2.94	2.44	0.50	814	118	252	251	283
E11	2.93	2.38	0.55	738	107	255	230	314
E9	1.45	0.99	0.46	752	109	577	573	629
E14(c)	1.48	1.04	0.44	731	106	---	---	708
E12	1.47	1.03	0.44	752	109	685	675	720
D11	1.47	0.99	0.48	724	105	833	825	865
D8	1.50	1.03	0.47	745	108	880	875	923
D12	1.47	0.99	0.48	738	107	915	912	929
E15	1.44	0.94	0.50	672	97.5	860	840	935
D13	1.47	0.97	0.50	667	96.7	895	880	964

(a) These specimens were tested in a "Nix Ox" catalyst purified hydrogen atmosphere; all others were tested in a palladium catalyst purified hydrogen atmosphere.

(b) The value of N_s is not reported because the tensile load did not drop off 5 percent before failure occurred.

(c) Values of N_c and N_s are not reported because before failure occurred, the load began to increase.

REPRODUCIBILITY OF THE
ORIGINAL PAGE IS POOR

TABLE B7. – SUMMARY OF CONTINUOUS CYCLING FATIGUE DATA FOR TYPE 347 STAINLESS STEEL IN HYDROGEN GAS AT 871°C (1600°F) AND AT AN AXIAL STRAIN RATE OF 10^{-3} SEC^{-1}

Specimen	Total axial strain range, $\Delta\varepsilon_t$	Axial strain range at $N_f/2$, percent		Stress range at $N_f/2$, $\Delta\sigma$		Fatigue life, cycles		
		Inelastic, $\Delta\varepsilon_{in}$	Elastic, $\Delta\varepsilon_e$	MN/m^2	ksi	N_o	N_s	N_f
C34	5.12	4.96	0.16	201	29.2[a]	--	--	139
B37	4.96	4.78	0.18	220	31.9	90	140	151
A37	4.93	4.74	0.19	234	33.9	82	171	178
C26	5.32	5.15	0.17	204	29.6	80	165	190
A36	4.97	4.80	0.17	230	33.3	120	200	241
B36	5.30	5.14	0.16	198	28.7	210	260	294
A29	4.97	4.77	0.20	208	30.1	100	352	356
B30[b]	4.96	4.80	0.16	179	25.9	150	210	359
C35	4.95	4.81	0.14	181	26.3	220	315	482
B35	3.00	2.81	0.19	243	35.2[a]	--	--	232
A38	3.20	3.02	0.18	209	30.3	255	410	437
A39	2.96	2.78	0.18	204	29.6	250	430	446
B31	2.97	2.81	0.16	177	25.7	320	445	479
C30	2.94	2.77	0.17	215	31.2[a]	--	--	479
C31	2.94	2.77	0.17	219	31.8[a]	--	--	516
B34	2.95	2.80	0.15	196	28.4[a]	--	--	517
C29	2.94	2.77	0.17	190	27.6[a]	--	--	553
A32	2.98	2.81	0.17	189	27.4	450	520	754
C32	1.70	1.55	0.15	209	30.3	500	700	767
C25[b]	1.50	1.33	0.17	201	29.2	800	1430	1522
A35	1.47	1.32	0.15	190	27.6	850	1805	1821
C33	1.48	1.32	0.16	203	29.5	900	1550	1889
C28	1.45	1.31	0.14	183	26.5[a]	--	--	1913
A33	1.44	1.33	0.11	158	23.0	1000	1720	2000
A31	1.28	1.12	0.16	187	27.1	1750	1850	2111
B38	1.50	1.35	0.15	196	28.4	800	1650	2124
B32	1.48	1.33	0.15	205	29.7	1200	1600	2245
B39	1.44	1.30	0.14	180	26.1	2100	2200	2545
B40	1.48	1.32	0.16	201	29.1	1400	1750	2850

(a) Values of N_o and N_s are not reported because anomolies in the load versus cycles record make their determination ambiguous.

(b) Hydrogen gas was purified using a copper chip drier and the specimen surface was similar to that obtained using a palladium-catalyst purifier.

TABLE B8. – SUMMARY OF CONTINUOUS CYCLING DATA FOR HASTELLOY ALLOY X IN HYDROGEN GAS AT 871°C (1600°F) AND AN AXIAL STRAIN RATE OF 10^{-3} SEC^{-1}

Specimen	Total axial strain range, $\Delta\varepsilon_t$	Axial strain range at $N_f/2$, percent		Stress range at $N_f/2$, $\Delta\sigma$		Fatigue life, cycles		
		Inelastic, $\Delta\varepsilon_{in}$	Elastic $\Delta\varepsilon_e$	MN/m	ksi	N_o	N_5	N_f
E39	5.27	4.96	0.31	461	66.9	88	155	172
D44	5.19	4.84	0.35	421	61.0	80	170	185
E34	5.01	4.67	0.34	466	67.6	90	182	185
D41	5.01	4.66	0.35	472	68.5[a]	--	--	193
E35	4.97	4.68	0.29	434	63.0	95	182	194
E38	4.96	4.65	0.31	438	63.5	100	192	219
D45	4.95	4.64	0.31	441	63.9	115	170	255
D40	4.96	4.62	0.34	411	59.6	150	268	277
E42	3.34	3.01	0.33	399	57.8	120	265	301
E40	3.00	2.70	0.30	448	65.0[a]	--	--	425
D36	3.00	2.67	0.33	449	65.1	185	440	469
D39	3.00	2.67	0.33	441	64.0[a]	--	--	473
E36	3.00	2.68	0.32	434	63.0	300	465	479
D37	2.95	2.62	0.33	431	62.5[a]	--	--	522
E33	2.96	2.59	0.37	414	60.1	290	582	596
D47	2.96	2.65	0.31	440	63.8	350	520	621
E41	1.65	1.33	0.32	447	64.8	450	900	981
D43	1.49	1.20	0.29	396	57.4[a]	--	--	1601
D35[b]	1.53	1.19	0.34	414	60.0	1000	1660	1731
D42	1.59	1.27	0.32	435	63.1	700	1650	1805
E31[c]	1.52	1.25	0.27	428	62.1[a]	--	--	1896
E37	1.53	1.23	0.30	388	56.3	960	1825	1998
D46	1.51	1.22	0.29	444	64.4	950	2000	2249
E32	1.51	1.22	0.29	403	58.4	1000	1950	2278
D38	1.48	1.18	0.30	392	56.8	--	--	2283

(a) Values of N_o and N_5 are not reported because anomolies in the load versus cycles record make their determination ambiguous.

(b) Hydrogen gas was purified using a copper chip drier and the specimen surface was similar to that obtained using a palladium-catalyst purifier.

(c) Specimen was covered with green oxide in test section because of a malfunction in the hydrogen gas purification system.

REPRODUCIBILITY OF THE
ORIGINAL PAGE IS POOR

TABLE B9. – SUMMARY OF CONTINUOUS CYCLING FATIGUE DATA FOR TYPE 347 STAINLESS STEEL IN HYDROGEN GAS AT 593, 649, AND 704°C (1100, 1200, AND 1300°F) AND AT AXIAL STRAIN RATE OF 10^{-3} sec^{-1}

Specimen	Temperature, °C (°F)	Total axial strain range, $\Delta\epsilon_t$	Axial strain range at $N_f/2$, percent		Stress range at $N_f/2$, $\Delta\sigma$		Fatigue life, cycles		
			Inelastic, $\Delta\epsilon_{in}$	Elastic, $\Delta\epsilon_e$	MN/m^2	ksi	N_o	N_s	N_f
A64	593 (1100)	3.04	2.62	0.42	690	100	308	317	327
A61		3.04	2.58	0.46	703	102	332	339	349
A62		3.02	2.59	0.43	696	101	367	383	400
A57	649 (1200)	2.97	2.57	0.40	625	90.7	205	235	264
A56		2.99	2.56	0.43	610	88.5	--	--	274
A55		2.98	2.59	0.39	607	88.0	244	257	281
A54		2.99	2.58	0.41	646	93.7	346	363	381
A60		1.51	1.18	0.33	519	75.2	1602	1603	1605
A59		1.54	1.20	0.34	523	75.9	1693	1704	1735
A58		1.52	1.21	0.31	502	72.8	1701	1732	1745
A40	704 (1300)	3.01	2.63	0.38	538	78.0	177	177	178
A41		3.06	2.62	0.44	591	85.7	--	--	232
A66		3.04	2.69	0.35	496	72.0	263	266	269

TABLE B10. – SUMMARY OF FATIGUE DATA FOR TYPE 347 STAINLESS STEEL AND HASTELLOY ALLOY X IN HYDROGEN GAS AT 760 and 871°C (1400 and 1600°F) WITH A 10-MINUTE COMPRESSIVE-STRAIN HOLD TIME AND AT AN AXIAL STRAIN RATE OF 10^{-3} SEC^{-1}

Specimen	Temperature, °C (°F)	Total axial strain range, $\Delta\epsilon_t$	Axial strain range at $N_f/2$, percent			Stress range at $N_f/2$, $\Delta\sigma$		Fatigue life, cycles		
				Elastic						
			$\Delta\epsilon_{in}$	$\Delta\epsilon_{ed}$	$\Delta\epsilon_{ei}$		ksi	N_c	N_z	N_f
Type 347 stainless steel										
A43	760 (1400)	4.85	4.64	0.32	0.21	507	73.5	114	124	136
A48		5.02	4.75	0.39	0.27	490	71.0	103	106	137
A44		5.04	4.82	0.34	0.22	436	63.2	122	150	156
A50		3.08	2.85	0.36	0.23	487	70.6	274	275	279
A51		3.01	2.76	0.36	0.25	470	68.2	311	317	322
A46		3.08	2.87	0.32	0.21	458	66.4	--	--	475
A47		1.58	1.37	0.33	0.21	420	60.9	711	725	746
A45		1.58	1.36	0.32	0.22	423	61.4	789	805	842
A49		1.55	1.33	0.34	0.22	443	64.2	837	845	939
A42		1.45	1.24	0.28	0.21	396	57.4	885	905	975
A52	871 (1600)	3.06	2.88	0.19	0.18	243	35.3	--	--	456
A63		2.98	2.88	0.18	0.10	221	32.1	--	--	506
A53		3.00	2.86	0.20	0.14	246	35.7	--	--	≥814[b]
Hastelloy alloy X										
D48	760 (1400)	3.05	2.67	0.63	0.38	931	135	111	130	148[c]
D49	871 (1600)	3.08	2.91	0.36	0.17	525	76.2	--	--	≥429[c]

[a]Strain rate was accidentally too low; $\dot{\epsilon} = 3.4 \times 10^{-4}$ sec^{-1}.

[b]Equipment malfunction resulted in damage to specimen and discontinuation of experiment. However, examination of the failed specimens indicated that substantial cracking had taken place; thus, the number of cycles was believed to be close to N_f.

[c]Specimen failed due to development cyclic deformation instability of necking in test section.

REPRODUCIBILITY OF THE ORIGINAL IS POOR

REFERENCES

1. Manual on Low Cycle Fatigue Testing. Spec. Tech. Publ. 465, ASTM, 1969.

2. Baldwin, E. E.; Sokol, G. J.; and Coffin, L. F., Jr.: Cyclic Strain Fatigue Studies on AISI Type 347 Stainless Steel. Proc. [illegible], vol. 57, 1957, pp. 567-581; discussion, pp. 581-586.

3. Jaske, C. E.; Mindlin, H.; and Perrin, J. S.: Low-Cycle Fatigue of Reactor Technology. vol. 15, no. 3, 1972, pp. 185-207.

4. Berling, J. T.; and Slot, T.: Effect of Temperature and Strain Rate on Low-Cycle Fatigue Resistance of AISI 304, 316, and 348 Stainless Steels. Spec. Tech. Publ. 459, ASTM, 1969, pp. 3-30.

5. Carden, A. E.; and Slade, T. B.: High-Temperature Low-Cycle Fatigue Experiments on Hastelloy X. Fatigue at High Temperature. Spec. Tech. Publ. 459, 1969, pp. 111-129.

6. Tackett, J.: Fatigue Data on Hastelloy Alloy X. Report of Stellite Division, Cabot Corp., 1976.

7. Slot, T.; Stentz, R. H.; and Berling, J. T.: Controlled-Strain Testing Procedures. Manual on Low-Cycle Fatigue Testing, ASTM-STP-465, American Society for Testing and Materials, Philadelphia, 1969, pp. 100-128.

8. Feltner, C. E.; and Mitchell, M. R.: Basic Research on the Cyclic Deformation and Fracture Behavior of Materials. Manual on Low-Cycle Fatigue Testing, ASTM-STP-465, American Society for Testing and Materials, Philadelphia, 1969, pp. 27-66.

9. Morrow, JoDean; and Tuler, F. R.: Low Cycle Fatigue Evaluation of Inconel 713C and Waspaloy. Transactions, ASTM, Series D. Journal of Basic Engineering, vol. 87, no. 2, June 1965, pp. 275-289.

10. Materials Properties Data Book. (ANSC Report 2275, Aerojet Nuclear Systems Company; SNP-1.) Revision of March 15, 1970.

11. Conway, J. B.: An Analysis of the Relaxation Behavior of AISI 304 and 316 Stainless Steel at Elevated Temperature. General Electric Report GEMP-730, Cincinnati, Ohio, December 1969.

12. Berling, J. T.; and Conway, J. B.: Effect of Hold Time on the Low-Cycle Fatigue Resistance of 304 Stainless Steel at 1200°F. Proceedings of the First International Conference on Pressure Vessel Technology, ASTM, pp. 1233-1246, New York, 1969. Also USAEC Report GEMP-702, Nuclear Systems Programs, General Electric Company, June 1969.

13. Jaske, C. E.; Mindlin, H.; and Perrin, J. S.: Low-Cycle Fatigue and Creep Fatigue of Incoloy Alloy 800. BMI-1921, February 1972.

14. Jaske, C. E.; Mindlin, H.; and Perrin, J. S.: Low-Cycle-Fatigue Evaluation of Reactor Materials. Progress on LMFBR Cladding, Structural, and Component Materials Studies During July 1971 through June 1972, Final Report, Task 32, BMI-1928, July 1972, pp. 2-70.

15. Jaske, C. E.; Mindlin, H.; and Perrin, J. S.: Influence of Hold-Time and Temperature on the Low-Cycle Fatigue of Incoloy 800. Journal of Engineering for Industry, vol. 94, no. 3, 1972, pp. 930-934.

16. Jaske, C. E.; Mindlin, H.; and Perrin, J. S.: Development of Elevated Temperature Fatigue Design Information for Type 316 Stainless Steel. Paper presented at the International Conference on Creep and Fatigue in Elevated-Temperature Applications, Philadelphia, September 1973, and Sheffield, England, April 1974.

17. Manson, S. S.; Halford, G. R.; and Hirschberg, M. H.: Creep-Fatigue Analysis by Strain-Range Partitioning. Design for Elevated Temperature Environment, the ASME, New York, 1971, pp. 12-24.

18. Halford, G. R.; Hirschberg, H. M.; and Manson, S. S.: Temperature Effects on the Strainrange Partitioning Approach for Creep Fatigue Analysis. Fatigue at Elevated Temperatures, ASTM STP 520, ASTM, 1973, pp. 658-669.

19. Coffin, L. F., Jr.: The Effect of Vacuum on the Low Cycle Fatigue Law. Metallurgical Transactions, vol. 3, 1972, pp. 1777-1788.

20. Sheffler, K. D.: Vacuum Thermal-Mechanical Fatigue Testing of Two Iron Base High Temperature Alloys. (TRW ER-7697, TRW Inc.; NAS3-6010.) NASA CR-134524, 1974.